Mechanical Properties of Polymer Blends 11

Z. Bartczak and A. Galeski

Contents

Z. Bartczak (✉) • A. Galeski
Department of Polymer Physics, Centre of Molecular and Macromolecular Studies Polish Academy of Sciences, Lodz, Poland
e-mail: bartczak@cbmm.lodz.pl; andgal@cbmm.lodz.pl

L.A. Utracki, C.A. Wilkie (eds.), *Polymer Blends Handbook*,
DOI 10.1007/978-94-007-6064-6_13,

Abstract

Mechanical properties of polymer blends, including strength and toughness, are described in terms of morphology, resulting texture, and elementary deformation mechanisms and cavitation. Basic principles of toughening of blends based on glassy, crystalline, and thermoset polymers are described. Toughening strategies involving crazing, cavitation, crystal plasticity, and other micromechanisms involving energy dissipation are presented. Cavitation during deformation arising from mechanical mismatch between differently oriented stacks of lamellae in a semicrystalline polymer, decohesion at interfaces, as well as internal rubber cavitation contribute to the toughness by activation of other mechanisms of plastic deformation of the surrounding matter. Internal cavitation, although augmenting the toughness, greatly reduces the strength of the material. Micromechanisms that are engaged in rubber-toughened blends were characterized with significant attention. Matrix and dispersed-phase properties, as well as interfacial effects, were considered in the interpretation of structure–property relationship for incompatible and partially compatible polymer blends. The dispersion of the second component of the blend and its influence on stress concentrations around inclusions were discussed. The concept of easy deformation paths connected with interparticle distances and shear orientation was considered.

The function of the interfaces, including compatibilizers, in plastic response of polymer blends, is also analyzed.

11.1 Introduction

In polymer blends, the structure is more complicated than in homopolymers because usually there are three structure components: dispersed phase, continuous phase, and interface. Strong bonding between blend components assures that the applied force is transmitted into the dispersed inclusions. Therefore, modification of blends by introducing compatibilizers is a common practice. Compatibilized blends differ from blends of incompatible polymers, apart from more discrete dispersion of a minor component, mainly by the structure and properties of the interface between components. Usually, the achieved toughness of well compatibilized blends allows for their large plastic deformation. There are several simultaneous and synergistic phenomena which give a contribution to toughening of polymer blends. The important factors are the recovery of macromolecular chain mobility at interfaces connected with the change in morphology of interfacial layers and the shift of the brittle-to-ductile transition to a lower temperature. The modification of interfaces often removes the additional relaxation processes which can appear in the system containing unmodified interfaces. Therefore, the limitations to the mobility of kinetics elements at interfaces due to interactions between the inclusions and the matrix are also removed.

Nowadays plain homopolymers are rarely used. Instead, the use of polymer blends dominates in many applications. There are a great variety of blends, including a broad range of materials of a matrix as well as dispersed phase. They differ in compatibility of components, incompatibility, partial miscibility, and inclusion size and shape. A range of micromechanisms including crazing, shear yielding, cavitation of various kinds, and plasticity of polymer crystal are engaged in deformation of polymer blends. Dependencies on temperature, deformation rate, concentration of components, molecular characteristics of components, and other factors influence the brittle-to-ductile transition, morphology, and phase structure. Therefore, this chapter was divided into subsections in which the behavior and mechanical properties of most important cases, related phenomena, and features of mechanical performance of polymer blends are discussed.

11.2 Plastic Deformation and Damage Mechanisms in Polymers

There are a large variety of mechanical responses of solid polymers. The range spans from brittle fracture through highly ductile behavior to rubber elasticity. Deformation processes of both glassy and semicrystalline polymers have been extensively explored in the past. For an overview of these numerous studies, see, e.g., Argon 2013; Balta-Calleja and Michler 2005; Haward and Young 1997; Michler and Balta-Calleja 2012. Above the elastic region, deformation of polymers is usually nonhomogeneous, especially when observed in the microscale. This is not only the case of polymers with clear heterogeneous morphology, such as semicrystalline polymers, block copolymers, or phase-separated polymer blends but also of homogeneous materials as amorphous glassy polymers. Plastic deformation and/or fracture mechanisms start to operate locally above the elasticity limit. Depending on the polymer molecular characteristics, such as chain flexibility and chain entanglement density, as well as test conditions (specimen geometry, loading mode, strain rate, temperature), three types of heterogeneous deformation are observed in the microscale: crazes, shear bands, and shear deformation zones (Michler and Balta-Calleja 2012). Among parameters controlling deformation, under standardized testing conditions, the molecular characteristics of the polymer remain the predominant parameter affecting the deformation mechanism.

Crazes are crack-like sharply localized bands of plastically deformed material, initiated when an applied tensile stress causes microvoids to nucleate at points of high stress concentrations that are created by surface scratches, flaws, cracks, dust particles, or other heterogeneities (Bucknall 1977; Haward and Young 1997; Kinloch and Young 1983). In homogeneous glassy polymers, crazes are usually initiated from microscopic surface flaws or embedded heterogeneities, like dust particles. Dust is difficult to avoid in processing (injection molding, extrusion) because it begins with pellets that become statically charged and attract airborne particles. Typical surface defects are small random scratches introduced during processing, machining, and handling. When these flaws are removed, e.g., by

cautious polishing, there is a marked increase in the critical stress of craze initiation, sometimes to the point at which tensile shear yielding and ductile drawing are initiated in relatively brittle polymers such as PMMA and PS (Argon and Hannoosh 1977). Crazes form in planes normal to the direction of maximum (tensile) principal stress and consist of highly oriented polymer fibrils of approximately 5–15 nm in diameter, stretched out in the direction of loading, and separated by elongated nanovoids. Crazes develop and propagate by two processes: by craze tip advance that allows fibrils to be generated and by craze width growth. In contrast to crack, the craze (which is, in fact, a highly localized yielded region, consisting of a system of alternating oriented polymer fibrils and voids) is capable of transmitting load. However, crazes are frequent precursors of brittle fracture since with the growth of the craze the most elongated fibrils break, which usually leads to the development of microcrack in the center of the craze. Due to the presence of voids, deformation of crazes is dilatational – the volume increases markedly with strain (Haward and Young 1997; Kausch 1983, 1990).

On the other hand, the shear bands and deformation zones are the result of shear processes and do not contain voids so that deformation advances at nearly constant volume. Shear bands can be either localized or diffuse, but even for very localized bands, their interface with bulk material is much thicker than for crazes. Thick bands and deformation zones are usually made of coalescing micro-shear bands.

The basic mechanisms involved in plastic deformation of glassy polymers are crazing and shear yielding (Argon 2013; Bucknall 1977; Haward and Young 1997; Kausch 1983, 1990; Michler and Balta-Calleja 2012), giving rise to the formation of crazes or shear bands and zones, respectively. For polymer crystals, plastic shear is realized through crystallographic mechanisms, primarily by crystallographic slips along and transverses to the chain direction, which are supported by the shear in interlamellar amorphous layers (Argon 2013; Bartczak and Galeski 2010; Oleinik 2003). Their collective activity gives rise to the formation of shear bands or deformation zones, similar to shear yielding in glassy amorphous polymers.

Crazing requires the presence of dilatational component in the stress tensor and may be inhibited by hydrostatic pressure. On the other hand, it is enhanced by the presence of triaxial tensile stress (Kinloch and Young 1983). Unfortunately, such a stress state exists ahead of large flaws or notches in relative thick specimens (plane-strain conditions). Therefore, the presence of sharp cracks, notches, or defects in thick specimens will favor craze initiation leading to brittle fracture, which is opposite to a bulk shear yielding mechanism that leads usually to ductile behavior.

Even the most brittle polymers demonstrate some localized plastic deformation – in front of the crack tip, there exists a small plastic zone where stretching of chains, chain scission, and crack propagation appear in a small volume. The size of that plastic zone is too small to manifest in macroscopic plastic yielding and the crack propagates in a brittle manner. The relative low energy absorbed by the sample on its fracture is almost entirely that dissipated inside the small plastic zone.

11.2.1 Brittle and Pseudoductile Polymers

Under given experimental conditions, chemically different polymers behave differently. For example, in tensile test at a low rate polystyrene tends to craze and is brittle while polycarbonate tends to yield and shows ductile behavior. Based on that, polymers are classified frequently as brittle or pseudoductile (i.e., generally showing a ductile behavior but changing to brittle at more severe conditions, e.g., at a lower temperature). According to this classification, brittle polymers (e.g., PS or PMMA) tend to fail by crazing, have low crack initiation energy (low unnotched toughness), and low crack propagation energy (low notched toughness). Pseudoductile polymers (e.g., PC, PET, PA, or PE) tend to fail by yielding, have high energy of crack initiation (high unnotched toughness), and relatively low energy of crack propagation (notch sensitivity, low notched toughness). The brittle or ductile response depends not only on the polymer itself but also on many extrinsic variables as specimen geometry, loading mode, and test conditions, so frequently the same polymer may either craze (i.e., be brittle) or yield (ductile) depending on external conditions. Argon (Argon et al. 2000; Argon and Cohen 2003) argued that with the exception of only a small class of pure metals, all other solids, including all solid polymers, should be actually classified as intrinsically brittle. Intrinsically brittle polymers only can change their response from brittle to ductile at certain specific experimental conditions (see Sect. 11.4.2.3).

11.2.2 Basic Mechanisms of Deformation

The brittle or ductile behavior of polymer and the preferred mechanisms of deformation and failure are controlled principally by two molecular parameters – the entanglement density and chain flexibility, determining an initiation stress for crazing or shear yielding, respectively. Depending on these parameters, one of the two basic deformation mechanisms (crazing or shear yielding) is selected as the dominating mechanism, so they occur separately in most cases. However, they also can be active simultaneously at different proportion in some polymer systems. Moreover, even a small change in the test conditions can result in a change from shear yielding to crazing or reverse. Crazing and shear yielding are considered to be independent processes, and the mechanism that at given experimental conditions requires the lower stress is activated first and becomes the dominant deformation mechanism that leads ultimately to the failure of the material.

11.2.2.1 Crazing and Entanglement Density

Crazes, in contrast to cracks, are load-bearing features owing to highly stretched fibrils connecting the walls of what would otherwise be a crack. Multiple crazes are actually the main source of ductility in amorphous polymers modified by blending with elastomers. However, crazes have also a big drawback as they frequently appear precursors of brittle fracture. This is due to high localization of deformation in crazes – large plastic deformation and related local energy absorption are highly

localized and confined to a very small volume of the material. Craze can be considered as a thin layer of polymer in which elastic and plastic deformation in the direction of principal tensile stress has occurred without lateral contraction. The lack of lateral contraction is due to voids created between fibrils. These voids can constitute up to approximately 50–75% of the volume of the craze (Haward and Young 1997). The thickness of a craze at the tip is below 10 nm, while a body of the mature craze is much thicker, by 2–4 orders of magnitude. Such significant thickening of the craze proceeds mainly by involving more bulk polymer at the interface into the plastic deformation zone due to strain hardening of the craze matter. This keeps molecular stretch and the void content quite uniform within the craze.

In the literature, there are many theories and models describing nucleation, initiation, and growth of crazes. They were discussed in several reviews, see, e.g., Argon (2013), Donald (1997), Kausch (1983, 1990), Michler and Balta-Calleja (2012). A craze is nucleated by an event of local plastic deformation by shear occurring in the vicinity of a defect and leading to the buildup of significant lateral stresses. This is followed by nucleation of nanovoids, relieving the triaxial constraints, and then by growth of these voids and strain hardening of polymer nanofibrils between voids as molecular orientation advances (Kramer 1983). The nanovoid nucleation stage is considered as a critical one. In highly entangled polymers, the load is distributed over different entanglements and different chains, and, as a consequence, the probability of breaking chains and void formation is lower. It is thus expected that a high entanglement density is unfavorable for craze initiation. Once a craze is initiated, it must grow both in width and length. The general mechanism of craze tip advance has been known to be meniscus instability process (Argon and Salama 1977). Kramer and Berger (1990) derived a detailed model of the craze growth. The craze will grow only when the deformation energy associated with the applied stress is larger than the surface energy needed to create a new surface. This surface energy per unit area of the void surface (Γ) is (Kramer and Berger 1990)

$$\Gamma = \gamma + \frac{1}{4} d_e v_e U_{ch} \tag{11.1}$$

where γ is the van der Waals surface energy, d_e is the entanglement mesh size, v_e is the entanglement density and U_{ch} is the bond energy of the polymer chain. The second term is the energy cost of elimination of entanglements crossing the interface, for example, by chain scission. It appears weighty – in PS of relatively low entanglement density ($v_e \sim 3 \times 10^{25}$ m^{-3}) is about equal to the van der Waals term, both being around 0.04 J/m^2. Increasing the entanglement density of the molecular network leads to a significant increase in Γ and, therefore, to an increase of the craze initiation stress. For PC, which has v_e higher by one order of magnitude than PS ($v_e \sim 3 \times 10^{26}$ m^{-3}), the additional contribution to Γ is 0.2 J/m^2, and consequently much higher stress would be required to initiate a craze. This explains why polymers of high entanglement density, as PC, often deform without crazes but readily form shear bands, instead. The dependence of the craze initiation stress on

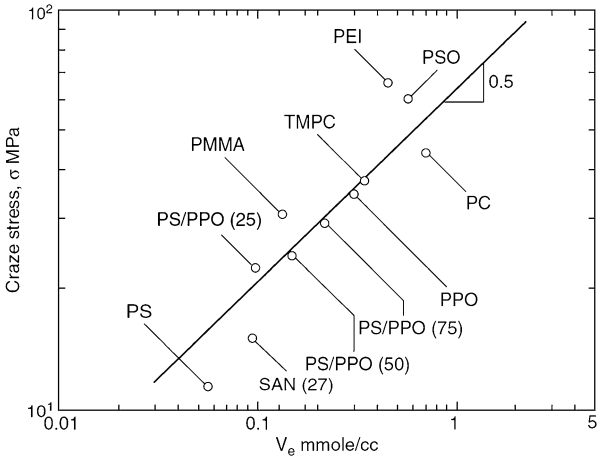

Fig. 11.1 Dependence of the craze initiation stress σ_e on the entanglement density v_e for various polymers and their miscible blends (From Wu (1990); reproduced with permission of Wiley)

entanglement density was confirmed by experimental data (Wu 1990, 1992). The following relationship holds for the stress of craze initiation σ_{craze} and the entanglement density v_e:

$$\sigma_{craze} \propto f_z \nu_e^{1/2} \tag{11.2}$$

where f_z is a parameter related to the free volume, reflecting the effects of the physical aging on the crazing stress. Craze initiation stress appears weakly dependent on temperature. A low entanglement density should result in low stress σ_{craze}, thus favoring crazing – see Fig. 11.1, illustrating the relationship of σ_{craze} and entanglement density v_e, for a series of homopolymers and miscible blends of polystyrene (PS) and polyphenylene oxide (PPO), obtained by Wu (1990, 1992). Crazing is initiated at very low stress in PS, which demonstrates the low entanglement density. Blending of PS with PPO results in a notable increase of entanglement density and hence the resistance to crazing – much higher stress is needed to initiate crazing in PPO-rich blends (e.g., in the blend containing 75 wt.% PPO) than in plain PS. On the other hand, polymers exhibiting high entanglement density, as. e.g., PC, tend to deform by shear yielding rather than crazing.

Brittle polymers, such as PS and PMMA, developing crazes at low strains below 1 %, can absorb a greater amount of energy if crazing involves a larger volume of the sample. This can be achieved by increasing the number of the crazes upon deformation due to appropriate structure modification, e.g., by introducing rubber particles. The resultant greatly increased the concentration of crazes is referred to as multiple crazing, which is now acknowledged to be the principal mechanism by which glassy crazable polymers modified with elastomer particles accommodate deformation (Bucknall 1977, 1997, 2000). The multiple crazing mechanism was demonstrated operational and highly effective in high-impact polystyrene (HIPS), ABS copolymer, rubber-toughened PMMA, and other similar systems (Bucknall 1977).

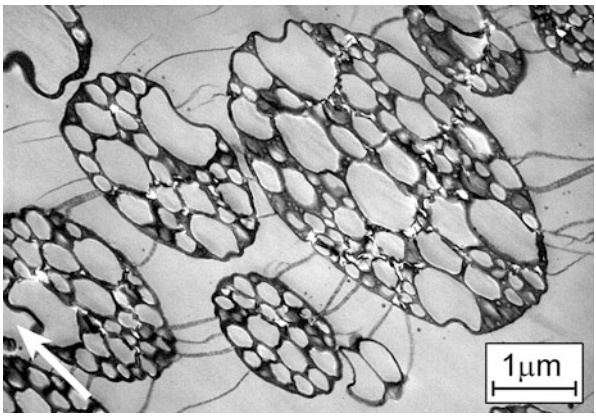

Fig. 11.2 Multiple crazing in HIPS: TEM micrograph of the ultrathin section of HIPS with salami particles of rubber and crazes at early stage of deformation. *Arrow* indicates tensile direction. Scale bar 1 μm (From Heckmann et al. (2005); reproduced with permission of Taylor and Francis)

The occurrence of multiple crazing was evidenced by optical and electron microscopy (Bucknall 1977; Michler and Balta-Calleja 2012) and by real-time small-angle X-ray scattering (Bubeck et al. 1991). In glassy polymers modified with elastomer particles (commonly called rubber-toughened polymers), the numerous crazes were found to be initiated near the equator of the cavitating rubber particle due to high stress concentration there (Bubeck et al. 1991; Bucknall 1977). Initiation of numerous crazes at rubber particles involves a relatively large volume of the glassy matrix into deformation, all dissipating energy, which results in a significant increase of toughness. Multiple crazing phenomenon is illustrated in Fig. 11.2.

11.2.2.2 Shear Yielding and Chain Flexibility

Bucknall (2000) depicted shear yielding as the process by which most of the ductile polymeric materials accommodate high strains. Shear yielding involves a displacement of matter during the deformation (molecules sliding past each other). In contrast to crazing, there is no change in the volume or density associated with shear yielding. As cohesion is not lost, no voids are created by shear yielding. Opposite to crazing, shear yielding is strongly temperature dependent. The dependence of the yield stress on temperature and strain rate can be described by the Eyring-type equation (Bauwens 1967; Roetling 1965). In this approach, a positive correlation is expected between chain mobility, yielding, and toughness. That correlation was verified experimentally by Wu (1990, 1992), who found dependence of the reduced normalized yield stress on chain stiffness, which can be defined by the following parameter:

$$C_\infty = \lim_{n\to\infty} \left(R_o^2/n_v l^2\right) \tag{11.3}$$

where $R_o{}^2$ is the mean-square end-to-end distance of an unperturbed chain, n_v is the number of statistical skeletal units, and l^2 is the mean-square length of a statistical unit. Rigid chains. such as liquid crystalline polymers. will have a high C_∞,

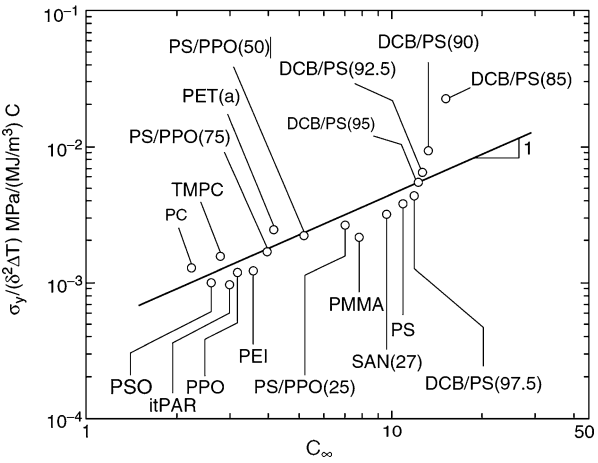

Fig. 11.3 Normalized reduced yield stress $\sigma_{yr} = \sigma_y/[\delta^2(\mathrm{Tg} - \mathrm{T})]$ versus characteristic chain stiffness, C_∞ (From Wu (1990); reproduced with permission of Wiley)

whereas flexible polymers, as, e.g., polyethylene, will demonstrate low values of C_∞. According to Wu (1990) C_∞ and v_e can be related by the equation:

$$v_e = \frac{\rho_a}{3\mathrm{M_v}C_\infty^2} \tag{11.4}$$

where $\mathrm{M_v}$ is the molecular mass of a statistical skeletal unit and ρ_a is the density of an amorphous polymer.

The stress initiating the shear yielding σ_y depends strongly on temperature and is additionally proportional to two parameters: $\Delta\mathrm{T} = \mathrm{T_g} - \mathrm{T}$ and to δ^2, where $\mathrm{T_g}$ and T are the glass transition temperature and the temperature of the test, respectively, while δ denotes the cohesive energy density. The reduced normalized yield stress was defined by:

$$\sigma_{yr} = \sigma_y/\left[\delta^2\left(\mathrm{T_g} - \mathrm{T}\right)\right] \tag{11.5}$$

The denominator $\delta^2(\mathrm{T_g} - \mathrm{T})$ accounts actually for the interchain effects (friction between chains) on the yield stress. Thus, the reduced yield stress defined above by Eq. 11.5 should be only a function of an intrachain property, characterized by the chain stiffness (Wu 1990, 1992):

$$\sigma_{yr} \propto f_y C_\infty \tag{11.6}$$

where f_y is a parameter related to the free volume, reflecting the effects of the physical aging. The above relation implies that the higher the chain stiffness, the lower its mobility and, therefore, the higher the reduced normalized yield stress. Figure 11.3 presents a plot of σ_{yr} as a function of the stiffness ratio, C_∞, constructed by Wu (1992) for a series of polymers and miscible blends. This experimental dependence, confirmed for a number of glassy polymers, shows that the yield

initiation stress increases with increasing chain stiffness of the polymer and that the reduced yield stress for polymers that are known ductile is lower than for those known brittle, as, e.g., PC and PS, respectively. Chains of PC exhibit low stiffness, $C_\infty = 2.4$ (Wu 1992), and PC prefers to deform by shear yielding while PS demonstrates a high chain stiffness, $C_\infty = 10.8$, which results in a high initiation stress for shear yielding. As a consequence PS appears vulnerable to crazing, which can be initiated at stress lower than that needed for initiation of shear yielding.

11.2.2.3 Molecular Criterion for Craze/Yield Behavior from Chain Structure Parameters

The competition between crazing and shear yielding determines which mode of fracture will predominate, so that the transition between crazing (which leads to brittle behavior) and shear yielding deformation mechanism (leading to ductility) is one of the key phenomena for toughness modification. Shear yielding wins the competition with crazing when the yield initiation stress is simply lower than the stress needed for initiation of crazing. The combination of Eqs. 11.2, 11.4, 11.5, and 11.6 leads to the following relationship that expresses the molecular criterion for dominant deformation mode (Wu 1990, 1992):

$$\frac{\sigma_z}{\sigma_{yr}} \propto \frac{\nu_e^{1/2}}{C_\infty} \left[= \left(\frac{\rho_a}{3M_v} \right)^{1/2} C_\infty^{-2} = \left(\frac{3M_v}{\rho_a} \right)^{1/2} \nu_e \right] \tag{11.7}$$

Henkee and Kramer (1984) evidenced the entanglement density to be a critical parameter determining whether the polymer will tend to deform by crazing or by shear yielding. A low entanglement density favors crazing, while the entanglement density rising above the critical value (roughly $v_e \sim 0.15$ mmol/cm^3 (Wu 1992)) results in a change from crazing to shear yielding. On the other hand, the flexibility of chains in thermoplastic polymers seems also to be likely an important parameter for this crazing/shear yielding transition, because when the pseudoductile polymer is cooled down below the temperature of its secondary relaxation process, it becomes brittle despite that entanglement density does not change at this temperature. Taking into account both entanglement density and chain stiffness parameters, the following classification was proposed:

1. Brittle polymers, for which $v_e < \sim 0.15$ mmol/cm^3 and $C_\infty > \sim 7.5$. They fracture by a dominant crazing mechanism and additionally exhibit a low crack initiation energy and a low crack propagation energy (resulting in low, both unnotched and notched, toughness). Examples are PS or PMMA.
2. Pseudoductile polymers, when $v_e > \sim 0.15$ mmol/cm^3 and $C_\infty < \sim 7.5$. They tend to deform by shear yielding mechanism prior to failure. They usually demonstrate a high crack initiation energy (resulting in high unnotched toughness) and a low crack propagation energy (low notched toughness). Examples are PC, polyesters (PBT, PET), or polyamides (PA6, PA6,6).

3. Intermediate class ($v_e \sim 0.15$ mmol/cm^3 and $C_\infty \sim 7.5$) demonstrating combined crazing/shear yielding deformation habit. Examples are some grades of PMMA, PVC, and POM.

According to the Eq. 11.7 both v_e and C_∞ provide a consistent prediction of the deformation behavior. It seems, however, that the entanglement density v_e can be considered as the primary parameter which controls the crazing behavior, whereas the chain stiffness parameter C_∞ is predominant in controlling the shear yielding behavior.

11.2.3 Plastic Deformation of Semicrystalline Polymers

There are three, currently recognized, principal modes of deformation of the amorphous material in semicrystalline polymers: interlamellar slip, interlamellar separation, and lamellae stack rotation (Argon 2013; Bowden and Young 1971; Butler et al. 1998; Haudin 1982; Oleinik 2003). Interlamellar slip involves shear of the amorphous phase between lamellae. It is relatively easy mechanism of deformation for the material above T_g. The elastic part of the deformation can be nearly entirely attributed to the reversible interlamellar slip. Interlamellar separation is induced by a component of tension or compression perpendicular to the lamellar surface. This type of deformation is difficult since a change in the lamellae separation should be accompanied by a transverse contraction and the deformation must involve a change in volume. Stacks of lamellae are embedded in the amorphous matrix, and the stacks are free to rotate under the stress. When the possibility of further deformation of the amorphous phase is exhausted, the deformation of crystalline materials sets in. Any additional deformation of the amorphous phase requires a change in the crystalline lamellae. Crystalline component of polymeric materials is deformed by crystallographic mechanisms, mostly crystallographic slips (Bowden and Young 1974; Lin and Argon 1994; Oleinik 2003). The concept was initially proposed by Peterson (1966, 1968) and developed by Shadrake and Guiu (1976) and Young (1974, 1988): an emission of dislocations from the edges of the lamellae across their narrow faces and their travel across crystals via crystallographic slip mechanism. Many of such subtle slips contribute to a macroscopic strain. Much evidence for the correctness of that mechanism was found in the past (Kazmierczak et al. 2005; Lin and Argon 1994; Seguela 2007; Wilhelm et al. 2004; Young 1988). The model of thermal nucleation of screw dislocations (Peterson 1966, 1968; Young 1974, 1988) was demonstrated to account fairly well for the plastic behavior of many crystalline polymers (Argon et al. 2005; Brooks and Mukhtar 2000; Crist et al. 1989; Darras and Seguela 1993; Seguela 2002). Dislocation theory predicts the correct order of magnitude of the yield stress (O'Kane et al. 1995).

It is commonly believed that the function of the amorphous phase, above the glass transition temperature, in yielding during tensile deformation of semicrystalline polymers is relatively small and is limited to transfer the stress between adjacent crystals (Seguela and Darras 1994). The stress is transmitted through

such elements as tie molecules, entanglements, etc., called "the tie-molecule fraction," An increase of the yield stress was observed with the increase in the tie-molecule fraction. Men et al. (2003) established that tie molecules are of lesser importance with respect to the deformation, while the entangled chains in amorphous phase play a decisive role.

Since all stress is transferred to crystals via amorphous layers, the amorphous phase appears nevertheless essential for load bearing of semicrystalline polymers, including yielding. Amorphous phase must be stressed at yield with a stress similar to plastically deformed crystals. On the other hand, when the stress in the amorphous phase exceeds its cohesive strength, it undergoes cavitation. Cavitation occurs in semicrystalline polymers, usually in tension. A triaxial local stress, contributing to negative pressure, is necessary for cavitation. If the plastic strength of crystals is low, then with an increase of the stress, it is easier to activate dislocation mechanisms of plastic deformation of lamellae rather than to disrupt the amorphous phase or the interface and create a cavity. In such a case, the deformation can proceed without cavitation. Opposite is the case when the breaking of an amorphous phase is easier than plastic deformation of crystals. Then cavities are generated in the amorphous phase during deformation prior to crystal yielding. However, the formation of voids changes rapidly the local stress state and by this can promote deformation of crystals. There are some ways of modification relations between strength of crystals and amorphous phase. First, it is by controlling the perfection, sizes, and number of crystals by crystallization process. Second, any modification of the amorphous component should result in changes of the material response to loading. Recently it was demonstrated that the amorphous phase can be subjected to various modifications without changing crystalline phase and morphology. Those modifications can greatly influence the yielding and deformation of semicrystalline polymers (Rozanski and Galeski 2013). The amorphous phase may be modified by removing of a low molecular weight fraction to increase its strength or by filling the free volume space with low molecular additives.

Many polymers cavitate during deformation at certain experimental conditions. The polymer morphology seems crucial for cavitation. It seems that the cavitation is generally easier in those semicrystalline polymers which are characterized by higher crystallinity and thicker, less defected crystals. However, it is difficult to separate the influence of crystallinity and crystal perfection. There is a kind of competition between two possible processes: cavitation of anamorphous phase and plastic deformation of crystals. If the crystals are defected and therefore become less resistant to plastic deformation, then their plastic deformation becomes relatively easy while the strength of the amorphous phase prevents for its cavitation. Conversely, if the crystals are thick and demonstrate a reduced number of defects giving rise to dislocations, the breaking of the amorphous phase may become easier and will occur first, prior to crystal yielding. Annealing causes some limited changes of crystal structure, including an increase of their thickness and perfection; however, it may cause also a significant change to amorphous phase and modify its cavitation ability. Average molecular weight and molecular weight distribution of polymers may also drastically change the yield cavitation stress (Kennedy et al. 1994). Also,

the deformation rate is an important factor: yields stress increases with deformation rate, and it becomes easier to initiate cavitation in the amorphous phase. Similar effect is due to lowering the temperature. If the cavitation occurs first, before significant deformation of crystals, then the stress at the apparent yield point is defined by cavitation, rather than by crystal plasticity.

Based on the facts presented above, the plastic deformation behavior of semicrystalline polymer materials and the structural changes accompanying the deformation of such materials are controlled by the properties of both crystalline and amorphous phases.

The most significant contribution to toughness comes from the plastic deformation of a material, which is a complex phenomenon involving both the crystalline and amorphous phases. As discussed in Sect. 11.2, the ability to an extensive plastic deformation, called ductility, requires an adequate flexibility of polymer chain segments in order to ensure the plastic flow on a molecular level. It is long known that the macromolecular chain mobility is a critical factor deciding on either brittle or ductile behavior of a polymer (Ferry 1970; Galeski 2002). The increase in the yield stress of an amorphous polymer with a decrease of the temperature is caused by a decrease of chain mobility, and vice versa, the yield stress can serve as a qualitative measure of macromolecular mobility. It was shown that the temperature and strain rate dependencies of the yield stress are described in terms of relaxation processes, similarly as in linear viscoelasticity. Also, the kinetic elements taking part in yielding and viscoelastic response of a polymer are similar: segments of chains, part of crystallites, and fragments of an amorphous phase. On the other hand, in semicrystalline polymers tested above their glass transition temperature, the yield stress is determined by the stress required for crystal deformation and not by the amorphous phase, provided that there is no cavitation. The behavior of crystals differs from that of the amorphous phase because the possibilities of motion of macromolecular chains within the crystals are subjected to severe constraints. Since the mobility of kinetic elements taking part in plastic deformation (mobile dislocations in crystals and shear strain carriers in amorphous phase) is lower at a lower temperature, the energy dissipated increases and can lead to local rise of temperature and produce deformation instability. The rate of plastic deformation increases drastically in such local plastic events referred sometimes as micronecks, and the material may fracture quickly hereafter. At a higher temperature the mobility of kinetic elements is higher, so less energy is dissipated and the local temperature increase is smaller. As a result, the deformation zone is stable and tends to extend to the whole gauge length of the sample. The material shows then a tough behavior.

The necessary condition for high plastic deformation is the possibility of motions of kinetic elements in a time scale as it follows from the deformation rate. The relaxation times and the activation energies are the parameters describing the kinetics of the conformation motions of macromolecules and larger elements taking part in the deformation.

Both massive voiding and shear yielding dissipate energy; however, shear yielding is often favored over voiding, especially under uniaxial stress, elevated

temperature, or slow deformation. Shear yielding dissipates the energy more efficiently (Horst and Spoormaker 1996).

The deformation of polymeric materials starts usually at scratches, notches, or internal defects because they are sources of local stress concentration, frequently well above the applied stress. Toughening of polymeric materials is based on the activation of such plastic deformation mechanisms which are activated at a stress lower than that required for triggering the action of surface and internal defects. Consequently, one of the important means of toughening appears to be a significant lowering of the yield stress of the material.

11.3 Blends

The comprehensive introduction to polymer blends is given in ▶ Chap. 1, "Polymer Blends: Introduction," while ▶ Chaps. 5, "Reactive Compatibilization," ▶ 8, "Morphology of Polymer Blends," ▶ 10, "Properties and Performance of Polymer Blends," ▶ 18, "Polyethylenes and Their Blends," and ▶ 21, "Miscible Polymer Blends" of this handbook are devoted to various aspects and detailed description of the formulation, structure, and morphology of polymer blends. Here, the attention will be briefly turned to such features of polymer blends that directly influence or determine their mechanical properties. In polymer blends, the structure is more complicated than in homopolymers because usually they have three components: dispersed phase, continuous phase, and interface. The interface has a finite thickness; hence it is the third component of the system. Applied force is transmitted onto the dispersed inclusions from the matrix via the interface. Therefore, the properties of the interface play a vital role in force transmission and overall behavior of a blend. Strong bonding between blend components prevents for slip between a matrix and inclusions, while weak adhesion is not efficient in stress transfer, but it may cause a certain amount of friction and may originate decohesion. Modification of blends by introducing compatibilizers is a common practice; therefore, the third component is *explicit* present in blends. It follows then that when considering mechanical properties, the polymer blends should be considered as the systems containing at least three components and with complicated interactions among them.

Compatibilized blends differ from blends of incompatible polymers, apart from more discrete dispersion of a minor component, mainly by the structure and properties of the interface between components. Usually, the achieved toughness of well compatibilized blends allows for their large plastic deformation. In plain crystalline polymers, the elementary mechanisms of plastic deformation are crystallographic slips. However, in simple drawing, the cavitation obscures the real crystallographic mechanisms. The origin of cavitation is the mechanical misfit between stacks of crystalline lamellae. In polymer blends, the interfaces between components are the other source of cavitation. Cavitation creates new internal surfaces; however, the energy dissipated for the formation of cavities is rather low. It is not so for the energy needed for the reorganization of the surrounding matter to accommodate cavities.

These and other considerations concerning mechanical properties of polymer blends will be presented in the forthcoming sections. The survey of existing data and applications shows that the main purpose of polymer modification by blending with other polymers is to modify their mechanical performance and primarily increase toughness. Therefore, in the forthcoming sections we will focus on issues related to polymer toughening which can be achieved by blending with other polymers, mainly those demonstrating elastomeric properties. That method of toughness modification is known under the name of "rubber toughening," because of rather historical reasons. Nowadays it is well established that the toughness can be successfully improved by thoughtful blending not only with classic rubbers but also with various other elastomers, selected other polymers, ready-to-mix polymer particles with core–shell morphology, and even mineral filler particles.

11.3.1 Low Strain Rate Deformation of Polymer Blends

Blending of a polymer with other immiscible polymers can lead to a substantial improvement of drawability and impact strength without a reduction in T_g. Blends of miscible polymers show a single glass transition at a temperature that is in between glass transitions of components. The position of glass transition of a miscible blend on a temperature scale determines its mechanical properties.

When the material is subjected to loading, it responds with deformation. Polymeric materials exhibit two types of mechanical response in elasticity range: in a glassy state the energy is stored as free energy, while in a rubbery state, the energy is stored as a change of macromolecular chain configurational entropy. The first type of elasticity is called energy elasticity and the second entropy elasticity or just rubber elasticity. The physical response of polymeric materials to a small strain or stress is then different because of different sources and different temperature and pressure dependencies. The first is a characteristic of glassy polymers and all inorganic and organic crystals and arises from interatomic and intermolecular interactions, while the second is a characteristic of polymers in a rubbery state and amorphous phase of crystalline polymers and is created by reversible shear and relaxation processes. The latter are specific for different polymers and determine their viscoelastic properties. Similar characteristics of elastic reaction to a small strain or stress concern polymer blends and their components. When a blend is composed of immiscible or partially miscible polymers, most of the free energy of deformation is stored in its matrix, less in dispersed inclusions. For miscible blends, the elastic response depends on their glass transition temperature. The rule of linearity between strain and stress was discovered by Hooke in the seventeenth century, and uniaxial strain or stress experiments can be described as below:

$$\sigma = E_o \varepsilon \tag{11.8}$$

where σ stands for stress, while ε for strain. The elastic constant E_o is called Young's modulus and it should be always defined at zero strain or zero stress;

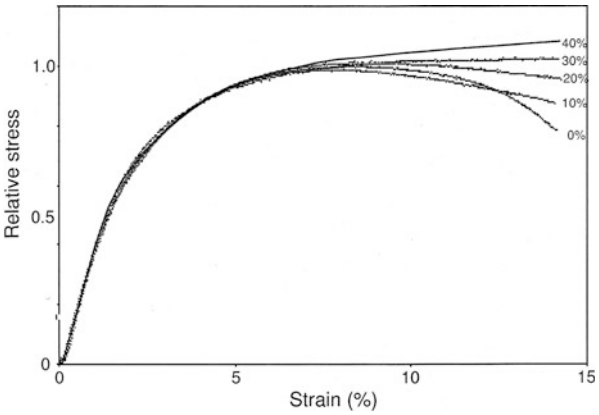

Fig. 11.4 Typical stress–strain curves for polypropylene blended with ethylene-propylene rubber (EPDM) at different rubber concentrations. Strain rate 10^{-2} s^{-1}, room temperature. The plot illustrates the relation of modulus and strain presented in Eq. 11.9 (From Gaymans (2000); reproduced with permission of Wiley)

hence it is called the tangent modulus. As the strain increases, the stress–strain relationship becomes gradually nonlinear. It was shown by Rose for metals (Rose et al. 1983) that the elastic response is modified by bulk decohesion arising from binding energy in the material in the following form:

$$\sigma = E_o \varepsilon \exp(-\alpha\varepsilon) \tag{11.9}$$

where α is a nonzero constant related to uniaxial decohesion strain. Equation 11.9 suggests that the tangent modulus progressively decreases with increasing tensile uniaxial strain (Argon 2013). However, for uniaxial compression, the modulus tends to monotonically increase. Equation 11.9 can be transformed to modulus dependence on ε as follows:

$$E(\varepsilon) = \frac{d\sigma}{d\varepsilon} = E_o (1 - \alpha\varepsilon) \exp(-\alpha\varepsilon) \tag{11.10}$$

Similar relations apply for polymers and polymer blends except that the binding energy for polymeric material is lower than for metals and nonlinearity of modulus is even more pronounced.

From Eq. 11.10, it is seen that the modulus decreases with increasing strain from the initial value of E_o eventually to 0, for strain of $1/\alpha$. The stress reaches then a maximum which is called yield stress, and the processes responsible for the phenomenon are called yielding (Fig. 11.4).

From the above discussion, it follows that most isotropic materials including polymeric materials behave for small strains in a very similar way all according to Eq. 11.10, differing only in a single parameter α. However, yielding in polymeric materials is reached due to other factors that come to play at slightly larger strain and not exhibiting yielding at strain $1/\alpha$ which is related to the binding energy and bulk decohesion as defined by Rose et al. (1983).

11.3.2 Yielding

Yielding in polymer blends is a very complicated event and is usually composed of several micromechanisms that are activated at various stages of deformation depending on the deformation rate, the temperature, deformation mode, and blend morphology.

In glassy homogeneous polymer blends below T_g, their internal morphology plays only a secondary role, in contrast to the temperature, which is the major parameter governing the yielding, especially in compression, shear, and hardness measurements.

One of the few compatible polymer blends in a large concentration range is polystyrene–polyphenylene oxide system (PS/PPO) (Yee 1976). In tension, with increasing PPO content, the deformation habit changes from the formation of crazes, as in PS to homogeneous deformation bands and shear bands, characteristic for PPO (Berger 1990); *see* also the data of Figs. 11.1 and 11.3. There are other partially compatible blends, for instance, SAN/PMMA blends, when the acrylonitrile content in SAN is about 10–30 % (Fowler et al. 1987; Suess et al. 1987). Other examples are amorphous quenched blends of PMMA and polyvinylidene fluoride (PVDF), which are compatible at high temperatures (Nasef and Saidi 2006; Neuber and Schneider 2001). The blend PMMA/PVDF shows a remarkable agreement with the additivity rule of the two components for the yielding in microhardness measurements (Martinez-Salazar et al. 1991). The yielding behavior of the blend material is well correlated with glass transition temperature resulting from the equation of glass transition superposition of Gordon and Taylor (1952).

Immiscible blends have nonhomogeneous morphology and their tensile deformation at yield is much more complicated than miscible systems. There are several mechanisms that are activated at various stages of deformation depending on the deformation rate, the temperature, glass transition temperature of the components, deformation mode, and blend morphology.

Bubeck et al. (1991) showed that in high-impact polystyrene (HIPS), there are crazing and cavitation engaged. The complex mechanism of plastic deformation in the blends leading to improvement of ductility and toughness was revealed. They used real-time X-ray measurements during tensile deformation HIPS samples to show that cavitation of the rubber particles actually precedes crazing of the matrix under tensile impact conditions. Cavities formed within the rubber particles can thus be identified as nuclei for a craze growth, which occurs through the meniscus instability mechanism proposed by Argon and Salama (1977).

Another example of rubber-modified glassy polymer was given by the study of polylactide blends (Kowalczyk and Piorkowska 2012). Blending polylactide (PLA) with poly(1,4-*cis*-isoprene), which is immiscible with PLA, can lead to a substantial improvement of drawability and impact strength without a decrease in Tg. In contrast to HIPS reported by Bubeck et al. (1991), the rubbery particles initiated crazing in PLA matrix at the early stages of deformation. Crazing was accompanied by cavitation inside rubber particles, which further

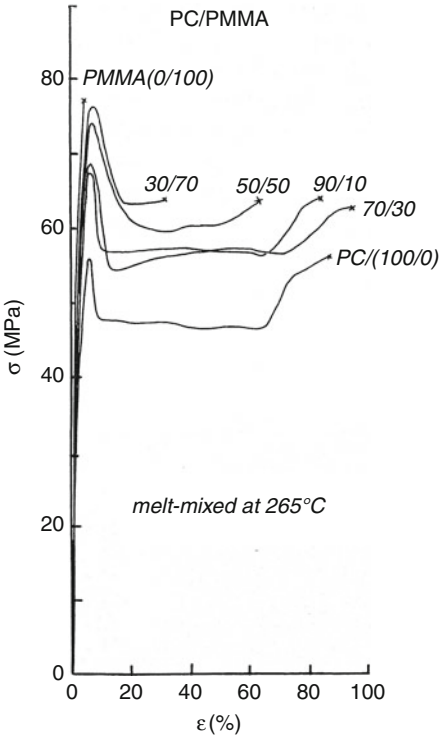

Fig. 11.5 The tensile stress–strain curves of the two-phase PC/PMMA blends, obtained at room temperature. The plots illustrate a stepwise transition of yielding by crazing characteristic of PMMA, to shear banding, characteristic of PC (From Kyu et al. (1991); reprinted with permission of Hanser Verlag)

promoted shear deformation of PLA. All three elementary mechanisms acting in the sequence appeared responsible for surprisingly efficient toughening of PLA by blending with a small amount of poly (1,4-*cis*-isoprene) – a major component of natural rubber. In comparison, plain PLA not containing rubber particles deforms initially via crazing, stronger at higher deformation rate and lower temperature, and then shortly undergoes shear banding. Separate cavitation is not then observed. The yield stress depends on the deformation rate and temperature; however, yielding is triggered and then controlled by the micromechanism of deformation which is activated first, at the lowest stress under given experimental conditions, selected from crazing, shear yielding or cavitation.

In Fig. 11.5, the stress–strain plots are depicted for a series of two-phase PC/PMMA blends with various concentrations. The phase-separated morphology was obtained by melt mixing. The position of the yield point on the stress–strain curves illustrates the stepwise transition of micromechanism of tensile deformation, characteristic of PMMA, which is crazing, to the mechanism of deformation, characteristic of PC – shear yielding.

As an example, the tensile deformation of polycarbonate/polyethylene blends is similar for a range of concentrations except for the magnitude of the yield stresses (Yee 1977). In this blend polycarbonate matrix undergoes strong yield shearing, and the decisive factor is the shear resistance of polycarbonate.

11.3.3 Necking

Crazes always tend to be perpendicular to the tensile deformation direction. They are typical dilatational zones of deformation. Since most of deformation is located in fibrils spanning the edges of a craze, a polymeric material is elongated, but its transversal size is not much changed. Hence, the neck is not formed. Cavitation usually helps to generate crazes and also does not cause formation of a neck. Necking is always associated with shearing and formation of shear bands whenever they are formed as a basic micromechanism of deformation or when they are triggered by crazes or cavities.

The way in which polymer blends change the shape upon deformation is not very different from other polymeric materials. The decisive role is played by micromechanisms triggered or stimulated by the presence of other components of the blend. The other key parameters are the temperature and strain rate. One may induce or inhibit shear banding by changing those process parameters and in that way control necking.

11.4 Toughening

11.4.1 Overview

The toughness is the property of resisting a fracture by absorbing and dissipating energy during deformation prior to ultimate fracture (Bucknall 1997). Strength, on the other hand, is the ability of the material to resist high stresses. Strengthening is usually achieved by suppression of plastic deformation mechanisms, sometimes to the extent that the material becomes brittle under normal loading conditions. On the contrary, high toughness can be obtained by promotion of plastic deformation, although most frequently at some tolerated loss of stiffness, strength, and creep resistance. Some reduction of stiffness, as in the case of rubber toughening, is acceptable if accompanied by substantial increase of toughness. A simple measure of toughness is the area below the stress–strain curve. Three typical cases are illustrated in Fig. 11.6: (1) very high strength by avoiding all defects and suppressing of plastic deformation (e.g., highly oriented fibers); (2) very high elongation at break, but low stiffness and strength, obtained by significant softening of the material (e.g., by plasticization); and (3) good stiffness and strength with a higher elongation, which can be obtained only due to widespread plastic deformation. The optimum case in toughening is, of course, the combination of relatively high value of stiffness, strength, and possibly high ultimate strain (curve (3) of Fig. 11.6). This requires some suppression of large, critical defects producing high stress concentrations leading to brittle fracture and promotion of extensive plastic deformation proceeding in large volume of the material, initiated at relatively high yield stress in numerous small, localized yield events. Plastic deformation must be stabilized by strain hardening to prevent excessive strain localization and premature crack propagation.

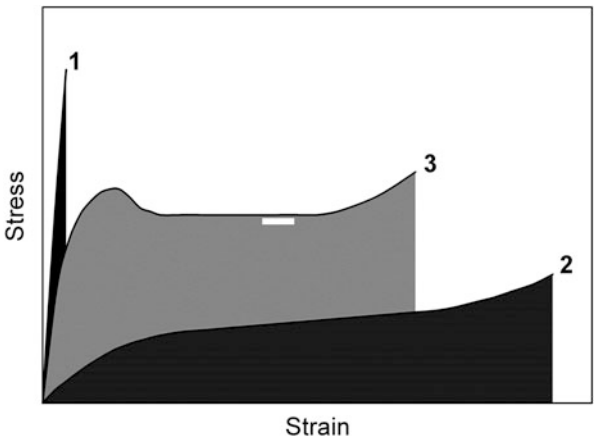

Fig. 11.6 Stress–strain curves illustrating toughness measured by the area below the curves. Curve (*1*) – high strength but low toughness; (*2*) low strength and high toughness; and (*3*) balanced good strength and toughness

Retaining strength and increasing plastic deformation are generally opposed requirements and are very hard to achieve simultaneously. In fact, the most popular and efficient practice of toughening by modification with elastomers (rubbers) suffers a drawback of a notable, sometimes serious, decrease in stiffness and strength of modified material due to relatively large content of a soft rubber (5–25 wt.%) (Bucknall 1977).

Toughness is one of the most complex mechanical properties. As it is greatly influenced by many morphological as well as micromechanical parameters, it is very difficult to control. Toughening can be realized by a particular morphology that permits lots of small local yielding events simultaneously in the entire volume of the material. This practically cannot be achieved in a homogeneous morphology, but only in heterogeneous one with specific morphology (e.g., small particles dispersed in the matrix) modifying the structure and structure-related micromechanical properties of the polymer at various scale levels. These modifications stimulate a large number of local plastic yielding and deformation processes on a nano- and microscale, all absorbing energy. They appear together in a large volume of the loaded material and result in large total energy absorption.

While many polymers can dissipate considerable amounts of energy through plastic deformation and appear tough at low deformation rate, they became brittle in the presence of notches and in high-rate impact loading. Therefore, toughening should be aimed not only to improve drawability at low rates but primarily to enhance the fracture resistance at impact conditions, especially in the most severe case when a notch is present in a thick sample. Consequently, the most frequent basis for assessment of toughening is the notched Izod (or Charpy) impact strength, determined in standardized impact tests of Izod or Charpy. This notched impact strength indicates the energy dissipated during impact fracture of relatively thick notched sample (according to the ISO 180 international standard of the Izod test, sample thickness must be greater than 3.2 mm and the striker speed $v = 3.5$ m/s).

11.4.2 Basic Principles of Toughening

11.4.2.1 Competition Between Plastic Deformation and a Terminal Process of Fracture

The toughness is administered by a competition between plastic deformation and a terminal process of fracture. The fracture is ultimately governed by stress and strain concentrations due to various structure imperfections like sharp notches, cracks, and other critical sized flaws or heterogeneities. Most commercial products made of polymers contain such imperfections. When the material is loaded, stresses become concentrated there, which results in high concentrations of strain and increase of the strain rate, all leading to very high localization of the deformation process. This localization can be high enough to trigger a brittle fracture. On the other hand, at some instances smaller, not critical, stress concentrations help also effectively to initiate the desired plastic deformation. Therefore, all these flaws and structure imperfections should be controlled precisely in quantity and size below critical in order to govern the fracture processes that limit material toughness. However, such a careful and precise control or management of the structure (flaws, imperfections) and surface (notches, scratches) of a product would be too difficult and expensive to be a practical solution for toughening, so that other measures to promote plastic deformation are necessary.

11.4.2.2 Intrinsic Brittleness

Argon (Argon et al. 2000; Argon and Cohen 2003) reasoned that with the exception of only a small class of pure metals, perhaps all other solids, including all unoriented solid polymers, are intrinsically brittle solids in the definition of Kelly et al. (1967) and will demonstrate brittle behavior at low temperatures and/or high strain rates, where a crack can propagate with little resistance, particularly in the presence of crack-like flaws and notches. While many polymers may appear quite tough at room temperature under low or moderate deformation rates, they became brittle at lower temperatures, in the presence of notches and in high-rate impact loading. Intrinsic brittleness denotes here that, in an otherwise flaw-free and homogeneous material, local tensile stress at the atomically sharp crack tip reaches the decohesion strength before local shear stresses concentrated at that crack tip initiate plastic flow (Kelly et al. 1967). Consequently, even the complete elimination of any notches, flaws, and other imperfection from the sample will not bring transformation of intrinsically brittle material to intrinsically ductile one, so that the approach seems of limited use for toughening. However, as already noted, intrinsically brittle polymers actually can exhibit a transition from brittle to ductile behavior at certain experimental conditions, e.g., higher temperature or lower deformation rate. That brittle-to-ductile transition is a crucial phenomenon in considering the toughness of polymers.

11.4.2.3 Brittle–Ductile Transition in Fracture

Stress–strain data collected for many rigid polymers deformed at various conditions revealed stronger dependence of the yield strength σ_y on temperature and strain rate

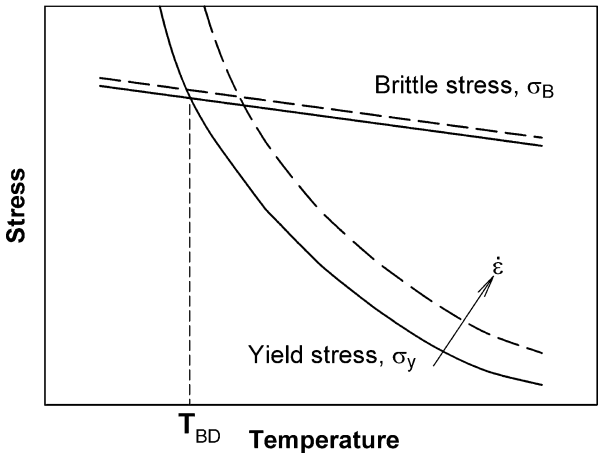

Fig. 11.7 Schematic representation of brittle-to-ductile transition in fracture (Davidenkov plot)

than that of brittle fracture strength σ_B (Vincent 1971): the yield stress σ_y decreases faster with increasing temperature T (typically by a factor of 10 between -180°C and room temperature) than the brittle stress (decrease only by factor of less than 2). The competition between the energy-absorbing plastic behavior characterized by the yield strength, having significant temperature and strain rate dependence, and the relatively temperature-independent brittle strength, governed by microstructural flaws or extrinsic imperfections, is illustrated schematically in Fig. 11.7 in terms of the well-known Ludwig–Davidenkov–Orowan criterion (Orowan 1949). This diagram, generic to intrinsically brittle solids, shows that for a given strain rate, there should be a transition from brittle to ductile behavior at a particular temperature T_{BD}, defined by the intersection of both curves – when increasing the test temperature above $T_{BD,}$ the yield strength becomes lower than the brittle stress, $\sigma_y < \sigma_B$, and the material changes its behavior from brittle to ductile. The dotted lines represent a higher strain rate resulting in a shift to higher stress values and, consequently, a shift of the brittle-to-ductile transition to a higher temperature (Vincent 1971). The brittle-to-ductile transition temperature is very sensitive to change in material parameters and test conditions, including specimen shape and size, temperature, or the deformation rate. For example, while the brittle strength relates to a tensile stress, the yield behavior responds only to a critical level of the effective (deviatoric) stress, σ_e. In the presence of sharp notches or other flaws, individual normal stress components can be substantially augmented by negative pressure, while the effective stress producing plastic flow remains equal to σ_e. This will result in a marked increase of the brittle-to-ductile transition temperature, as is well known in the notch impact testing.

11.4.2.4 Strategies and Options for Toughening

One of the possibilities to obtain tough polymeric materials is of course synthesis of new polymers, which would appear to be intrinsically ductile instead of intrinsically brittle. However, this is perhaps fundamentally impossible, or at least such attempts

are not economically justified. Analysis of the Davidenkov plot of Fig. 11.7 demonstrates that the only possibility of improving toughness of an intrinsically brittle rigid polymer is then by moving the brittle-to-ductile transition temperature well below the temperature range of the expected application of that material. This can be done either by an increase of the brittle strength, without altering plastic deformation mechanisms, or by reduction of the yield strength which makes plastic deformation easier. The first alternative can be realized through careful modification in both synthesis technology and processing to exclude critical sized flaws and extrinsic imperfections, as, e.g., dust particles. When such structural imperfections are well controlled in quantity and size and are limited to only subcritical size comparing to the size of the imperfections that control ultimate stress σ_B, the brittle strength can increase above the level of the initial yield strength. As a consequence, such polymer sample will tend to deform plastically. Once plastic deformation is initiated, it will result in molecular alignment due to advancing deformation and in neutralization of some of the effects of small imperfections still present in the structure which can eventually elevate, even substantially, the fracture toughness across the extension direction. This approach is always an option, but often is either not possible or technologically not profitable (Argon and Cohen 2003; Lin and Argon 1994). In such a case, the only practical choice left is to decrease the global plastic resistance of the modified polymeric material and shift in this way the brittle-to-ductile transition temperature T_{BD} to a lower temperature, below the temperature range of the expected applications. As a result, toughness of the material can be improved, even substantially, but inevitably in expense of some loss of its strength, and perhaps also stiffness and creep resistance. However, that sacrifice of stiffness and strength is often tolerable. Actually most of the approaches to toughening have followed this route, which when wisely practiced can be very effective (Argon 2013; Argon and Cohen 2003).

The other general rule in polymer toughening is to take advantage of the deformation mechanisms already operating in a particular polymer and only stimulate its response to loading to procure an extensive deformation and therefore large energy dissipation. In many approaches to polymer toughening, it has been assumed that incorporation of compliant rubber particles might impart toughness to a brittle polymer by a notion arising from the simple rule of mixtures, i.e., hoping that very flexible rubber could alleviate the brittleness of the matrix. However, in nearly every instance, when such practices are adopted, the beneficial effect of improved toughness actually does not arise from the added modifier directly, but rather through its indirect stimulation of very effective matrix response (Argon 2013), such as, multiple crazing in glassy polymers, providing widespread dilatational plasticity or an extensive plastic deformation promoted by significantly lowered plastic resistance due to conversion of a continuous solid material into porous (cellular) solid as a result of particle internal cavitation or debonding at the particle–matrix interface. This transition not only relieves volumetric strain but also greatly modifies the yield conditions for the matrix material and facilitates extensive yielding and plastic deformation of the matrix. Another example is cavitation-induced modification of the stress state allowing deformation of

preferentially oriented crystals within ligaments of the semicrystalline matrix between particles, the orientation of which had been induced by the presence of matrix–particle interfaces or by processing.

Glassy Polymers

Glassy polymers are frequently capable of dissipating locally significant amounts of energy per unit volume through viscoelastic–plastic flow, most frequently, highly localized either in crazes or thin shear bands. Bucknall (2000) estimated for crazable polymers, like polystyrene, that locally, within the craze or thin deformation zone, energy absorption per unit volume of a glassy polymer is high, on the order of 100 MJ/m^3! However, the amount of the material involved in the deformation is very limited, roughly to the thickness of the craze, i.e., single micrometers, and fracture is, therefore, essentially brittle. Such a small amount of material involved in the process of energy absorption through the plastic deformation occurring within a craze is too small to give the material a satisfactory fracture resistance and toughness. The problem is the acutest when the specimen or structure contains sharp notches, surface scratches, cracks, voids, or other structural imperfections that could cause a severe localization of the deformation, frequently so strong to end up with the brittle-like fracture, even due to a single craze. Therefore, strategies of toughening should be directed primarily towards maximizing the volume of the material participating in such deformation by multiplication of deformation events like crazes or deformation bands. Concurrently, some reduction of overall deformation resistance is needed to ease craze nucleation or initiate yielding as well as to avoid premature fracture of crazes, since failure in crazable polymers is caused by fracture of the craze matter. Many effective procedures have been advanced to reach toughening by the reduction of overall deformation resistance to promote new crazes and avoid premature craze fracture (Argon 2013; Bucknall 1977, 2000; Kausch 1983, 1990; Michler and Balta-Calleja 2012).

There are several methods known to improve the toughness of glassy polymers, e.g., by co-polymerization, by mixing with another miscible polymer, or by incorporation of a second phase through the blending process, like particles of other thermoplastic polymers or rubbers, fine particles of inorganic materials, or even very small voids. By dispersion of particles of the second phase, the energy dissipating deformation processes that are native to the matrix (either crazing or shear yielding) can be notably intensified and stabilized. The selection of the active deformation mechanisms depends primarily on the details of the matrix chemistry, and the modification by incorporation of the second phase usually does not alter it.

For glassy brittle polymers prone to crazing, such as PS or PMMA, apart from blending with non-crazable polymers miscible with them in order to alter the entanglement density and hence increase the craze flow stress above the distortional plastic resistance (Wellinghoff and Beaer 1978), the majority of approaches to their toughening were based on the incorporation of compliant heterogeneities, like soft spherical elastomer particles. Such particles appeared very effective in increasing the craze concentration by promotion of craze nucleation at lowered overall plastic resistance, as, e.g., in high-impact polystyrene (HIPS) or ABS. The rubbery

particles not only initiate crazes but also participate in their stabilization and act as craze terminators. This approach to toughening has been well developed practically and was described in many fine books and reviews (Argon 2013; Balta-Calleja and Michler 2005; Bucknall 1977, 1997, 2000; Collyer 1994; Kinloch and Young 1983; Michler and Balta-Calleja 2012). Very similar methods of toughness modification by incorporation of rubber particles are also widely used for toughening of semiductile glassy polymers that tend to deform by shear yielding. A further approach to additional toughening of crazable polymers by lowering the craze resistance through "plasticization-on demand" by low molecular weight diluent accelerating craze plasticity, which was prepackaged in inclusions, was also explored (Brown et al. 1989; Gebizlioglu et al. 1990). This method while appearing quite effective in certain ranges turns ineffective at high strain rates, mainly due to limitations of the stress-enhanced processes of case II diffusion which govern the local plasticization process (Argon et al. 1999; Piorkowska et al. 1993; Qin et al. 1999).

Thermoset Polymers

Epoxies and other thermoset resins are used widely as matrix materials in composites reinforced with long and short fibers as well as with fine particles and in other bulk applications. Therefore, the problem of alleviating their brittleness has attracted much attention. Incorporation of soft compliant particles into epoxies, in order to achieve a toughening effect similar to HIPS, has basically failed (Sultan and McGarry 1973) because of elementary reasons that these thermosets demonstrate notably in high plastic resistances due to cross-linking, which leads to a dense and robust molecular network. Consequently, they do not form crazes as PS or other glassy polymers do. Nevertheless, incorporation of well dispersed, small and compliant particles has demonstrated to be effective in promoting cavitation of particles under stress localized in planar zones (Sue 1992; Sue and Yee 1996) which give rise to craze-like dilatational bands similar to those observed on crazing of glassy polymers (Lazzeri and Bucknall 1995), a response similar to the cavitational craze process found in spherical-domain block copolymers (Schwier et al. 1985). It was also shown that use of rigid particulate fillers can also be quite effective through the crack pinning mechanism (Shaw 1994).

Semicrystalline Polymers

Many semicrystalline polymers, such as high-density polyethylene (HDPE), polypropylene (PP), polyacetals (POM), or polyamides (PA), are generally known to be quite tough at usual conditions of deformation, i.e., away from low temperatures and at moderate rates. Unfortunately, they also appear notch brittle, particularly under impact loading and at low temperatures. These and other semicrystalline polymers have been, however, successfully toughened by incorporation of elastomeric particles which, when present at certain conditions, triggered an extensive plastic deformation of the semicrystalline matrix through common crystallographic slip and interlamellar shear mechanisms. The primary function of rubbery particles here is again to bring about reduction of plastic resistance of the matrix, based on the same deformation mechanism as these are active already in the plain polymer.

Much of the recent work has been concerned on toughening of polyamides (Borggreve and Gaymans 1989; Borggreve et al. 1987; Dijkstra et al. 1994a; Gaymans 1994, 2000; Muratoglu et al. 1995a, c, d; Wilbrink et al. 2001; Wu 1985, 1988). These studies highlighted the correlation between toughness improvement and the critical interparticle distance, found in such blends. This interparticle distance was tried to relate mechanistically to a specific form of preferential "edge-on" orientation of lamellar crystals around particles that was shown to reduce markedly the overall plastic resistance of the polymer matrix (Muratoglu et al. 1995a, c, d). It was postulated that such a preferential local orientation could be obtained at the matrix–particle interfaces, not only for rubbery particles but also for other particles, including stiff particles of a mineral filler (Bartczak et al. 1999a, b, c). Considerable work was carried out on isotactic polypropylene (iPP) using both elastomeric particles (Jiang et al. 2000; Martuscelli et al. 1996; Liang and Li 2000; Liu et al. 2013; Nitta et al. 1998, 2005) and mineral filler (Chan et al. 2002; Cioni and Lazzeri 2010; Gong et al. 2006; Lazzeri et al. 2004; Thio et al. 2002; Zuiderduin et al. 2003; Dubnikova et al. 2004; Lin et al. 2010; Weon et al. 2006). Toughening of high-density polyethylene with both elastomeric and stiff particles was also studied extensively (Bartczak et al. 1999b, c; Deshmane et al. 2007; Yuan et al. 2009), and the effect of the critical interparticle distance was explored here, too.

11.4.3 Rubber Toughening

The invention of rubber toughening is one of the milestones in the history of the plastic industry (Bucknall 1977). In the late 1940s, high-impact polystyrene (HIPS) and acrylonitrile-butadiene-styrene (ABS) were developed by compounding butadiene rubber into PS or SAN, respectively. Both HIPS and SAN demonstrate a heterophase morphology with compliant micron-sized particles dispersed in the rigid matrix. The success of these products has led not only to the formulation of their improved grades, but also to the idea that the principle of rubber toughening could be applied to all other types of plastics, not only to crazable glassy polymers. Since then modification of polymers by blending them with other polymers, mostly compliant elastomers, to create a continuous matrix-dispersed inclusion morphology, commonly referred to as rubber toughening (due to rather historical reasons), has been successfully applied to many amorphous polymers such as PS, SAN, or PC (Hourston and Lane 1994; Parker et al. 1990), as well as to semicrystalline ones, including polyamides (Abate et al. 1992; Billon and Haudin 1997; Borggreve and Gaymans 1988, 1989; Borggreve et al. 1987, 1988, 1989a; b, Bucknall et al. 1989; Cimmino et al. 1986; Dijkstra and Gaymans 1994a, b; Dijkstra et al. 1994a, b; Epstein 1979; Flexman 1979; Gaymans 1994, 2000; Gaymans et al. 1990; Gaymans and Dijkstra 1990; Gaymans and van der Werff 1994; Gonzales-Montiel et al. 1995a, b, c; Hobbs et al. 1983; Janik et al. 1995; Kayano et al. 1997; Lu et al. 1993, 1995, 1996; Majumdar et al. 1994a, b, c, d, e; Margolina and Wu 1988; Muratoglu et al. 1995c, d; Okada et al. 2000; Oshinski et al. 1992a, b, 1996a, b, c, d;

Ramsteiner and Heckmann 1985; Scott and Macosko 1995; Takeda et al. 1992; Takeda and Paul 1992; Wilbrink et al. 2001; Wu 1983, 1985, 1987, 1988, 1989), polypropylene (Gensler et al. 2000; Harrats and Groeninckx 2005; Jang et al. 1984, 1985; Jiang et al. 2000, 2004b; Liang and Li 2000; Liu et al. 2013; Martuscelli et al. 1996; Nitta et al. 1998, 2005; Tiwari and Paul 2011; Utracki and Dumoulin 1995; van Der Wal et al. 1998), polyacetal (Flexman 1988; Kloos 1985; Xie et al. 1997), and thermoplastic polyesters such as polyethylene terephthalate and polybutylene terephthalate (Abu-Isa et al. 1996; Arostegui and Nazabal 2003; Brady et al. 1994; Cecere et al. 1990; Hage et al. 1997; Hale et al. 1999a, b, c, d, e; Hert 1992; Hosti-Miettinen et al. 1995; Hourston and Lane 1994; Hourston et al. 1991, 1995; Kanai et al. 1994; Kang et al. 1997; Laurienzo et al. 1989; Loyens and Groeninckx 2002, 2003; Mouzakis et al. 2001; Neuray and Ott 1981; Okamoto et al. 1994; Park et al. 2000; Penco et al. 1995; Polato 1985; Sanchez-Solis et al. 2000; Tanrattanakul et al. 1997). Rubber-modified polyamide 6,6 was the first marketed super-tough engineering blend (Epstein 1979; Flexman 1979; Wu 1987) with more than tenfold improvement in toughness when compared to the pristine parent polymer. Brittle thermosets like epoxies have also been toughened by blending with elastomers (Shaw 1994; Yee et al. 2000).

It has been established that the fracture toughness could be increased significantly by adding a relative small amount (usually from 5 to 25 wt.%) of a suitable elastomer to the thermoplastic matrix. Optimum particle size appropriate to toughen satisfactorily a rigid polymer varies, depending on properties of the host polymer (matrix), primarily on its inherent fracture mechanism, but is commonly within the range of 0.1–5 μm. As a general rule, brittle glassy matrices that tend to craze benefit more from large rubber particles size, typically between 2 and 3 μm. On the other hand, matrices that can absorb energy via shear yielding are effectively toughened with relatively small particles, on the order of 0.5 μm or less. Very fine particles, as, e.g., those smaller than 0.05 μm in blends based on polyamide, do not take part in toughening process (Gaymans et al. 1990; Oshinski et al. 1992a, 1996b), since they need higher stress to cavitate. The immiscibility and phase separation appear very important as a rubber dissolving in the matrix acts merely as a plasticizer, which reduces the glass transition temperature and hence seriously affects the stiffness but with only limited influence on toughness. Optimum commercial rubber-toughened glassy polymers (phase-separated blends), such as HIPS and ABS, demonstrate toughness about one order higher than the unmodified matrix material (PS, SAN). Similar, impressive results were obtained for elastomer-toughened semicrystalline polymers. Toughness of several glassy and semicrystalline polymers toughened by elastomers is given in Table 11.1.

The most important feature of rubber toughening is that the fracture of the toughened polymer is substantially postponed – material becomes ductile and undergoes extensive plastic deformation, usually according to the same mechanism as the pristine parent polymer, prior to reaching the failure limit – at the expense of a limited, yet usually tolerated reduction of stiffness, yield strength, and creep resistance (Bucknall 1977; Kinloch and Young 1983). This change from brittle to ductile behavior is possible due to the reduction of the overall plastic resistance of

Table 11.1 Toughness of selected polymers and their blends with rubbers

Matrix polymer	Predominant fracture mechanism	Typical notched Izod impact strength (J/m)	Polymer–rubber blend fracture mechanism	Optimum rubber diameter (μm)	Typical notched Izod impact strength of the blend (J/m)
PS	Crazing	21	Crazing	2.5	130
SAN	Crazing	16	Crazing and yielding	0.75	780
PMMA	Crazing	16	Crazing and yielding	0.25	80
POM	Yielding	110	Yielding	<0.5	910
PP	Yielding	20–40	Yielding	0.1–0.4	500–700
PA	Yielding	40–60	Yielding	0.1–0.4	1100

the matrix material below the brittle fracture strength. The desired changes in the deformation behavior and the balance of properties are achieved by a suitable dispersion of the soft elastomer or rubber in the polymer matrix, in the form of small spherical inclusions (particles). The dispersed particles can have a form of homogeneous or heterogeneous particles (as, e.g., "salami" particles in HIPS or core–shell particles (Cruz-Ramos 2000)).

It has been established that the use of phase-separated, well-dispersed elastomer with a suitable particle size allows to bring a large volume of the matrix into the process of plastic deformation, resulting in absorption of a significant amount of energy. Concurrently, rubbery particles frequently help to limit the growth and breakdown of voids and crazes and prevent in this way an initiation of a crack and premature failure. A number of quite different mechanisms of such toughening have been proposed in the past, but all of these rely on a dispersion of elastomer particles within a glassy or semicrystalline matrix. These have included energy absorption directly by rubber particles (Buchdahl and Nielsen 1950; Merz et al. 1956), energy dissipation upon rubber cavitation, or debonding at rubber–matrix interface (Sultan and McGarry 1973), matrix crazing (Bucknall 1977, 2000) or shear yielding (Newman 1978) or a combination of both (Bucknall 1977, 2000). The early hypothesis attributed toughness enhancement to dissipation of energy in the elastomeric phase either directly (Buchdahl and Nielsen 1950) or by the effect of bridging cracks by rubber particles (Merz et al. 1956). The amount of energy absorbed at impact was attributed to the sum of the energy to fracture the rigid matrix and the work to break the elastomeric particles encountered on the crack path. This hypothesis was dismissed soon since it was estimated that the total energy associated with the rubber deformation and break can account for only a small fraction of the observed enhanced impact energy (Bucknall 1978). Consequently, this mechanism can play only a minor role in toughening of rigid polymers. In the late 1960s Schmitt (1968) and Kesskulla (1970) proposed that the rubber particles can not only deflect or terminate cracks but can also act as stress concentrators, which efficiently initiate crazes in their very surroundings. Microscopic examination of deformed HIPS revealed formation of numerous crazes at

interfaces of rubber particles in their equatorial regions, which confirmed that hypothesis (Bucknall and Smith 1965). The role of rubber particles as stress concentrators, able to initiate extensive crazing, turned out crucial for toughening of the matrix. Bucknall proposed the mechanism of toughening by the so-called multiple crazing (Bucknall 1977), which became the basis of many toughening approaches developed later. It has been established and widely accepted that the deformation process involving crazing is initiated at surface of numerous elastomer particles, simultaneously in many sites of the matrix (Bucknall 1977, 2000; Collyer 1994). The primary function of elastomer particles is to modify the stress field in the surrounding matrix (stress concentrations, relief of the triaxial stress state upon cavitation), which can promote a widespread deformation of the matrix (Bucknall 2000). In rubber-modified crazable polymers, crazes are initiated under an applied tensile stress at points of maximum principal strain, which is typically near the equator of rubber particles (where maximum concentration of the stress is observed), and propagate outwards, normal to the direction of maximum tensile stress, although deviations may occur because of an interaction between the neighboring particle stress fields (Kinloch and Young 1983) (cf. Fig. 11.2). Craze propagation is terminated when another particle is encountered by a craze, which prevents the growth of very long crazes. As a result, a large number of small crazes are produced in polymer modified with rubber particles, in contrast to a small number of large crazes formed in the same polymer in the absence of elastomer. This mechanism is effective enough for absorption of large amounts of energy, which results in a substantial enhancement of impact strength of the material. Similar scenario of initiation of widespread plastic deformation at rubber particles (at points of maximum shear stress) holds also when the dominating deformation mechanism of the matrix is shear yielding rather than crazing.

The addition of rubber particles promotes energy absorption through the initiation of crazing or local yielding phenomena in the proximity of numerous particles, followed by an extensive plastic deformation that involves quite a large volume fraction of the sample. Such a toughening mechanism can be described by the following sequence (Bucknall 1977, 1997; Kim and Michler 1998b; Michler 2005; Michler and Balta-Calleja 2012):

1. **Stress concentration:** Tensile elastic deformation results in the generation of stress concentrations around the modifier particles, due to different stiffness of particles from the matrix. The stress concentration leads to the development of a triaxial stress in the rubber particles as well as in their surrounding within matrix.
2. **Voids formation:** Due to the stress concentration and/or thermal stress, a higher triaxial or hydrostatic stress builds up inside particles and gives rise to nano- or microvoids formation through cavitation inside particles or debonding at the particle–matrix interface which substantially modifies the local stress state (e.g., partially relieves triaxial stress in front of the crack tip) and matrix response to the stress (through a change of the sensitivity of the yield stress to mean stress). Due to void formation the volume strain is released and constraints imposed earlier by incompressible rubber particle on a neighboring matrix are relieved.

All of this can reduce the sensitivity of the material towards crazing and promote shear yielding.

3. **Local yielding:** Initiation of local yielding of the matrix occurs in the points of the highest stress concentrations, usually around the equatorial zone of a particle (plastic strain softening). The mechanism of that local yielding of the matrix can be either multiple crazing (fibrillated or homogeneous crazes), extensive shear yielding, or some combination of both. In semicrystalline matrices, local shear yielding proceeds by shear of crystals (crystal plasticity involving primarily crystallographic slip mechanisms) and amorphous layers (interlamellar shear) (Argon 2013; Oleinik 2003). If the shear yielding mechanism is active, then weak shear bands become to develop in the matrix between the voided/debonded particles at an angle of around 45° to the direction of the maximum principal tensile stress, simultaneously with continuous growth of voids.
4. **Extensive deformation stabilized by strain hardening** of the yield zone, mostly due to increasing matrix deformation, although stretching of the rubber phase to high strains can make a significant contribution to this, especially when the rubber is well bonded to the matrix and its content is high. The strain hardening stabilizes deformation process and prevents its localization which could result in a generation of crack and premature fracture. This stabilization is especially important when multiple crazing is the dominating mechanism of deformation. In specimens containing sharp notches or cracks, rubber particles can cause also crack tip blunting and consequently crack stop.

The selection of the dominant deformation mechanism in the matrix depends not only on the properties of this matrix material but also on the test temperature, strain rate, as well as the size, shape, and internal morphology of the rubber particles (Bucknall 1977, 1997, 2000; Michler 2005; Michler and Balta-Calleja 2012; Michler and Starke 1996). The properties of the matrix material, defined by its chemical structure and composition, determine not only the type of the local yield zones and plastic deformation mechanisms active but also the critical parameters for toughening. In amorphous polymers which tend to form fibrillated crazes upon deformation, the particle diameter, D, is of primary importance. Several authors postulated that in some other amorphous and semicrystalline polymers with the dominant formation of dilatational shear bands or extensive shear yielding, the other critical parameter can be the interparticle distance (ID) (the thickness of the matrix ligaments between particles) rather than the particle diameter.

11.4.3.1 Stress Concentrations

Particles dispersed in the matrix (as elastomer or other polymer inclusions in polymer blends or block copolymers, filler particles in composites, impurities) similarly to small voids initiate stress concentrations in loaded material due to the difference in stiffness between particle and the matrix. These stress concentrations are highly localized – they decrease rapidly with distance from particle or void (as r^{-3}), and at a distance of particle radius ($R = D/2$), the stress concentration almost disappears (see Fig. 11.8a). The intensity of stress concentration at the particle–matrix interface depends on the properties of both materials, as shear

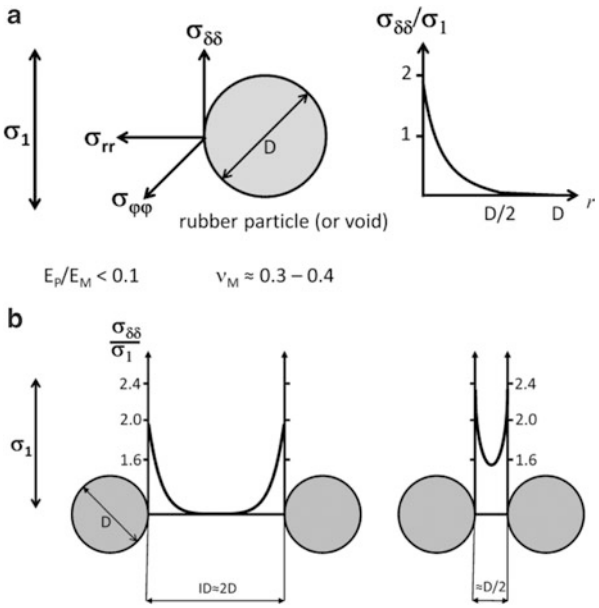

Fig. 11.8 (**a**) Stress components in the equatorial plane of the rubber particle under the remote tensile stress of σ_1 and the change of the tensile stress $\sigma_{\delta\delta}$ with the distance r from the interface. (**b**) Stress concentrations overlap between the close particles when the interparticle distance is about 2D (*left*) and D/2 (*right*) (Drawn after Michler and Balta-Calleja (2012))

moduli and Poisson's ratio of the particle and the matrix, respectively, while it does not depend on the particle diameter D. The elastic stress concentration at rubber particle–rigid matrix interface depends mainly on the ratio of the moduli of rubber and matrix G_R/G_M and reaches the maximum value of slightly above than 2 for $G_R/G_M < 0.001$ and is already near 2 for $G_R/G_M = 0.1$(Oxborough and Bowden 1974). This indicates that $G_R/G_M < 0.1$ is practically enough for high stress concentrations that can lead to effective toughening. However, the absolute size of the stress concentration region increases with increasing particle diameter D – the size of the equatorial stress concentration zone is approximately D/2. An initiation of the local deformation (e.g., through initiation of crazes) should be the most effective, when the size of the stress concentration region correlates with the typical size of the plastic zone (note that typical craze thickness in PS is in the range 0.2 – 1 μm and the most effective rubber particles in HIPS appear to be of similar size). If the particle diameter decreases, then the size of the stress concentration zone and also the size of initiated plastic zone decrease, too. The minimum size of the deformation zone, which is double the thickness of the typical transition layer between the plastically deformed material and its undeformed surrounding, determines roughly the smallest effective particle radius for craze initiation. The small rubber particles are, therefore, unable to initiate any plastic deformation of the matrix by crazing, although, as will be discussed in Sect. 11.5, it may appear effective in the promotion of the shear yielding.

The stress concentration fields of the neighboring particles overlap when the interparticle distance ID becomes small, approximately below the particle diameter. Rough estimations, assuming regular packing of uniform particles in cubic lattice,

demonstrate that average interparticle distance ID decreases to around D at the rubber volume concentration of $\phi \approx 10$ vol.% and to D/2 at $\phi \approx 15$ vol.% (Michler and Balta-Calleja 2012). The resultant stress field between particles can be estimated by simple superposition of stress concentration field of isolated particles, as illustrated in Fig. 11.8b. Due to that superposition the stress concentration at the equatorial plane of particles which are placed close enough (ID < D/2) is higher than for isolated particles, and the stress concentrations extend over the entire cross section of the matrix interparticle ligament.

An inevitable side effect of compliant elastomeric particles (or voids) dispersed in rigid polymer matrix is a reduction of the yield stress of the material. As a first approximation the Ishai–Cohen effective area model (Ishai and Cohen 1968), considering a unit cube with a spherical particle of radius R at its center, can be used for estimation of the reduction of the yield stress:

$$\frac{\sigma_y(\phi)}{\sigma_y(0)} = 1 - \pi R^2 = 1 - \pi\left(\frac{3\phi}{4\pi}\right)^{2/3} = 1 - 1.21\phi^{2/3} \tag{11.11}$$

where $\sigma_y(\phi)$ is the yield stress of a blend containing a volume fraction ϕ of voids or compliant inclusions with the radius R, and $\sigma_y(0)$ is the yield stress of the pristine matrix. Another dependence was found experimentally for rubber-toughened PMMA deformed in compression (cavitation inhibited) (Gloagen et al. 1993):

$$\frac{\sigma_y(\phi)}{\sigma_y(0)} = 1 - 1.375\phi \tag{11.12}$$

Although different, both Eqs. 11.11 and 11.12 demonstrate a clear dependence of the yield stress on volume fraction alone. The above equations apply to uniform distribution of particles. Significantly higher local stress concentrations, leading to a deeper reduction of the yield stress, and higher toughness can be expected when the rubber particles are not dispersed uniformly but form a pseudo-network morphology (Bucknall 2000).

When shear modulus of a rubber is much smaller than that of the matrix ($G_R/G_M < 0.1$), the high stress concentrations around rubber particles can additionally cause a significant increase of the deformation rate (Bucknall 2000), in addition to modification of the stress state reducing locally the yield stress.

At temperature below glass transition temperature of the elastomer, its modulus becomes similar to that of the matrix, i.e., $G_R/G_M \approx 1$. As a consequence, stress concentrations weaken substantially, and rubber particles are not able any more to reduce the yield stress enough to produce significant toughening. Additionally, the stress required to cavitate a particle that becomes glassy increases dramatically, which practically stops any internal cavitation of particles and also leads to the disappearance of the toughening effect. In impact tests, like Charpy or Izod, the minimum temperature at which any toughening can be observed is usually about 10 K higher than the actual T_g (Bergen 1968) due to relatively slow relaxation and

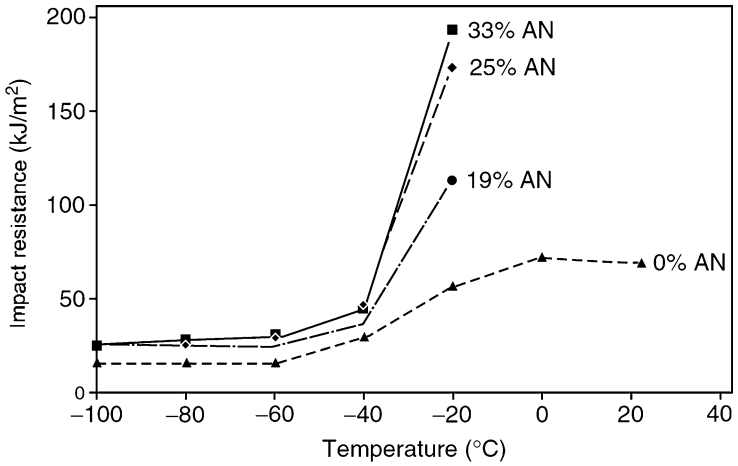

Fig. 11.9 Impact resistance of SAN of various compositions blended with PBA/SAN core-shell particle impact modifier (From Heckmann et al. (2005); reproduced with permission of Taylor and Francis)

high deformation rate. The effect is illustrated in Fig. 11.9 for different SAN copolymers toughened by blending with core–shell particles containing the poly (butylacrylate) (PBA) rubber core. One can observe here that toughness of the blends is enhanced only above the glass transition temperature of the rubber phase, which is below –40 °C, independently on properties of the matrix (the differences in toughening efficiency with changing composition of the matrix observed above T_g of the rubber are related primarily to the agglomeration habits of particles) (Heckmann et al. 2005).

In contrast to soft rubber particles, the stiff particles dispersed in a softer matrix (particles of stiff polymer or particulate filler, $G_R/G_M \geq 1$) respond on tensile loading with the concentration of the tensile stress in the polar regions ($\sigma_r/\sigma_o \approx 1.8$) and compressive stresses around particle equator. If the adhesion between the matrix and particles is poor, the concentration of tensile stress at the particle–matrix interface can result in debonding and formation of voids in polar region of particles. These voids become the source of new stress concentrations, similar to that around isolated void or rubber particle. Further elastic or plastic stretching of the matrix can lead to the expansion of these polar voids towards the equator and their eventual merging. This produces a single relatively large and elongated void around the particle. The voids created by debonding initiate stress concentrations, advantageous for matrix yield and deformation around the void equator. More frequently, however, due to other factors, the stiff particles debonded from the matrix initiate crack and followed by brittle fracture rather than yielding of the matrix.

In addition to the stress concentrations upon loading, which arise from a difference in stiffness of the matrix and elastomeric modifier, there are thermal stresses generated around particles due to the difference in thermal expansion

coefficient of the matrix and the elastomer. Upon cooling after melt processing, both the matrix and modifier phase contract, but with a different degree, which results in compressive or tensile radial stresses at particle–matrix interfaces. Elastomers shrink on cooling more than a glassy matrix, so that the tensile thermal stresses are produced, while, for stiff mineral fillers, which show expansion coefficient lower than the matrix, thermal stresses are compressive.

The thermal tensile stress developed in spherical rubber particle in the radial direction can be determined from the following relation (Beck et al. 1968):

$$\sigma_{rr} = \frac{2(\alpha_R - \alpha_M)\mathrm{E_R E_M}\Delta\mathrm{T}}{6(1-2\nu_R)\mathrm{E_R} + 3\mathrm{E_M}(1-\nu_M)} \tag{11.13}$$

where α is coefficient of thermal expansion, ν is Poisson's ratio, E is the Young's modulus, and the subscripts M and R refer to the matrix and rubber, respectively. It can be noted that similarly to intensity of stress concentrations, thermal stresses do not depend on the particle diameter. They depend strongly on Poisson's ratio, especially when the ν_R approaches the value 0.5. Thermal stresses of 1.3 MPa and 9.6 MPa can be estimated for a glassy matrix, like PS, and rubber particles with the Poisson's ratio of $\nu_R = 0.49$ and 0.499, respectively (Michler and Balta-Calleja 2012). The thermal tensile stresses acting at a rubber particle–matrix interface together with the radial component of stress concentrations can induce debonding at interface when particles show poor interfacial strength. For well-bonded particles, an isotropic tension (negative hydrostatic pressure), which is produced inside particle, leads to their increased volume dilatation. This results in an increase of free volume and hence easier initiation of cavitation as well as reduction of the glass transition temperature. A significant reduction of T_g by 12–19°C was observed experimentally for polybutadiene inclusions dispersed in polystyrene (Bates et al. 1983).

Thermal stresses generated in the matrix around rubber particles have a radial tensile component and tangential compressive components. These tangential components reduce the effective stress concentration in the equatorial zone of the rubber particle.

11.4.3.2 Particle Cavitation

Rubber particle cavitation, i.e., formation of holes inside of rubber inclusions, is one of the most important ways in which toughened polymer can respond to tensile stress. Although recognized already in 1970s, this phenomenon was initially believed to be merely a secondary process, triggered by extensive shear yielding or crazing of the surrounding matrix, and not significant for toughening. With increasing experimental evidence, that opinion has gradually changed and there has been a growing understanding and acceptance of cavitation importance. Now it is widely accepted that cavitation within rubber particles is, in fact, a decisive step in toughening (Argon 2013; Argon and Cohen 2003; Bucknall 2000, 2007a, b; Bucknall and Paul 2009, 2013; Michler and Balta-Calleja 2012). Although

cavitation itself involves little energy absorption, it allows for the subsequent enhanced, sometimes massive, deformation of the matrix, which appears the primary source of the energy absorption.

In the middle of thick sample or in front of the crack tip, the stress state is triaxial (plane-strain conditions). It occurs also in front of the notch in Izod and Charpy notched samples. Such a stress state makes plastic deformation more difficult than the biaxial stress under plane-stress conditions and favors brittle fracture as the surrounding stressed material resists the lateral contraction which is needed to maintain a constant volume on deformation. The rubber particles respond to a high level of triaxial stresses produced by near plane-strain conditions with cavitation or sometimes with debonding, if the rubber–matrix interfacial adhesion is low. Both processes create voids either inside rubber particles or at their interfaces, respectively. Cavitation manifests with the easily observed stress whitening in the deformation zone (Ban et al. 1988; Gaymans et al. 1990). The volume strain experiments demonstrated that rubber cavitation begins at low strains (2–6 %) (Borggreve et al. 1989a; Bucknall et al. 1989) under triaxial stress when the matrix material is still in the elastic region.

The stress needed to initiate cavitation of an elastomer particle is a function of the cohesive energy density of that elastomer, chain entanglements, and presence of any inhomogeneities inside the elastomer particle (as, e.g., precavities, small crystallites, or foreign impurities) (Gent 1990; Kramer 1983; Wu 1989). The number of entanglements depends on the molecular weight and its distribution of the elastomer. Cavitation becomes easier for lower molecular weight and narrows its distribution (Brown and Ward 1983). Any defect or heterogeneity, if present inside the elastomer particle, can result in a significant reduction of the cavitation stress of that particle. The cavitation stress decreases further with an increasing inhomogeneity (defect) size to the micron-scale length (Gent 1990). However, it is frequently observed that rubber particles dispersed in the matrix, even those much smaller than 1 μm, cavitate quite easily under dilatational stress. This implies that there must be another mechanism for nucleation of nanovoids and cavitation, which is independent on the presence of occasional micron-scale defects and is inherent in the behavior of rubbers themselves, perhaps at the level of individual chain segments. Bucknall reasoned that since resistance to dilatation in rubbers arises almost entirely from weak van der Waals interactions, and shear occurs easily, it could be expected that under high triaxial tensile stresses, the distribution of polymer chains within the expanded volume of the elastomer become unstable, giving rise to nucleation of the nanovoid (Bucknall 1997). Calculations of Lazzeri and Bucknall (1993) and Bucknall et al. (1994) confirmed that hypothesis and demonstrated that even for particles as small as 0.2 μm in diameter, the energy barrier for cavitation is quite low and can be overcome easily with the aid of thermal energy.

Impact tests of pre-cavitated samples of rubber-toughened Nylon (pre-cavitation obtained by a slight tensile pre-straining at low deformation rate) demonstrated their impact behavior very similar to samples without initial cavities (Gaymans 1994). Similar results were reported by Dasari et al. (2010) for polypropylene and PP/$CaCO_3$ nanocomposites pre-cavitated during processing. They observed that the

voids in both plain iPP and composite acted in a similar way as the cavitating rubber particles in rubber-toughened polymer systems; i.e., the preexistent voids expanded at the early stage of the PP matrix deformation and subsequently triggered large plastic deformation of the surrounding matrix in the form of isolated and domain-like deformation zones (Dasari et al. 2010). The above findings demonstrate that the cavitation process itself, although crucial for toughening, is not a major energy-absorbing mechanism. It is rather the plastic deformation of the matrix, which follows the cavitation step.

Upon formation of voids, the constraints imposed on the matrix are locally eased, and the triaxiality of the stress is relieved, at least partially, around each cavitated elastomer particle ahead the notch or the running crack (Bucknall 1977; Donald 1994; Kinloch and Young 1983). Due to a notable reduction of constraints, the stress state around these particles, especially within thin matrix ligaments between neighboring cavitated particles, can be converted from a triaxial to a nearly biaxial one (plane-stress conditions). When the stress concentrations are present around voided particles (they actually become even slightly stronger than prior to internal particle cavitation), the change of the stress distribution from plane-strain to plane-stress conditions might be advanced enough to depress locally the yield strength and initiate plastic deformation. Shear yielding is favored by plane-stress, whereas crazing is preferred under plane-strain conditions (constraints reduced, yet not fully dismissed). Therefore, the primary effect of cavitation is usually an enhancement of shear yielding mechanism in the matrix (Bucknall 2000; Bucknall et al. 1989). Formation of cavities results in local decrease in the hydrostatic stress component and a corresponding increase in the deviatoric (shear) component, and a higher stress concentration factor (Bucknall et al. 1989). Another important result of cavitation is conversion of the material from a continuous solid to the porous (cellular) structure, which demonstrates modified sensitivity to the mean stress on yielding. Consequently, the matrix can yield easier, even at the plane-strain conditions ahead of the notch. This feature will be discussed further in Sect. 11.5.3.

Once the rubber particles have cavitated, the surrounding matrix is free to yield and stretch in a way it was previously impossible. The deforming shell of the matrix enclosing cavitated particle extends biaxially, which increases the volume of the cavitated particle. If the particle is isolated, that deformation of the adjacent matrix is limited by constraints imposed by yet undeformed surroundings. However, if particles are closely spaced, the thin matrix ligaments between them may become yielded fully across, which results in extensive plastic deformation in large volume of the sample and evolution of the shape of the cavitated rubber particle from spherical to ellipsoidal or sausage-like shape, elongated in the direction of local principal stretch due to high extension of the matrix ligaments around particle (Muratoglu et al. 1995d), as illustrated in Fig. 11.10.

It is sometimes suggested that rubber particles lose completely their ability to sustain a stress once they have cavitated. This is actually not true except only for a very few cases. First exception is when voids are formed along particle–matrix interfaces due to debonding (poor adhesion). Transfer of stress between the matrix

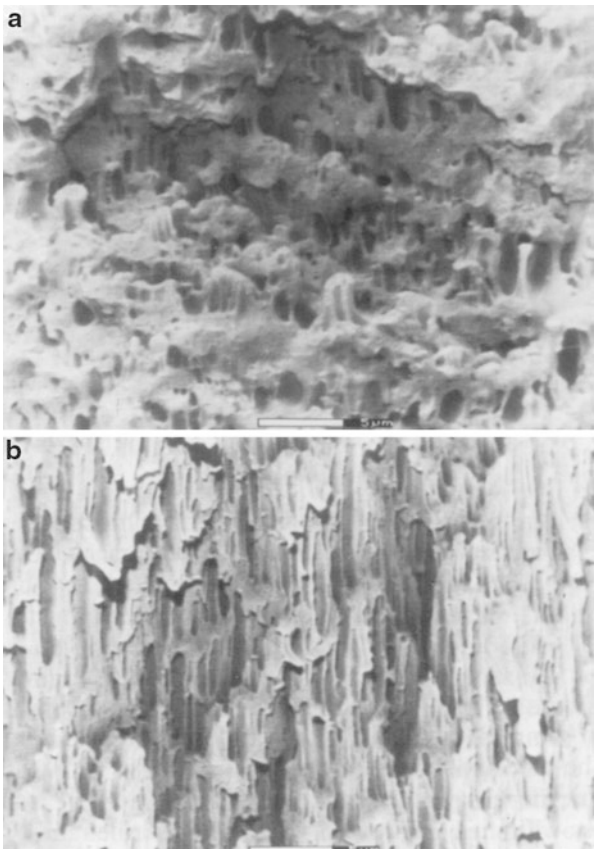

Fig. 11.10 SEM micrographs of cavitated tensile sample of polyamide 6,6 modified with 19 wt.% EPDM rubber: (**a**) stress-whitened zone outside the neck region and (**b**) stress-whitened zone inside the neck region. The scale bar represents 5 μm (From Muratoglu et al. (1995d); reproduced with permission of Elsevier)

and such debonded particles is very limited. The other case is when crazes formed away from rubber particle intercept it upon their growth. In such a case, a significant lateral contraction must accompany elongation of the particle in the applied stress direction. As this contraction proceeds, debonding at the particle/craze interface occurs, and the void is created. This void grows then under increasing load, which can lead to premature craze breakdown and subsequent crack initiation.

For homogeneous rubber particles with high interfacial strength (strong adhesion) to the matrix, their cavitation results in the formation of the void in the center of the particle. When a void is formed, the rubber particle transforms into a continuous thick spherical shell around the void, in which the stress and strain are no longer uniform. As the void grows, the rubber shell is expanded by biaxial tension. The strain is distributed in this shell nonuniformly: the inner face of the shell must deform most, close to the ultimate stretch, which results in substantial strain hardening, whereas the outer layer, contacting the matrix, deforms much less. The expanding rubber shell bonded to the matrix can transmit load and also contribute to strain hardening of the entire material with an advance deformation of the matrix and the rubber, initiated by its cavitation. However, further expansion

of the void can lead eventually to the rupture of the most strained rubber segments in the inner layer close to the void, and consequently the entire shell can fail by progressive tearing (Bucknall 2000).

In all cases, a premature rupture of the rubber will restrict extensive deformation of the matrix as it leads to the formation of voids larger than critical, resulting in fast crack initiation and propagation. When rubber rupture occurs later, after some advance of matrix deformation, the orientation-induced hardening of the matrix can alleviate to some extent the effect of such flaws and the material is allowed to deform further.

Frequently fibrils are formed inside the rubber particle, especially in cross-linked or heterogeneous particles, as, e.g., particles with stiffer sub-inclusions or core–shell morphology. These fibrils, anchored both sides at particle–matrix interfaces or bridging a particle stiff core/inclusion with the matrix matter at the interface, are clearly load-bearing elements of the structure, which make a major contribution to the strain hardening. The fibrillar morphology of cavitated particle is the most effective for stress transfer and contribution in strain hardening that prevents premature fracture since stress and strain across fibrils are uniform and can be high, simultaneously in all fibrils. The experimental evidence indicated that the stress in the fibrils formed in core–shell particle reached much more than 30 MPa (Starke et al. 1997). Bucknall (1997) claimed that a low-level cross-linking of the rubber is desirable for homogeneous rubber particles, as it allows a still early cavitation of the particles and high strains by fibrillation, while the fibrils would have high strength. Excessive cross-linking, also that caused by photodegradation effect (e.g., in outdoor applications), can lead, however, to a marked reduction or even loss of the impact strength due to stiffening of the rubber and impediment of cavitation.

Various morphologies of cavitating rubber particles were considered by Kim and Michler (Kim and Michler 1998a, b). Depending on the original morphology of the particle (homogeneous, heterogeneous with inclusions, core–shell) and adhesion between particle and the matrix, which can be modified broadly by addition of various compatibilizers, different modes of cavitation or debonding can be observed: from single-site cavity in the center of a homogeneous inclusion, through multiple internal cavitation, to multiple cavitation with formation of fibrils in the shell of the core–shell particle or around debonding particle which had been moderately bound to the matrix, cf. Fig. 11.11. The most favorite situation is when rubber forms fibrils rather than a single smooth shell around cavity since contrary to a single shell around void, fibrils are strained uniformly and therefore can transmit higher stress and participate effectively in strain hardening (in a similar manner as fibrils in a craze), which stabilizes advancing deformation of the matrix and prevents premature initiation of a crack. The presence of fibrils controls also the size of the microvoids and prevents expansion of the void to the overcritical size which could quickly end up in crack formation.

Observations of rubber cavitation and growth of the voids offer an additional explanation for the enhanced shear yielding of the matrix (Donald and Kramer 1982). The presence of many closely packed particles which can cavitate enables

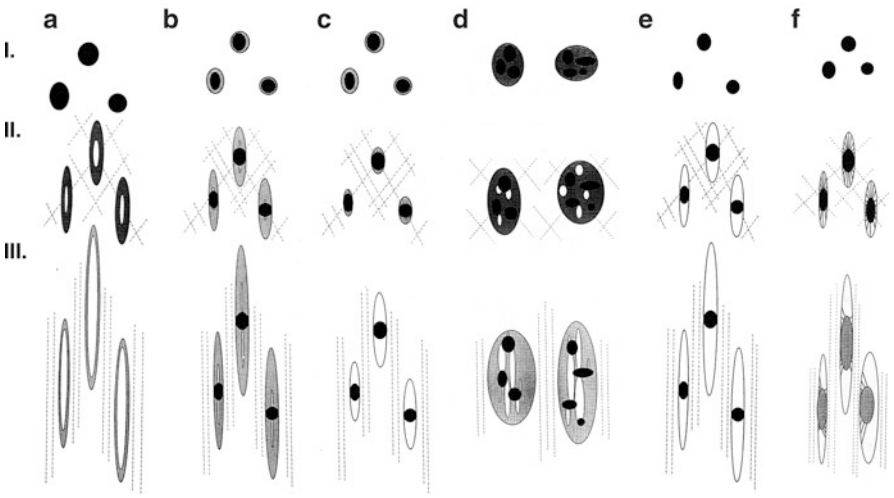

Fig. 11.11 Various morphologies produced by cavitation and debonding: (**a**) single cavitation in homogeneous particles (e.g., PA/BA blend); (**b**) single cavitation in heterogeneous particles (blend PP/ethylene–propylene block copolymer with low content of ethylene); (**c**) fibrilized cavitation (PP/PA/SEBS-g-MA blend); (**d**) multiple cavitation in heterogeneous particles (PP/LLDPE/SEBS-g-MA blend); (**e**) single debonding (PP/ethylene–propylene random copolymer blend); and (**f**) fibrilized debonding at the interface (PP/EPDM blend). *I* – initial morphology, *II* – low strain, *III* – high strain (Adapted from Kim and Michler (1998b); with permission of Elsevier)

relief of the local buildup of hydrostatic tension produced by localized shear process (proceeding at constant volume). Thus, possibly soon after initiation of cavitation and the development of some initial shear yielding, the constrained conditions might be fully relieved by expansion of numerous cavities distributed densely over the process zone, which changes the structure of the material into cellular, in which thin cell walls are under plane-stress, so that even the relatively thick bulk specimens may behave as if the matrix were everywhere under plane-stress conditions. Shear deformation occurs more readily under biaxial rather than at triaxial stress state, and cavitation of the rubber particles therefore favors local shear yielding deformation. However, if the matrix does not shear readily, but like polystyrene is far more prone to crazing, then this mechanism is not available and rubber cavitation followed by expansion of created voids is more damaging.

11.4.4 Core–Shell Particles

A very effective way of toughening is the use of core–shell particles instead of homogeneous rubber particles. The core–shell particles were commercially introduced as PVC impact modifiers in 1958 and since that time, their use has continuously expanded into new toughening applications, which now include a wide variety of engineering polymers (Cruz-Ramos 2000). In contrast to other impact

modifiers, as homogeneous rubber particles, which are most frequently formed by high shear forces during blending of a molten matrix polymer with an elastomer, the core–shell particles are preformed by emulsion polymerization prior to mixing with the host polymer. This makes a major difference between core–shell particles and other types of impact modifiers: the size and size distribution of core–shell particles are set during the synthesis process and continue the same after they are introduced and dispersed in a matrix of a host polymer, whereas elastomer particles formed in the blending process have the final size depending heavily on processing conditions.

The typical architecture of core–shell particles consists of a soft core, made up of a rubbery polymer, surrounded by relatively thin shell of rigid polymer that is grafted to the core. The core in commercial materials is usually a cross-linked rubber based on poly(butyl acrylate) (PBA), poly(butyl acrylate-co-styrene), or poly(butadiene-*co*-styrene). It provides the soft second phase that induces toughening similarly to homogeneous rubber particles in conventional blends. The shell of the particles consists of a polymer that is chemically grafted onto the core and generally is much stiffer since it has a much higher glass transition temperature than rubber of the core. Typical polymers used for a shell in commercial products are homo- and copolymers of PMMA and styrene–acrylonitrile copolymers (SAN) (Cruz-Ramos 2000). Two basic functions of the shell are (1) to prevent adhering of particles from one to another during the drying after emulsion polymerization process and (2) to provide a good dispersion and compatibility of particles with the matrix of the host polymer – the shell gives the particle a layer that physically binds the rubber core to the surrounding matrix and prevents particle coalescence upon blending.

There are several advantages on the use of core–shell particles as impact modifiers. The main is a relatively easy control of the matrix–particle morphology of the final blend. The particles, preformed prior to blending, have defined size and narrow size distribution, and dispersing them within the matrix does not alter these, independently on the processing conditions. Good and uniform particle dispersion can be achieved relatively easy. The shell, grafted to the rubbery core, provides usually sufficient bonding between particles and the matrix. Due to versatility of the emulsion polymerization, the particles of various sizes can be produced and selected for blend formulation according to particular demands. All this allows for a relative easy modification and fine-tuning of the impact strength and other mechanical properties of the material. Furthermore, the small size with a narrow size distribution and the uniform spatial distribution in the matrix make possible formulation of transparent impact-modified blends. The mechanism of the toughness improvement is the same as in the case of materials modified by homogeneous rubber particles, although cavities in core–shell particles are frequently stabilized by the core–shell structure, and this prevents coalescence of voids of neighboring particles, in which coalescence would lead to critical flaw and crack initiation (Michler and Bucknall 2001).

Another type of the core–shell particles is by multilayer particles that consist of a glassy core, a thin intermediate rubber layer, and an outer glassy shell (Lovell and

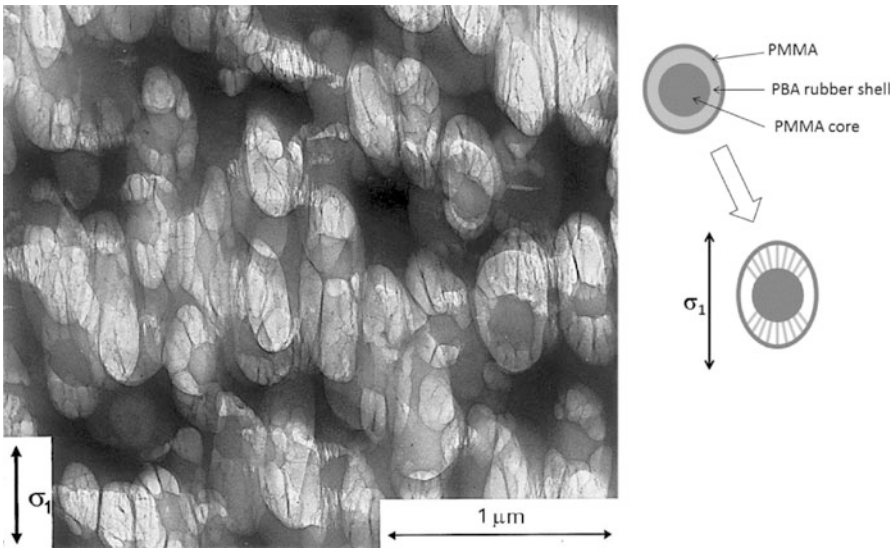

Fig. 11.12 TEM micrograph of fibrillar cavitation of the core–shell multilayer particle in the SAN/PBA blend; tension direction vertical (From Starke et al. (1997); reproduced with permission of Springer)

El-Aaser 1997; Michler and Bucknall 2001; Shah 1988; Starke et al. 1997). An example is the particle with the core of cross-linked PMMA, ca. 180 nm in diameter, poly(butyl acrylate-*co*-styrene) (PBA) rubber shell of approx. 40 nm thickness, and an additional outer thin-grafted PMMA shell added for improved bonding with the matrix (Michler and Bucknall 2001; Starke et al. 1997). The overall particle diameter was approximately 260 nm. Compounding of particles with SAN results in acrylonitrile–styrene–acrylate copolymer. Due to rigid core and relative low amount of the rubber, such multilayer particles with rigid core allow for better balance between toughness and stiffness of the final toughened material. The other extremely important benefit is that cavitation of such particles proceeds via nucleation of many small nanovoids in thin intermediate rubber shell. With subsequent expansion of these voids, a quite regular fibrillar morphology develops within the rubber shell with elongated fibrils anchored well to the rigid core and the outer shell (rubber had been grafted to both core and the outer shell). The morphology of cavitated particles is shown in Fig. 11.12.

As discussed in the previous section, such extended fibrils are effective load-bearing elements of the structure, which make a major contribution to strain hardening. Multiple cavitation and formation of fibrils results in uniform stress and strain distribution in these fibrils, which prevents their premature fracture, stabilizes cavities, and allows for effective stress transfer across the rubber shell. All of this brings a significant contribution of particles in strain hardening and stabilization of the matrix material extensive deformation. The stretching of fibrils is very similar to drawing of fibrils from the walls of a craze and generates

substantial stress, which can be estimated even above 100 MPa at room temperature for highly elongated fibrils (Michler and Balta-Calleja 2012). The experimental evidence indicated the stress in the fibrils formed in core–shell particle exceeded well 30 MPa (Starke et al. 1997). Such a high stress transmitted to the hard polymer core can be high enough to involve its yielding, which if happen would provide an additional effective mechanism of energy absorption upon impact. The plastic deformation of the core of particles was indeed observed by Michler and Bucknall (2001).

Taking all above into account, the multilayer core–shell particles seem to be suited very well for toughening of rigid polymers, as they provide a relatively good balance between toughness and stiffness of the impact-modified material, in contrast to modification with homogenous rubber inclusions, which frequently leads to unacceptable deep reduction of stiffness of toughened material. However, to get full benefit of potential of modification with core–shell particles, these particles must be carefully designed (with respect to particle composition, layer thickness, overall diameter, selection, or adequate chemical modification of the outer layer to ensure good adhesion to the matrix) and custom made for a particular blend and its application.

It is well known that the particle size needed to toughen a rigid polymer depends on inherent fracture mechanism of the matrix. In general, brittle glassy matrices that tend to craze benefit more from large rubber particles, of diameter exceeding 1 μm. Smaller particles, below 0.5 μm diameter, are, in turn, effective in toughening matrices in which shear yielding is a main deformation mechanism. Since typical core–shell particles have a diameter well below 1 μm (usually in the range of 0.25–0.5 μm), they are used most frequently for toughening of non-crazable polymers, in which shear yielding is a dominant deformation mechanism. Core–shell particles were used as effective impact modifier in many polymers, including PC (Kayano et al. 1996; Lovell and El-Aaser 1997), PMMA (He et al. 1998; Laatsch et al. 1998; Lovell and El-Aaser 1997; Lovell et al. 1993; Shah 1988; Vazquez et al. 1996), PVC (Lutz and Dunkelberger 1992), PA (Aerdts et al. 1997; Kesskula and Paul 1994; Majumdar et al. 1994d), PBT, and PET (Brady et al. 1994; Hage et al. 1997). Preparation of larger particles by emulsion polymerization to be used for toughening of crazable polymers, like PS, received also some amount of attention (Cruz-Ramos 2000).

11.4.5 Rigid Particles (Fillers)

The idea of toughening with rigid particles instead of soft rubber particles has attracted great attention because incorporation of rigid particles would contribute to a greatly enhanced stiffness of the modified material in addition to possible toughness improvement, while modification with elastomers always leads to an inevitable reduction in modulus. The rigid particles can be either particles of a particulate filler or particles of another polymer, stiffer than the matrix polymer. The possibility of simultaneous enhancement of both toughness and stiffness would be a significant advantage of rigid particles over traditional rubber toughening.

Stiff particles dispersed in the polymer matrix increase its modulus, and if there is strong adhesion between particles, they can also increase the yield strength. However, in the case of low or missing interfacial strength, debonding appears on loading readily while still in the elastic region as stiff particles are unable to deform to any significant degree. The microvoids created around particles due to debonding should not form immediately upon application of stress as this may reduce the elastic modulus. Ideally, debonding should occur at stress only slightly lower than the yield of the pristine matrix. As it is often the case, it prevents any increase of the yield strength of the system, unwanted for toughening. The microvoids created at interfaces act as stress concentrators, like cavitated elastomer particles. Widespread particle debonding in the deformation zone close to notch root or fracture surface transforms this zone into a porous solid and helps to relieve plastic constraints imposed earlier on the matrix by rigid and hardly deformable particles (Bartczak et al. 1999b, c; Muratoglu et al. 1995a, d; Thio et al. 2002; Tzika et al. 2000; Wilbrink et al. 2001) and make yield easier due to modification of yield sensitivity to the mean stress. The related change in the stress state can initiate local yielding process and consequently lead to an improved toughness. This however can be achieved only in the case of small, semi-equiaxed, and homogeneously distributed particles, since large particles create large voids when debonding, with the disadvantage of void coalescence and formation of cracks of overcritical length. On the other hand, very small particles, well dispersed in the matrix, require high mean stress for debonding, while agglomerates of such very small particles, which are difficult to destroy in processing, can rupture easily on loading and produce sharp cracks reaching quickly the critical length (Kim and Michler 1998a, b; Michler 2005; Michler and Balta-Calleja 2012). Clustering of rigid particles can also result in the formation of quite large unbounded inclusions, which, similarly to very large particles, upon separating from the matrix, can act as supercritical flaws that trigger a brittle response (Argon and Cohen 2003).

In the case of filler particles in shape of fibers or platelets (as, e.g., organoclays), oriented randomly, the distribution of voids created at their interfaces on loading can be not homogeneous enough to produce a uniform porous structure needed for successful toughening. Therefore, toughening with anisotropic rigid particles seems more difficult than with semi-equiaxed ones.

It has been suggested (Bucknall 1978; Kinloch and Young 1983; Lavengood et al. 1973) that rigid particulate fillers might be used to increase the toughness of brittle glassy polymers by initiating multiple crazing. Under an applied stress, rigid particles do induce tensile stress concentrations in the matrix and debond from the matrix readily, which generate stress concentrations sufficient to initiate crazing, yet near the particle poles rather than the equator, as it was for rubber particles. On the other hand, due to limited adhesion between the rigid particulate filler and the matrix, the filler particles do not appear particularly as effective craze or crack terminators. To act as efficient terminators, the second phase has to be adequately bonded, while rigid particles when called to do this job may have already become debonded from the matrix. Consequently, rigid particles of particulate fillers debonding from the matrix prior to yield point demonstrate low ability to act as

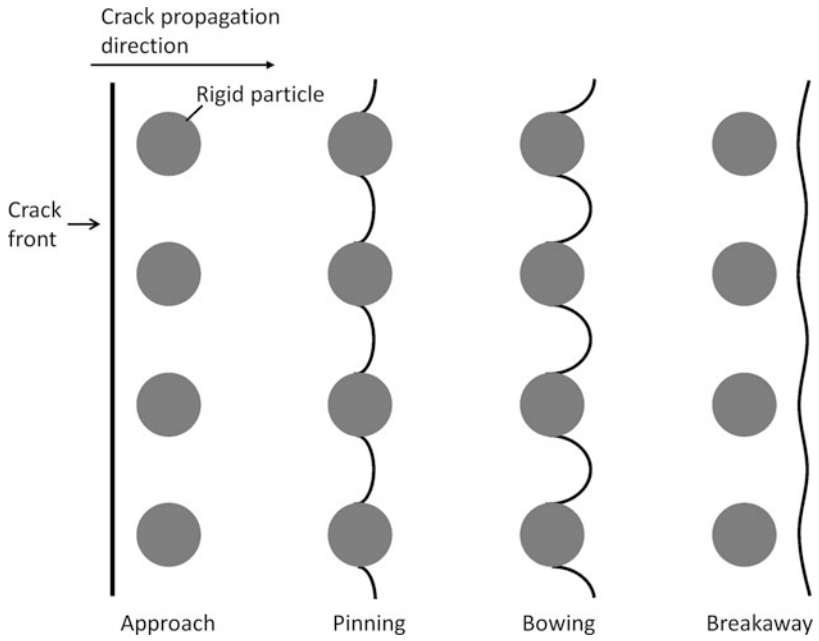

Fig. 11.13 Schematic representation of the crack pinning mechanism (Drawn after Kinloch and Young (1983))

effective craze and crack terminators, which results in much poorer toughening performance when compared with well-bonded rubber particles.

Several investigations have demonstrated that incorporation of particulate fillers such as silica or alumina trihydrate can improve the toughness of thermosets, like cross-linked epoxies (Shaw 1994). The mechanism considered responsible for an increase of impact resistance is different than that of rubber particles effective in promoting cavitation under stress localized in planar zones (Sue 1992; Sue and Yee 1996), giving rise to craze-like dilatational bands (Lazzeri and Bucknall 1995). Particles of filler are expected to impose stress concentrations in epoxy matrix due to a substantial modulus difference between particle and the matrix. However, this is usually not considered as significant. Instead, a mechanism based essentially on the impeding characteristics of the particles was proposed (Evans 1972; Green et al. 1979; Lange 1970). The mechanism, called the crack pinning mechanism (Lange 1970), postulates that a propagating crack front, when encountering an inhomogeneity, as, e.g., well-bonded filler particle, becomes temporarily pinned at that point. An increase in load increases the degree of bowing between pinning points caused by adjacent particles, resulting in both a new fracture surface and an increase in the length of the crack front, as illustrated schematically in Fig. 11.13. These processes will absorb some amount of energy and therefore lead to an increase of the fracture toughness of the resin. Although incorporation of the filler can lead to a noticeable toughness improvement, this is generally much smaller than

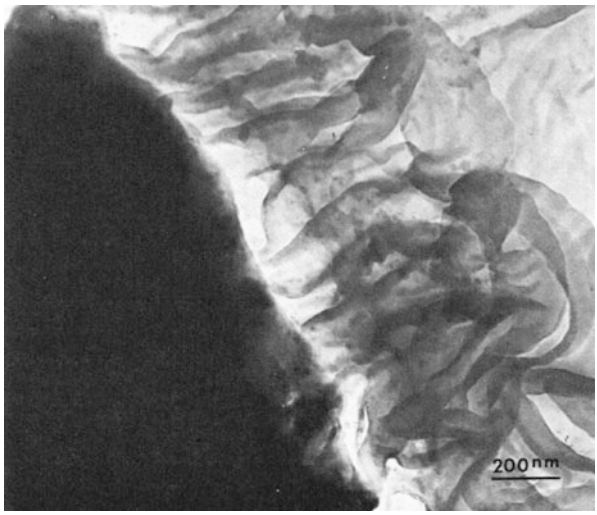

Fig. 11.14 TEM micrograph of polyethylene thin film with a particle of $CaCO_3$ (seen as a continuous *black* region in the left-hand side). Crystalline lamellae seen as *black ribbons* when oriented edge on against interface (From Chacko et al. (1982); reproduced with permission of Wiley)

that obtained with cavitating elastomer particles. Thus, in the direct comparison, rubber modification would prevail, although a substantial stiffness increase accompanying toughness enhancement is a major advantage of rigid particle toughening and this method may be preferred for some applications.

Another possibility of improvement of impact strength with rigid particles was demonstrated for notch-sensitive semicrystalline polymers, like polyamides, polyethylene, or polypropylene. Many studies investigating toughening of polyamides with elastomer particles (Borggreve and Gaymans 1989; Borggreve et al. 1987; Dijkstra et al. 1994a; Gaymans 1994, 2000; Muratoglu et al. 1995a, c, d; Wilbrink et al. 2001; Wu 1985, 1988) emphasized the correlation between toughening and the critical interparticle distance. This distance was correlated with a specific form of preferential crystal orientation around particles (with crystalline lamellae oriented locally edge on with respect to the particle–matrix interface and with the low energy/low plastic shear resistance (001) crystallographic plane oriented parallel to that interface). Such an orientation was shown by Muratoglu et al. (Bartczak et al. 1999a, b, c; Muratoglu et al. 1995a, c, d) to reduce markedly the plastic resistance of the layer of polymer matrix around the particle due to possibility of activation of the easiest crystallographic slip system, (001) [010] of polyamide crystals (Lin and Argon 1992). Bartczak et al. (1999a, b, c) postulated that such a preferential local orientation can be obtained at the matrix–particle interfaces, not only in the system consisting of PA matrix and rubbery particles but also for other polymers and particles, including stiff particles of other polymers or mineral fillers. They demonstrated it for polyethylene modified with various elastomers and $CaCO_3$ particles of various sizes. Figure 11.14 presents the TEM micrograph illustrating an oriented layer formed in polyethylene around the particle of $CaCO_3$.

Bartczak et al. (1999a) proposed that the driving force for such a unique crystal orientation around particle is the secondary nucleation at the interface, enhanced

due to the difference in interfacial energy when lamella grows in bulk and in the edge-on contact with the substrate, here the particle surface. This energy difference results in faster growth of those lamellae which maintain contact with particle surface and are oriented edge on, and consequently in the formation of the preferred crystal orientation in a thin layer around particle. Thickness of this specially oriented layer of reduced shear plastic resistance is defined for a given polymer, while independent on the type and size of particles. It was determined approximately 150 nm for Nylon 6 (Muratoglu et al. 1995a) and around 300–400 nm for HDPE (Bartczak et al. 1999a). When the interparticle distance in the blend is reduced below double the oriented layer thickness (300 nm for PA or 800 nmm for PE, respectively), the matrix ligaments consist almost entirely of the oriented material of low plastic shear resistance. They create then easy deformation paths, which percolate the sample. Upon sample loading and particle debonding, the stress concentrations induced by microvoids initiate easily the plastic deformation of crystals within these ligaments just relieved from constraints by debonding of neighboring particles, massive formation of microvoids, and then conversion of the material within deformation zone into a cellular solid. Deformation of ligaments results in an extensive plastic deformation in a large volume of the sample and high energy absorption, exactly the same as in the case of toughening with cavitating rubber particles. It was demonstrated experimentally that a big jump of impact resistance (approximately one order of magnitude) occurred in blends of PE with various elastomers and PE filled with stiff $CaCO_3$ particles, in all systems for the same critical interparticle ligament thickness of approximately 800 nm (Bartczak et al. 1999b, c), which indicates that the same toughening mechanism has to be activated for rubber and rigid particle toughening.

Toughening with rigid particles has two significant advantages over rubber toughening: (a) First, it leads to simultaneous improvement of both toughness and stiffness, in contrast to rubber toughening, which always reduces material stiffness, as illustrated in Fig. 11.15. (b) The other benefit of toughening with rigid particles is its insensitivity to the test temperature (again in contrast to their rubber toughened counterparts). As mentioned earlier, in Sect. 11.4.3.1 at temperature below T_g of the elastomer used for toughening, the stress required to cavitate a particle which became glassy increases dramatically. This practically stops any internal particle cavitation and leads to disappearance of the toughening effect (rubber is usually well bonded and cannot debond from the matrix). In impact tests, the minimum temperature at which any toughening can be observed is usually even about 10 °C higher than actual T_g (Bergen 1968). This is not the case of rigid particles toughening as it relies on particle debonding which does not depend on temperature dramatically. As a result, semicrystalline polymers toughened with rigid particles remain tough in a wide range of temperatures down to around T_g of the matrix polymer (Bartczak et al. 1999c) – cf. Fig. 11.16. Therefore, for polymers with matrices of low glass transition temperature, toughening with stiff fillers has a clear advantages over rubber modification.

There are several prerequisites for successful toughening with rigid particles: particles must be small enough and with narrow size distribution in order to prevent

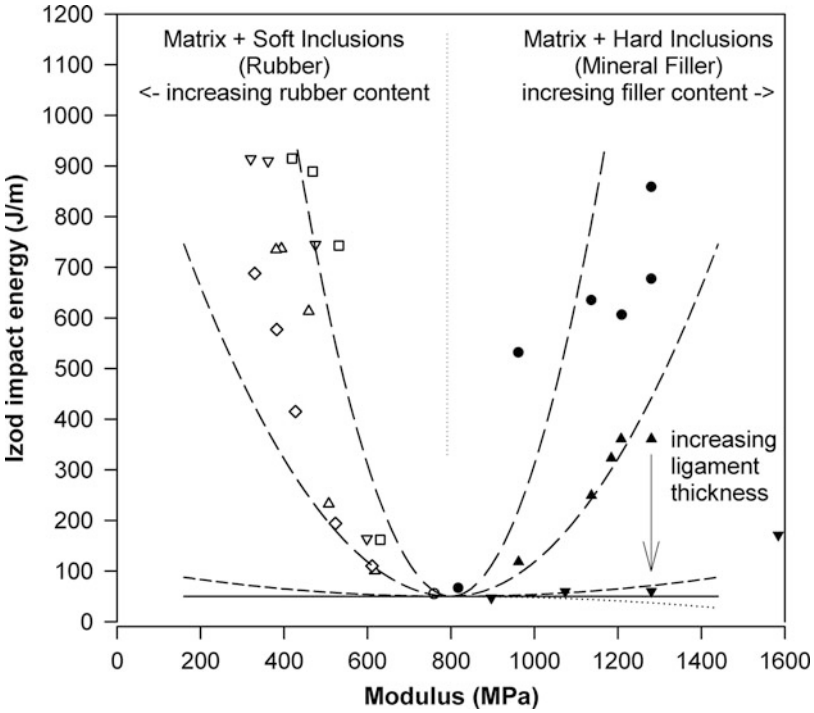

Fig. 11.15 Schematic plot of possible routes of toughening of semicrystalline polymers with soft particles (e.g., rubber, *left* branch) and hard particles (e.g., mineral filler, *right* branch) (From Bartczak et al. (1999c); reproduced with permission of Elsevier)

crack initiation at the microvoids of overcritical size formed around large particles due to their debonding, and particle dispersion must very good and their spatial distribution uniform to avoid clustering and to obtain an optimum interparticle distance, below the critical, set by matrix properties. The aspect ratio of particles should be close to unity to avoid very high stress concentrations (Zuiderduin et al. 2003). Moreover, adhesion between filler and the matrix must be kept as low as possible to allow easy particle debonding prior to matrix yielding. However, as the debonding stress increases with decreasing particle diameter, the filler particles cannot be too small since very small particles will not debond prior to the matrix yield and the mechanism will not work. Another negative consequence of very small particles is their tendency to form agglomerates or clusters. The composite suffers severely from clustering of rigid particles into quite large unbounded inclusions, which upon separating from the matrix often act as supercritical flaws, triggering a brittle response (Argon and Cohen 2003). Loose agglomerates can also rupture across, giving rise to the development of a sharp crack, cf. Fig. 11.17.

All above show that there is only a limited range of average size and size distribution of particles to be used for toughening; moreover, particles must have

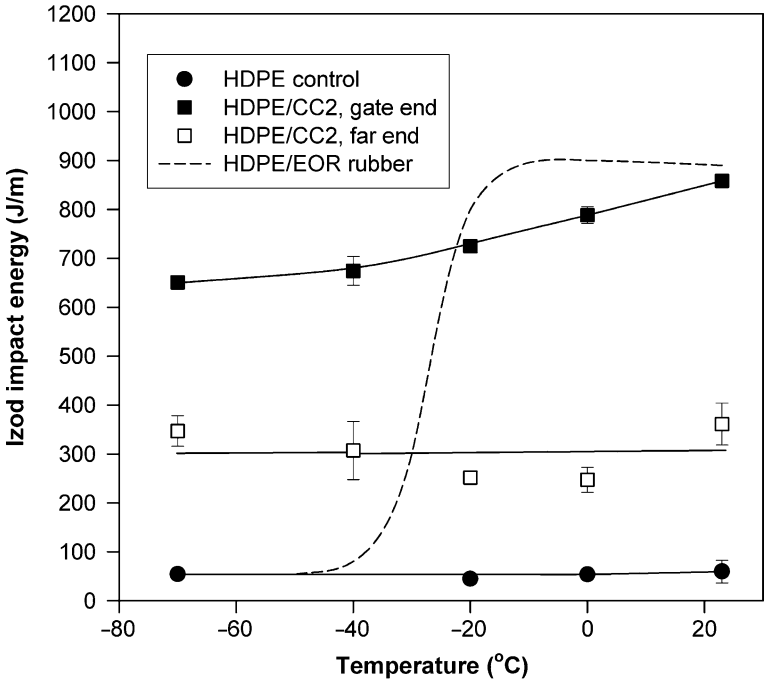

Fig. 11.16 The dependence of notched Izod impact energy on temperature for the HDPE/$CaCO_3$ (80:20vol./vol.) and HDPE/ethylene–octene rubber (78:22 vol./vol.) blends (From Bartczak et al. (1999c); reproduced with permission of Elsevier)

an appropriate surface treatment that promotes good dispersion but at the same time highly reduces or completely eliminates adhesion to the matrix. Furthermore, there is a strong need of optimum processing protocol, utilizing very high shear forces in order to obtain a very good and uniform particle dispersion, which is essential for toughening effect. A nonuniform dispersion causes some ligaments may become too thick to do deform easily. Particle clustering often results in supercritical flaws. All these effects can lead to material embrittlement instead of expected toughening. The method of toughening with rigid particles, with its potential and strong limitations, was analyzed in detail by Argon and Cohen (Argon and Cohen 2003).

Successful toughening with rigid particles, mainly of $CaCO_3$, was reported for high-density polyethylene (Badran et al. 1982; Bartczak et al. 1999b, c; Deshmane et al. 2007; Fu et al. 1993; Lazzeri et al. 2005; Lei and Zhou 2000; Liu et al. 2002; Wang et al. 1997; Yuan et al. 2009), polypropylene (Bartczak 2002; Chan et al. 2002; Cioni and Lazzeri 2010; Gong et al. 2006; Kamal et al. 2012; Lazzeri et al. 2004; Lin et al. 2008, 2010, 2012; Thio et al. 2002; Weon et al. 2006; Yang et al. 2006, 2007, 2009; Zuiderduin et al. 2003), Nylon 6 (Ou et al. 1998; Wilbrink et al. 2001), POM (Bartczak 2002), and aliphatic polyketone (Zuiderduin et al. 2006). On the other hand, a need of fulfillment of all severe preconditions mentioned above makes toughening with rigid particles very difficult, which in turn

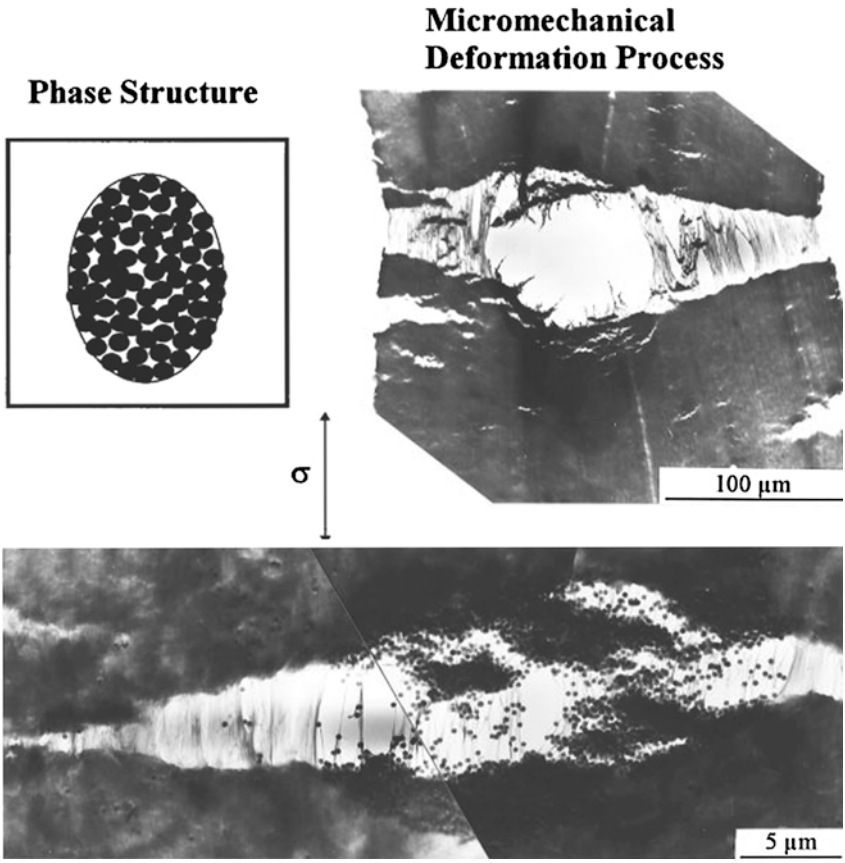

Fig. 11.17 Characteristic deformation structure depending on the phase structure of PP filled with SiO_2 particles demonstrating tendency to agglomeration (From Kim and Michler (1998a); reproduced with permission of Elsevier)

makes often the modification with rubbery particles more attractive in industrial practice.

The described above toughening mechanism of semicrystalline polymers proposed by Muratoglu was criticized by Hwang et al. (2006) who, on the basis of computer simulation, suggested that the observed preferred orientation of crystals which led to toughness improvement of studied samples might result from, or be significantly amplified by, oriented crystallization induced by shear during sample injection molding, possibly much enhanced within interparticle ligaments, rather than by interfacial energy differences postulated by Bartczak et al. (1999a, b, c). It was also questioned on other grounds by Bucknall and Paul (2009, 2013), who remarked inconsistency of the Muratoglu's hypothesis with recent work by Huang et al. which shows that the impact behavior of 80/20 rubber-toughened blends based on the amorphous polyamide (Zytel 330) is very similar to that of 80/20 blends

based on semicrystalline PA6 (Huang et al. 2006a, b; Huang and Paul 2006), which may suggest that crystalline structure and morphology of the matrix are inessential for toughening with particles.

11.5 Plastic Deformation Mechanisms in Toughened Polymer Blends

11.5.1 Overview of Micromechanical Behavior

As it was already discussed in Sect. 11.4.3, the modification of a rigid thermoplastic polymer with rubber particles promotes energy absorption through the initiation of local yielding in the close proximity of particles, followed by the extensive deformation involving large volume of the sample owing to dense arrangement of rubber particles. This deformation mechanism can be described by the following sequence (Bucknall 1977, 1997; Kim and Michler 1998b; Michler 2005; Michler and Balta-Calleja 2012):

- Buildup of stress concentrations around particles and negative pressure inside
- Generation of microvoids due to cavitation or debonding of rubber particles that alters the stress state in the surrounding and modifies matrix response by reducing locally the yield stress
- Initiation of local yielding by an accessible mechanism (crazing, shear yielding)
- Extensive plastic deformation stabilized by strain hardening, resulting in large energy absorption

The dominant mechanism of deformation depends mainly on the type and properties of the matrix polymer, but can vary also with the test temperature, the strain rate, and the morphology, shape, and size of the modifier particles (Bucknall 1977, 1997, 2000; Michler 2005; Michler and Balta-Calleja 2012; Michler and Starke 1996). Properties of the matrix determine not only the type of the local yield zones but also the critical parameters for toughening. In amorphous polymers with the dominant formation of crazes, the particle diameter, D, is of primary importance, while in some other amorphous and in semicrystalline polymers with the dominant formation of dilatational shear bands or intense shear yielding, the interparticle distance ID, i.e., the thickness of the matrix ligaments between particles, seems to be also an important parameter influencing the efficiency of toughening. This parameter can be adjusted by various combinations of modifier particle volume fraction and particle size.

It is now widely appreciated that independently on the actual mechanism of plastic deformation dominating the matrix response and brought about by modification with rubber particles, the critical step in toughening is generation of microvoids, common for all toughening mechanisms (Argon 2013; Argon and Cohen 2003; Bucknall 2000, 2007a, b; Bucknall and Paul 2009, 2013; Michler and Balta-Calleja 2012), not only in rubber toughening but also in toughening with rigid particles (Argon 2013). Cavitating or debonding particles facilitate the development of voids and then activation of dilatational yielding in the deformation zone

close to the fracture surface. The primary role of cavitating/debonding particles is to alter the stress state in the surrounding matrix. Such a change enables matrix to yield at moderate stress, even under plane-strain conditions (see Sect. 11.5.4) which initiate an extensive plastic deformation of the matrix (Bucknall 2000). This is possible because generation of microvoids by closely spaced cavitating/debonding particles converts the material in the deformation zone from continuous solid into a porous (cellular) solid, which is generally the most effective way to reduce plastic resistance of the material (Argon and Cohen 2003).

Depending on matrix characteristics and test conditions, its deformation, which has been triggered by the formation of microvoids, can proceed according to several mechanisms, including multiple crazing, shear yielding, or combination of both, or crystal plasticity mechanisms supported by shear of interlamellar amorphous layers, if the material is semicrystalline. It is not completely clear whether cavitation of rubber particles is the necessary precondition for multiple crazing. It seems that the triaxial stress at equatorial regions of rubber particles induced by stress concentrations may be alone sufficient to induce crazes. However, cavitation increases additionally the stress concentration (as the ratio of moduli of cavity and the surrounding, determining the stress concentration, falls to 0) and this must enhance craze initiation. Therefore, cavitation increases the efficiency of toughening by multiple crazing and perhaps allows to obtain the desired effect at lower rubber content. On the other hand, particle cavitation must certainly occur in order to induce the shear yielding of the matrix – prior to cavitation the extrinsic constraints and those imposed on the matrix deformation by well-bonded rubber particles do not allow for dilatation (as rubber is nearly incompressible), which in turn highly restricts deformation by shear, especially when sample is thick or in front of the notch or crack tip. The microvoids developed by cavitation help to alleviate these constraints and convert the stress state within interparticle ligaments from plane-strain towards plane-stress conditions, which corresponds to an increase in the shear component and thereby to reduction of the yield strength. Additionally, as the volume strain is released, the material sensitivity towards crazing is reduced. All of this might facilitate shear yielding in ligaments between particles, much less constrained now.

11.5.2 Criteria of Rubber Particle Cavitation

As discussed in the previous section, cavitation of rubber particles is practically necessary for toughening. In this section, some conditions important for cavitation to occur will be discussed.

The criteria for cavitation in polymers modified with rubbers were modeled by Lazzeri and Bucknall (Bucknall et al. 1994; Lazzeri and Bucknall 1993, 1995). They are based on energy release rate principles similar to those used in fracture mechanics. Void nucleation and expansion in elastomer particles are accompanied by the formation of a new surface, significant stretching of the surrounding layers of elastomer, and the stress relaxation in the adjacent matrix. All of these are driven by

the release of energy stored both in the particle itself and in the surrounding rigid matrix material. The model was simplified and did not account for any additional effects resulting in an energy barrier restricting void formation. The essential condition for void growth is that the volumetric strain energy release rate dU/dr must be greater than the rate at which energy is absorbed in increasing the surface area and stretching the adjacent layers of rubber. Considering the blend as an assembly of small volume elements, each consisting of a spherical elastomer particle of radius R which is surrounded by a rigid elastic shell of the outer radius Q (particle volume fraction is $\Phi_p = R^3/Q^3$), the total energy released upon cavitation can be calculated from the difference of potential energy of that element prior to and after cavitation (Lazzeri and Bucknall 1993). The simplified example in which a rubber particle of radius R is held at a fixed volume strain ε_v and forms a single void of radius r_{vd} can be described with the following equation:

$$U_p(r_{vd}) = \frac{2}{3}\pi R^3 K_R \left(\varepsilon_v - \frac{r_{vd}^3}{R^3}\right)^2 + 4\pi r_{vd}^2 \Gamma_r + 4\pi r_{vd}^3 G_R f\left(\lambda_f\right) \tag{11.14}$$

where $U_p(r_{vd})$ is the potential energy of the rubber particle; r_{vd} is the radius of the cavity in the center of the particle; ε_v is the current volume strain of the particle, including the void; R is the radius of the particle; G_R, K_R are the shear and bulk moduli of the rubber; Γ_r is surface energy of that rubber; and λ_f is the extension ratio of the rubber at fracture in biaxial tension. The function $f(\lambda_f)$, which typically has a value close to 1, represents energy lost in tearing the thin layer of rubber that is very close to the expanding void surface, where $\lambda > \lambda_f \approx 10$.

Calculations based on this model demonstrated that the main parameter controlling cavitation is the size of rubber particles – the critical volume strain at cavitation, ε_v(cav), increases as the particle size is decreased, principally because the strain energy release rate depends on the size of the local volume element. The model predicts that when the shear modulus of the rubber is small, the relationship between logarithms of critical volume strain at cavitation ε_v(cav) and the particle diameter D should be approximately linear (Bucknall 1997, 2000), which, in fact, was confirmed by experimental data of PVC blends reported by Dompas et al. (1994a). They demonstrated that a decrease of particle size caused an increase of critical strain to a maximum value $\varepsilon_v(\text{cav}) = 0.0128$, where the specimens did not cavitate any longer and yielded before any cavitation happened. The observed dependence of log(ε_v (cav)) on log (D) was almost linear and could be fitted with a straight line calculated with Eq. 11.14, although an upward shift in experimental ε_v(cav) was seen, related most probably to several simplifying assumptions used for model formulation (Bucknall 2000). There are strong indications that similar relationships between D and ε_v(cav) to the described above, predicted by Eq. 11.14, apply to other polymer blends containing soft rubber particles ($G_R \approx 0.1$ MPa) (Bucknall and Paul 2009). Apart from size, the other important factors which affect cavitation are the surface energy Γ_r (energy needed to create a new surface inside the rubber particle) and the shear modulus of the rubber G_R,

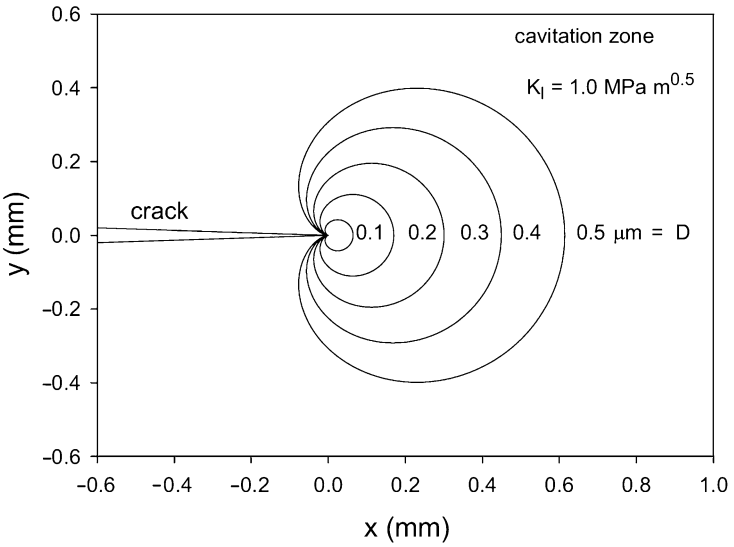

Fig. 11.18 Map of cavitated zone in plane-strain region, showing dependence of zone boundary on the particle diameter when $K_I = 1$ MPa $m^{0.5}$. Critical mean stresses calculated with bulk modulus K = 3GPa and data of Dompas et al. (Dompas and Groeninckx 1994) (From Bucknall and Paul (2009); reproduced with permission of Elsevier)

determining the work done in biaxial extension of the rubber shell upon void expansion. On the other hand, any additional energy barrier restricting formation of cavities, which was not taken into account in model calculations, would additionally increase critical volume strain and corresponding stress.

Figure 11.18 illustrates the effects of particle size on cavitation around a crack tip, calculated by Bucknall and Paul (2009) using Eq. 11.14 with $K_I = 1.0$ MPam$^{1/2}$ and ε_v(cav) from the line fitting the data of Dompas et al. (1994a). For fine particles the cavitated zone is very small, yet with increasing particle diameter, D, this zone expands distinctly outwards from the crack tip. Such behavior helps to explain observations that very small particles are not effective in toughening (Gaymans et al. 1990; Oshinski et al. 1992a, 1996b), which was usually interpreted as a result of an inability of very fine particle to cavitate. The results of calculations of Bucknall and Paul presented in Fig. 11.18 show that the difference in efficiency of toughening by fine and large particles can be explained without making an assumption that very small particles are unable to cavitate. According to these authors, problems arise simply because critical volume strain ε_v(cav) and stress are very high for fine particles, which limits noticeably the size of the cavitated yielded zone, which raises the probability of brittle fracture. In the limit, ε_v(cav) becomes so high that the void-free blend would yield under plane-strain conditions at the very high shear stress, still before reaching the particle cavitation stress. However, as the stress needed for craze nucleation is lower than the stress needed for shear yielding and so reached first, a craze will develop from the notch tip instead of shear zone

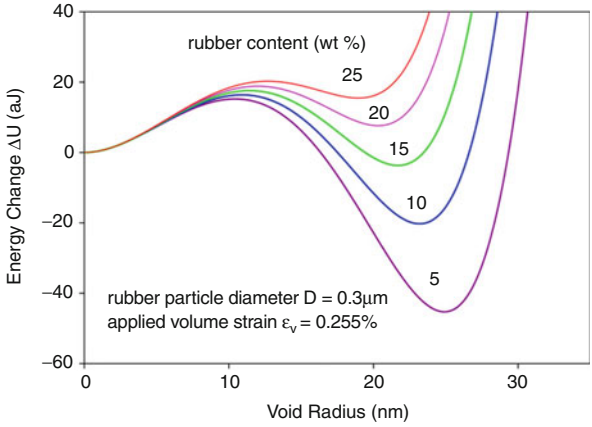

Fig. 11.19 Energy curves for a cavitating rubber particle, calculated using Eq. 11.14 in blends with D = 0.3 μm, $\Gamma_r = 35$ mJ/m^2, and $\varepsilon_v = 0.255$ %, showing the effect of varying rubber particle concentration at a critical particle size. Energy in aJ (atto-Joule; 1 aJ = 10^{-18} J) (From Bucknall and Paul (2013); reproduced with permission of Elsevier)

and a crack will be initiated before a significant amount of energy has been absorbed in ductile deformation by shear (Bucknall and Paul 2009). For a typical blend (Young's modulus E = 2 GPa and Poisson's ratio of $\nu = 0.4$), a stress intensity factor K_{IC} of 1.0 MPam$^{1/2}$ corresponds to a fracture surface energy $G_{IC} = 420$ J/m^2, which is sufficient to form and rupture a single mature craze. By contrast, increasing D (above about 0.03 μm (Bucknall and Paul 2009)) enables the particles to cavitate before reaching the yield point and consequently reduces the shear yield stress, which at this stage becomes a function of the volume fraction of cavitated particles (see Sect. 11.5.4).

Further calculations made by Bucknall and Paul (2013) illustrate additionally the influence of rubber concentration on cavitation, which is shown in Fig. 11.19. This figure compares curves of calculated energy change upon cavitation for blends containing various weight fractions of rubber particles, all with diameters of D = 0.3 μm. A fixed applied strain $\varepsilon_v = 0.255$ % was chosen for illustrating the sensitivity of the energy balance to the change in rubber content. It is clear in this example that blends containing up to15 wt.% of rubber can cavitate at the specified applied volume strain but blends with 20 % or 25 wt.% rubber cannot, as there is no net energy fall: $\Delta U = U_p(r_{vd}) - U_p(0) > 0$. For these high rubber concentrations, the volume strain ε_v has to be increased in order to induce cavitation. Taking into account that increasing rubber concentration reduces the yield stress, the volume strain required for cavitation of such particles could be not reached before the yield point. This may indicate that the range of particle size ready to cavitate narrows with increasing rubber content.

Summarizing, the extent of cavitation and hence the level of toughness which can be achieved depend mainly on the particle size, although also partially on rubber concentration and its properties, as, e.g., shear modulus or surface energy, as well as on test conditions (especially temperature and strain rate). Cavitation resistance increases when either the shear modulus or the surface energy of the rubber is increased, similarly to the effect of reduced particle size. Most notably, increasing the shear modulus of the rubber phase due to cross-linking, change of

chemical composition, or simply reduction of the test temperature increases critical volume strain for cavitation ε_v(cav), which eventually results in a reduction, sometimes dramatic, of fracture resistance of the blend (Gaymans 2000). The same shear modulus term accounts also for the brittle–ductile transition observed in many toughened polymers near T_g of the rubber phase (already discussed in Sect. 11.4.3.1), where G_R changes dramatically.

11.5.3 Shear Yielding

Analysis of the stress field and deformation behavior in front of the tip of sharp notch or crack allows to calculate principal stresses and estimates the size of the plastic zone ahead of the crack tip. Under assumption that the material near the crack tip is an elastic–plastic continuum, the radius of the plastic zone on the crack plane can be expressed, according to Irwin (1964):

$$r_p = \frac{1}{2\pi}\left(\frac{K_I}{m_p \sigma_{1y}}\right)^2 \tag{11.15}$$

where K_I is the stress intensity factor, σ_{1y} is the first principal stress at yield, and m_p is the plastic constraint factor, which reflects the amount of constraint on the developing plastic zone, created by the surrounding elastic material. This increases the stress necessary for the yield to occur above that needed in uniaxial tension, i.e.,

$$m_p = \frac{\sigma_e}{\sigma_y} \tag{11.16}$$

where σ_e and σ_y are the effective yield stress and the yield stress in uniaxial tension, respectively. The value of m_p depends upon the stress state around the crack tip. The value of $m_p = 1$ is for plane-stress conditions ($\sigma_3 = 0$), while according to Irwin and Paris (1971), the increased constraints in plane strain (where $\sigma_3 = v(\sigma_1 + \sigma_2)$ to the first approximation may be represented by assuming $m_p = \sqrt{3}$, which implies that the stress needed to yield in plane strain is higher than in uniaxial tension: σ_e (plane strain)$=\sqrt{3}\,\sigma_y$; thus, the radius of the plastic zone in plane strain is only one third or perhaps even less than that of plane stress. Another approach predicts the relation $m_p = 1/(1 - 2v)$, which for typical rigid polymer with the Poisson's ratio of $v = 0.4$ results in the size of the plastic zone under plane strain smaller than under plane stress by a factor of 25 (Bucknall and Paul 2009). The yield envelopes calculated for 80:20 PA6/rubber blend under the plane-stress and plane-strain conditions using the pressure-dependent von Mises criterion are shown in Fig. 11.20 (Bucknall and Paul 2009). The calculated sizes are probably underestimated because of simplified calculations, which have not allowed for stress redistribution sizes of real plastic zone in similar materials to be about double those shown in Fig. 11.20. Nevertheless, even after necessary adjustments, it appears clearly that the size of the yield

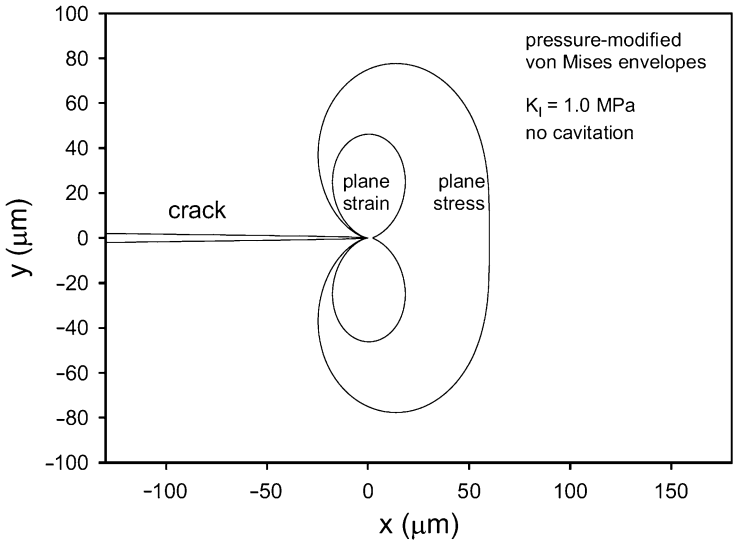

Fig. 11.20 Pressure-dependent von Mises yield envelopes under plane-stress and plane-strain condition of loading, calculated with $K_I = 1.0$ MPa $m^{0.5}$, for void-free 80:20 PA6/rubber blend with Poisson's ratio $v = 0.4$ and pressure coefficient $\mu = 0.36$ (From Bucknall and Paul (2009); reproduced with permission of Elsevier)

zone under plane strain is too small to enable a notched specimen to overcome its susceptibility to brittle fracture (Bucknall and Paul 2009).

Since a blend containing high concentration of cavitated rubber particles becomes cellular solid (porous) rather than continuous material, Eq. 11.15 does not apply to it any longer and any analysis of the plastic zone size must be based on yield criteria appropriate for the porous solid. Free from the constraints of continuum mechanics, the cavitated plastic zones formed in polymer blends are able to increase substantially in radius even under plane-strain conditions (Bucknall and Paul 2009).

The commonly used criterion for shear yielding in cavity-free rigid polymers is a pressure-modified von Mises criterion (Ward 1983):

$$\sigma_e \geq \sigma_{y0} + \mu \mathrm{P} = \sigma_{y0} - \mu \sigma_m \tag{11.17}$$

where σ_e is the effective stress, σ_{y0} is the yield stress in pure shear ($\sigma_m = 0$), μ is the pressure coefficient, P is pressure, and σ_m is the mean stress. The effective stress σ_e is given by

$$\sigma_e = \sqrt{\frac{(\sigma_1 - \sigma_2)^2 + (\sigma_2 - \sigma_3)^2 + (\sigma_3 - \sigma_1)^2}{2}} \tag{11.18}$$

and the mean stress σ_m is defined as follows:

$$\sigma_m = -\mathrm{P} = \frac{\sigma_1 + \sigma_2 + \sigma_3}{3} = \mathrm{K}\,\varepsilon_v \tag{11.19}$$

where K is bulk modulus and ε_v is the volume strain. Typical values of K at room temperature are 3.5 GPa for a glassy polymer and 2.0 GPa for a rubber.

The presence of voids increases markedly the pressure sensitivity of the material. Gurson (1977a, b) modified the von Mises criterion to be used for porous solid that contains well-distributed small voids. He applied a continuum treatment to a cavitated ductile material containing a volume fraction Φ_{vd} of voids and obtained the following yield criterion:

$$\sigma_e \geq \sigma_{yt}\sqrt{1 - 2\Phi_{vd}\cosh\left(\frac{3\sigma_m}{2\sigma_{yt}}\right) + \Phi_{vd}^2} \tag{11.20}$$

where σ_{yt} is tensile yield stress of the rigid polymer matrix and Φ_{vd} is the volume fraction of voids. His analysis leads to the conclusion that yielding occurs through the formation of dilatation bands, which allows the original voids to expand as plastic flow proceeds in the intervening ligaments between voids.

By further modification of this approach to account for pressure sensitivity of the initial material, Bucknall and Paul (2009) obtained the following equation for pressure-sensitive material containing small voids, which can be applied to the description of a polymer blend in which all rubber particles have already fully cavitated:

$$\sigma_e \geq \left(\sigma_{yo} - \mu\sigma_m\right)\sqrt{1 - 2\Phi_{vd}\cosh\left(\frac{1.5\sigma_m}{\sigma_{yo} - \mu\sigma_m}\right) + \Phi_{vd}^2} \tag{11.21}$$

where $\sigma_{yt} = \sigma_{y0} - \mu\sigma_m$ is tensile yield stress of the rigid polymer matrix (pressure sensitive) and Φ_{vd} is the volume fraction of voids. For pure shear conditions ($\sigma_m = 0$), the above Eq. 11.21 reduces to the simple rule of mixtures:

$$\sigma_e = \sigma_{y0}(\Phi_{vd}) = \sigma_{y0}(0)(1 - \Phi_{vd}) \tag{11.22}$$

It was postulated (Bucknall and Paul 2009) that the same equation can be used also for the approximation of yield in pure shear of rubber-toughened blends, which contain only void-free rubber particles or the combination of cavitated and void-free particles with the total volume fraction of intact and cavitated particles ϕ replacing Φ_{vd} (pure shear):

$$\sigma_e = \sigma_{y0}(0)\,(1 - \phi) \tag{11.23}$$

Of course, this equation cannot be considered as a universal relationship, applicable also to other deformation modes. Other dependencies of the yield stress

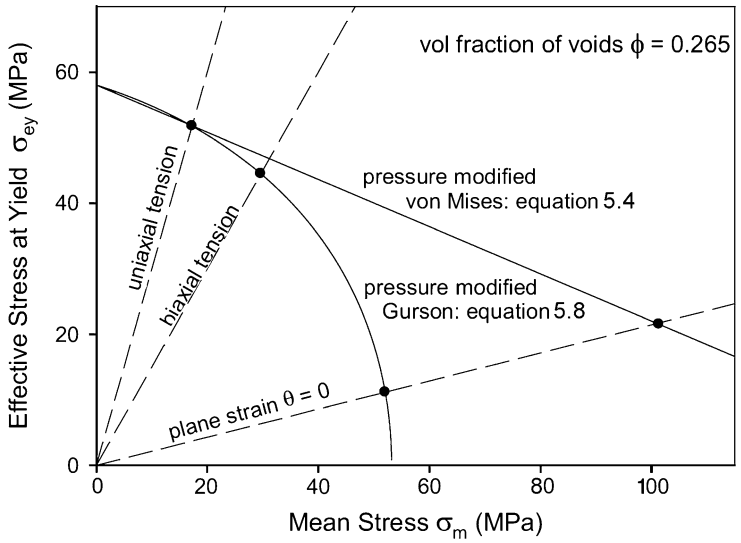

Fig. 11.21 Comparison between pressure-modified von Mises criterion for a void-free blend (Eq. 11.17 with $\mu = 0.36$) and the pressure-modified Gurson criterion for the same blend, now fully cavitated (Eq. 11.21) (From Bucknall and Paul (2009); reproduced with permission of Elsevier)

on concentration were presented in Sect. 11.4.3.1 (Eqs. 11.11 and 11.12) for uniaxial tension and compression and can be also considered in the context here. Both predict, however, a direct dependence of the yield stress on concentration as the Eq. 11.23 above.

Figure 11.21 illustrates the application of criteria of Eqs.11.17 and 11.21 to shear yielding at the crack tip in a model blend of rigid polymer with 20 wt.% of soft rubber ($\phi = 0.265$) prior and after cavitation of the rubber particles, respectively. The plot was constructed by Bucknall and Paul (2009) with data of dry PA6 ($v = 0.4$, $\mu = 0.265$, $\sigma_{yt} = 70$ MPa) used for the matrix. Tensile stress of PA6 matrix $\sigma_{yt} = 70$ MPa corresponds to yield stress in pure shear of $\sigma_{yo} = 78.4$ MPa. Blending with the soft rubber reduces those to $\sigma_{yt} = 51.5$ MPa and $\sigma_{y0} = 57.6$ MPa, respectively. Under plane strain, the construction line meets the pressure-modified von Mises curve (calculated with Eq. 11.17 at a mean stress of $\sigma_m = 100.4$ MPa where $\sigma_1 = \sigma_2 = 107.6$ MPa and $\sigma_3 = v(\sigma_1 + \sigma_2) = 86.0$ MPa) and $\sigma_e = 21.5$ MPa. This shows that pressure sensitivity helps to alleviate the adverse effects of notch tip constraint on shear yielding. The lower curve in Fig. 11.21 calculated for the same blend but with all rubber particles cavitated (Eq. 11.21) demonstrates a significant departure from the curve of non-cavitated blend, but practically only in the plane-strain conditions. This means that differences between voids and well-bonded soft particles become prominent only when the material is subjected to large dilatational stresses as in the presence of triaxial stress (plane strain). The curve calculated for the fully cavitated blend intersects the plane-strain construction line at $\sigma_m = 52.1$ MPa and $\sigma_e = 11.1$ MPa (corresponding to the stress state of

$\sigma_1 = \sigma_2 = 55.8$ MPa, and $\sigma_3 = 44.7$ MPa), i.e., well below the yield stress for the same blend with non-cavitated, continuous rubber particles.

The results presented in Fig. 11.21 are very meaningful as they clarify some of the key issues concerning the contribution of void formation to toughness in polymer blends. It appears that the cavitation is extremely important in notched specimens because it allows the blend to yield under plane-strain conditions at still moderate stresses due to increased sensitivity to the mean stress. It implies that this modification of yielding does not result from eliminating geometrical constraints and converting a state of plane-strain to plane-stress state, as it has been frequently postulated in the past (Bucknall and Paul 2009).

Cavitation enables the plastic zone, including the plane-strain region in front of the notch or crack tip, to react to dilatational stresses by expansion in volume and an increase in radius. To get the maximum toughness, two conditions must be satisfied: a widespread cavitation ahead of the crack tip and extensive involvement of the matrix in plastic deformation. To engage the matrix fully in an energy absorption through deformation, shear yielding should be the dominant mechanism of deformation. The chains must be long enough to prevent premature failure and allow accommodation of high strain. Moreover, in most cases, participation of the rubber phase in the strain-hardening mechanism is also required. To achieve this, the rubber should be strongly bonded to the matrix and to any internal sub-inclusions, when particles have heterogeneous morphology. This implies that the formation of voids through internal cavitation, especially multiple, resulting in formation of fibrils inside particle, is more efficient in toughening than particle debonding, as internal cavitation allows for higher load transfer into particle and hence better stabilization of deformation owing participation of the elastomer phase in strain hardening. The range of cavitation and thereby the level of achieved toughness depends primarily on the particle size and additionally on the degree of cross-linking of the rubber phase, surface energy, and test conditions (temperature and strain rate).

11.5.4 Dilatation Bands

The mechanism for rubber toughening in non-crazing polymers has been explained by Lazzeri and Bucknall (1993, 1995, 2000) who demonstrated that rubber particles can facilitate formation of microvoids and activate dilatation yielding in the deformed zone close to the fracture surface. They concluded that yielding in the blend sample occurs through the formation of dilatation bands, containing cavitated rubber particles, which allows the original voids to expand as plastic flow develops in the band and to relieve the dilatational stress. There is broad evidence that rubber particle cavitation in several different polymers is indeed concentrated within band-like zones of high shear strain (Lazzeri and Bucknall 1995; Sue 1992). Similar cavitated yield zones have been reported in the literature concerning metals, where they have been referred to as "dilatation bands." Such dilatation bands form because when an element of material is restrained in two dimensions, the only

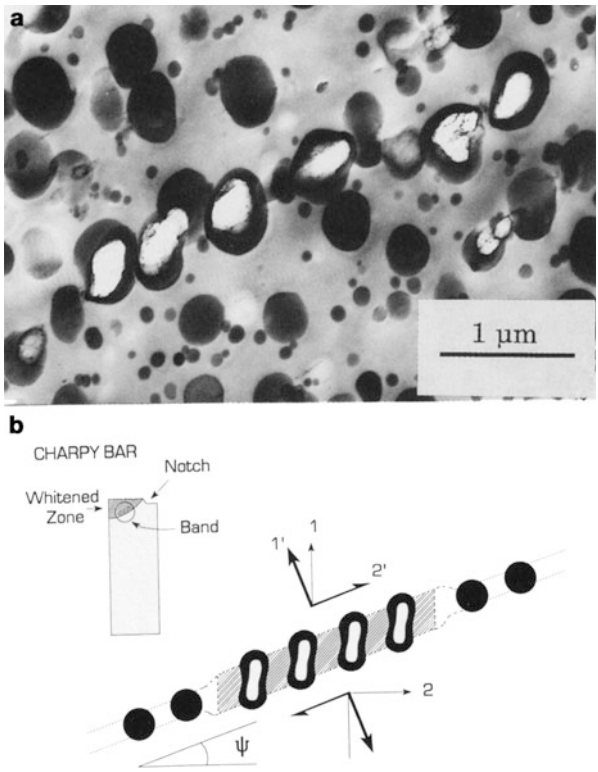

Fig. 11.22 (**a**) Transmission electron micrograph of an $0s0_4$-stained ultrathin section from a fractured Charpy specimen of rubber-toughened PA6, showing a dilatation band. (**b**) Sketch showing the location of band in the broken Charpy bar and the strains within the band (From Lazzeri and Bucknall (1995); reproduced with permission of Elsevier)

modes of deformation compatible with the imposed constraints are simple shear parallel to the plane and volume dilatation normal to it. The presence of both results in formation of a dilatation band, as illustrated in Fig. 11.22.

The inclination angle Ψ of the band to the principal tensile axis depends on the sensitivity of the yield stress to the mean stress (pressure) – cf. Eq. 11.17. The following equation was obtained (Lazzeri and Bucknall 1993):

$$\cos 2\Psi = -\frac{2\mu}{3}\frac{(\sigma_o - \mu\sigma_m)}{(\sigma_1 - \sigma_2)} \tag{11.24}$$

where Ψ is the inclination angle of the band, μ = pressure sensitivity coefficient, $\sigma_m = -\mathrm{P}$ is the mean stress, and σ_1 and σ_2 are principal stresses in the deformation plane. For anisotropic material not sensitive to pressure, $\mu = 0$, and containing no voids, the angle between the principal tensile axis and the normal to the band is $\Psi = 45^{\circ}$. For polymers, in which yielding depends on pressure, Ψ is about 38°. Introduction of voids into the shear bands through cavitation increases significantly the pressure dependence (see the Sect. 11.5.3) and leads to further reduction in Ψ, so that dilatation bands respond to stress by both increasing thickness and

undergoing shear in a plane. The inclination angle eventually falls to zero when the void volume fraction reaches 0.53 (Lazzeri and Bucknall 1993). This rotation of the band plane reduces resistance to crack tip opening; at the crack tip plane, $\Theta = 0^{\circ}$, yielding occurs entirely in response to tensile stresses applied normal to the bands, which in that respect may resemble crazes. Some examples of craze-like cavitated shear bands have been reported for rubber-toughened epoxy by Sue (1992).

11.5.5 Crazing

Multiple crazing is the basic deformation mechanism of all disperse systems with an amorphous brittle matrix prone to crazing, including rubber-toughened grades of PS, SAN, PMMA, and related glassy polymers. On the other hand, it does not seem to play a significant role in the process of energy absorption in the blends based on ductile glassy polymers (such as PC), semicrystalline polymers, or thermosetting resins. In the above mentioned blends of amorphous brittle polymers, the matrix is a brittle thermoplastic, which tends to form crazes at strains between 0.3 % and 1 % and fractures shortly afterwards. Although macroscopically brittle, these polymers appear ductile on the length scale below 1 μm, within a single craze, and would absorb a considerable amount of energy if this ductility could be extended over a large volume of the material. Multiple crazing, first observed in HIPS, is an extensive crazing in which individual crazes are nucleated by numerous rubber particles dispersed in the matrix. Those rubber particles are also able to terminate crazes. As a result, large number of short crazes is developed in the material, which engages much more of its volume in plastic deformation events, and consequently notably higher energy dissipation is observed.

The soft rubber particles dispersed in glassy matrix act as stress concentrators (see Sect. 11.4.3.1) and like microscopic surface scratches can constitute the sites of effective craze initiation. Bubeck et al. (1991) used real-time X-ray measurements on HIPS to show that crazing of the matrix under tensile impact conditions is actually preceded by cavitation of the rubber particles. Cavities formed within the rubber particles can thus be seen as the real nuclei for the craze growth, which occurs through the meniscus instability mechanism proposed by Argon and Salama (1977). Cavitated particles initiate crazes in the immediate matrix adjacent to their equatorial regions. The crazes propagate then outwards through the matrix perpendicularly to the direction of principal tensile stress until termination by other rubber particle encountered along the propagation path. This produces secondary cavitation within encountered particle and crazing around. At higher rubber concentration (above approximately 15 vol.%), the stress concentration fields of neighboring particles overlap, which results in stress concentrations higher than around isolated particles. In such interparticle zones, broader crazes and craze bands develop roughly perpendicularly to the principal tensile stress and propagate from one particle to the other, cf. Fig. 11.8 in Sect. 11.4.3.

One of the serious difficulties in developing a quantitative description of toughening with elastomer particles is the lack of a suitable criterion for craze initiation.

Several criteria were developed in the past by Sternstein and Ongchin (1969), Oxborough and Bowden (1973), and Argon and Hannoosh (Argon 2011; Argon and Hannoosh 1977) suffer from serious flaws (Bucknall 2007a). Recently Bucknall (2007a, b) demonstrated that the craze initiation can be considered as a frustrated fracture process which actually falls within the scope of linear elastic fracture mechanics (LEFM); therefore, the Griffith equation, modified accordingly, can be regarded as an appropriate criterion for craze initiation. It is evidenced that rubber particles can be effective craze initiation sites, e.g., microscopic surface scratches. In order to act as craze initiators, the elastomer particle must cavitate internally first to form rubber-reinforced spherical holes, in which the rubber provides significant reinforcement, but only when it becomes highly strained. Such a behavior pattern was confirmed experimentally (Bubeck et al. 1991). Using LEFM approach and treating cavitated rubber particles as isolated spherical voids embedded in a homogeneous matrix, the following equation of the critical stress for craze initiation by cavitated particle can be formulated:

$$\sigma_{1craze} = \sqrt{\frac{\pi E G_{craze}}{2(1-\nu^2)D}} \tag{13.25}$$

where σ_{1craze} is the critical tensile stress for craze initiation, E is the matrix Young's modulus, G_{craze} is the energy absorbed in forming unit area of a new craze, and D is the diameter of the cavitated particle. Typically, in well-prepared tensile specimens of glassy crazable polymer (plain, not modified), the critical stress $\sigma_{1craze} \approx 20$–$50$ MPa. It can be estimated that G_{craze} is small, between 0.1 and 1 J/m^2.

Equation 11.25 becomes inaccurate with increasing rubber concentration, ϕ, and the average stress in the matrix raising much above the applied tensile stress σ_1. A simple solution might be to apply the rule of mixtures and assume the crazing stress is proportional to $(1 - \phi)$. However, comparison with experimental data demonstrates that this method leads to a substantial overestimation of the yield stress for HIPS blends, where multiple crazing is the dominant mechanism of deformation. Bucknall and Paul (2013) found that much better fitting the data, for both HIPS (Bucknall et al. 1986) and ABS (Ricco et al. 1985), can be obtained by using the effective area model proposed by Ishai and Cohen (1968), who assumed that cracks and shear bands tend to follow paths of minimum resistance through heterogeneous or porous solids and formulated the dependence of stress on rubber concentration (cf. Eq. 11.11 in Sect. 11.4.3.1). Applying this model to materials in which multiple crazing is the dominant mechanism, the critical tensile stress can be obtained:

$$\sigma_{1craze}(\phi) = \left(1 - \pi\left(\frac{3\phi}{4\pi}\right)^{\frac{2}{3}}\right)\sigma_{1craze}(0) = \left(1 - 1.21\phi^{\frac{2}{3}}\right)\sqrt{\frac{\pi E G_{craze}}{2(1-\nu^2)D}} \tag{11.26}$$

where $\sigma_{1craze}(\phi)$ is the stress at which crazes propagate and thicken in a blend containing volume fraction ϕ of rubber particles, and $\sigma_{1craze}(0)$ is the limiting crazing stress at very low rubber contents.

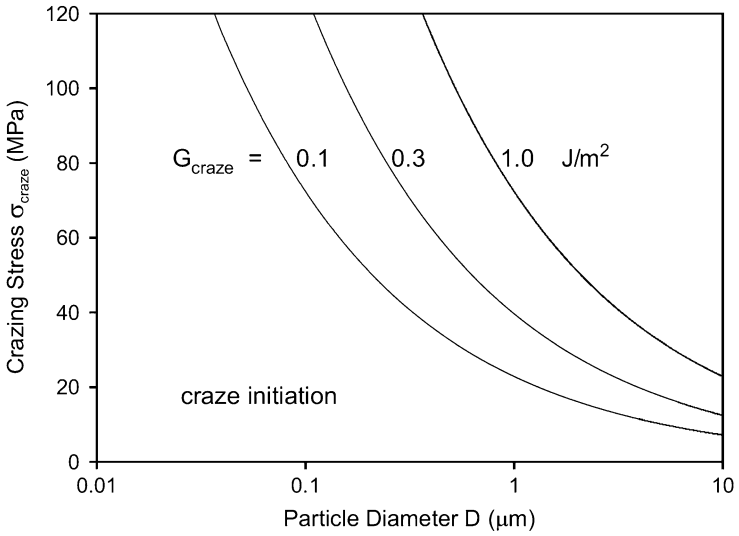

Fig. 11.23 Critical tensile stress for craze initiation as a function of (cavitated) rubber particle diameter, calculated using Eq. 11.26 with three different values of G_{craze}, the specific energy of craze initiation (From Bucknall and Paul (2009); reproduced with permission of Elsevier)

Equations 11.25 and 11.26 predict the proportionality of the critical craze initiation stress on the inverse square root of the particle diameter. It allows to estimate that σ_{1craze} decreases with increasing particle diameter from above 100 MPa to the level of below 20 MPa for large particles, exceeding 1 μm in diameter (typical values of E = 2.8GPa and $v = 0.4$ assumed for calculation) (Bucknall and Paul 2009); see Fig. 11.23 illustrating strong dependence of the critical stress for craze formation on particle size. That size dependence implies that for particles which are large enough, σ_{craze} must eventually decrease below the shear yield stress of the fully cavitated blend, which becomes independent of D after complete cavitation of particles (cf. Sect. 11.5.3). In this way, crazing can emerge as the dominating mechanism for large particles, in contrast to smaller particles which upon cavitation will initiate preferably the shear yielding in the same matrix. The process begins with primary cavitation of larger particles, which then initiate crazes that propagate outwards. These can induce secondary cavitation and crazing in other particles encountered by a propagating craze. Such a picture is supported by experimental evidence that in many blends tested at impact conditions, crazing is accompanied by dilatational shear yielding and that increasing particle size suppresses shear yielding while promoting crazing as an active mechanism (Bucknall 1977; Bucknall and Paul 2009). The exception is HIPS, which demonstrates almost no signs of ductility under tensile load.

Crazing is a mechanism of plastic deformation that is extremely localized. Even when the number of crazes in the sample is substantially increased, as in the case of multiple crazing in rubber-toughened blends, their early stages of development

engage much less of the matrix volume into plastic deformation than the shear yielding mechanism. Therefore, less energy is usually dissipated in crazing, and toughness improvement may appear below that demanded. Moreover, crazes, if have not been stabilized sufficiently, can quickly degrade to cracks, which inevitably leads to a premature failure. As a result, toughness of the blend which responds to load with crazing is usually lower compared to the blend responding with shear yielding. This explains the appearance of an upper ductile–brittle transition (see section "Rubber Concentration" and Figs. 11.26 and 11.27), observed for some blends, in which toughness falls down as the particle diameter increases. This transition is presumably a result of the change of active deformation mechanism from shear yielding, which is promoted by smaller particles, to crazing which is related to large particles present in the blend.

For effective performance of multiple crazing as the toughening mechanism, the craze growth must be controlled and stabilized. Crazes can be stabilized efficiently by rubber particles, provided these particles can transmit loads and consequently participate in strain hardening of the blend. The particles, especially large ones, tend to cavitate prior to craze initiation and their ability to transmit load depends strongly on their morphology after cavitation. From this point of view, the worst case is when particles are weakly bonded to the matrix and tend to debond from the matrix rather than cavitate internally. Debonding prevents any stress transfer from the matrix into the particles, which then cannot participate in the strain-hardening process and therefore are not able to stabilize craze. As a result, such material with particles debonded usually fractures shortly after craze initiation in nearly brittle fashion. The homogeneous particles, which are well bonded to the matrix, tend to cavitate internally in a single site and form a single void which is surrounded by the continuous rubber shell. Their ability to transfer stress is much higher than debonded particles, but participation in strain hardening is moderate, as the continuous rubber shell does not deform uniformly and eventually fails by progressive tearing with advance of the strain (Bucknall 2000). As a result, cracks can develop relatively early, and toughening effect may be unsatisfactory, especially when particles are large, e.g., few microns in diameter (which is just the optimum size for craze initiation). The most advantageous situation is when the particles are not only bonded well to the matrix but show additionally heterogeneous structure: either contain harder sub-inclusions dispersed inside or have a core–shell morphology. When the internal sub-inclusions or the core is bonded well with the surrounding rubbery phase, then cavitation is frequently followed by a stable fibrillation of the rubber. These fibrils, strongly bonded both to the core or sub-inclusion and to the surrounding matrix matter, can deform uniformly by stretching to high strains, close to the ultimate stretch of the rubber. This enables an effective participation of rubber in strain hardening which greatly helps to stabilize crazes. Consequently, properly formulated and balanced blends made with heterogeneous particles, which are ready to cavitate and form internal fibrils and thereby able to stabilize crazes, show frequently quite large elongations to break, sometimes up to above 50 %, and can even demonstrate a super-tough behavior at impact conditions.

11.5.6 Structure–Property Relationships

Important factors were found to affect the fracture behavior. These can be divided into three main groups related to:

- Matrix material:
  - Molecular weight
  - Entanglement density
  - Ability to crystallization and crystallinity
- Dispersed-phase material:
  - The type of the elastomer
  - Rubber modulus
  - Interfacial bonding
  - Concentration
  - Particle size/interparticle distance
- Sample and test parameters:
  - Sample shape and dimensions
  - Test method (deformation mode, presence of notch)
  - Test speed
  - Test temperature

Below, a short description of these parameters related to the properties of the matrix and the modifier dispersed in the matrix is presented. Sample and test parameters will be not addressed here.

11.5.6.1 Matrix Properties

Toughening of the polymer blend depends on the deformation mechanisms that dominate mechanical response of the host polymer (matrix), where most of energy is dissipated during deformation and fracture. These mechanisms are determined generally by the chemical structure of that polymer, including the repeat unit, chain architecture, molecular weight, and its distribution. Apart from crystal plasticity governing deformation of polymer crystals, the main deformation processes in polymers are shearing and crazing. Each of these mechanisms allows for different level of toughening, also because the starting level, i.e., the toughness of the pristine host polymer, is very different for brittle crazable polymers and quasi-ductile polymers which tend to deform by shear yielding. The selection of the active deformation mechanisms depends principally on details of the matrix chemistry (Bucknall 1977). As already discussed in Sect. 11.2, if the chains of the matrix polymer demonstrate low entanglement density and are stiff under the test conditions, like in PS, then crazing is promoted in tensile loading. On the other hand, if the chains are much more flexible and demonstrate higher entanglement density, then the shear deformation initiated by shear yielding is the dominant mechanism, as, e.g., in PC or PVC deformed at room temperature. These polymers exhibit secondary relaxation processes below their glass transition temperature. These relaxation transitions indicate some limited segmental mobility of the chain backbone which become allowed at temperature range between the lower, secondary relaxation and the glass transition temperature. These localized main-chain motions

facilitate parts of the macromolecules to slide past each other and initiate shear deformation when material is loaded. As a consequence, these polymers can exhibit ductile behavior already below their glass transition temperature. Temperature of the secondary relaxation determines then the brittle–ductile transition temperature (Kausch 1987). On the other hand, some of stiff glassy polymers like PS or SAN lack this type of secondary relaxation process below their T_g and consequently are not able to shear at the desired scale and deform at room temperature preferentially by crazing, instead. If this energy dissipating craze mechanism is not stabilized properly, e.g., by dispersed rubber particles, it leads shortly to crack formation and brittle fracture. PMMA, with a mobility of the side groups beginning near room temperature and also mobility of parts of the main chain slightly above room temperature (as indicated by the secondary relaxation process at 50 °C), appears at room temperature to be in the intermediate range and can deform by shear yielding, by crazing, or by both mechanisms simultaneously, depending on particulate test conditions. Generally, crazing seems to dominate in tension at low temperatures and/or at high deformation rates, when the molecules have very limited time to rearrange under the stress, and also at conditions of triaxial tensile stress. In contrast to these situations resulting in brittleness, when enough time is given for possible chain rearrangement (e.g., at higher temperature, above the secondary relaxation temperature, and/or at low deformation rates), the polymer tends to yield in shear.

The details of the matrix chemistry determine not only the stiffness of the chain but also the tendency to form entanglements. Again, as discussed in Sect. 11.2, the density of chain entanglements, generally related to chain stiffness (cf. Eq. 11.4), influences markedly the choice of the deformation mechanism: low entanglement density promotes crazing, while polymers exhibiting high entanglement density tend to deform by shear yielding. Both the chain stiffness and entanglement density are intrinsic properties of the chains and therefore are difficult to modify by physical methods without interfering chain chemistry. The entanglement density can be increased, and thus vulnerability to crazing reduced, practically only by blending a polymer with another polymer, which is fully miscible with it and demonstrates higher flexibility. That blending leads to the formation of the uniform network consisting of stiff and flexible chains, and characterized by increased overall entanglement density. Such modification is possible for only a few polymer pairs that demonstrate complete miscibility, as, e.g., PS and PPO (cf. Fig. 11.1).

Polymers that deform preferentially by crazing demonstrate usually low fracture toughness. This toughness can be enhanced quite substantially by a suitable modification, e.g., by adding an elastomer, but the resulting toughness of the modified material, although much increased compared to the pristine polymer, can be still lower than the toughness of many quasi-ductile polymers that tend to deform by shear yielding rather than crazing. These quasi-ductile polymers, in general, demonstrate significantly higher initial toughness than brittle, crazable polymers and usually are also much more receptive for toughening. As a result, super-tough materials can be formulated on the basis of those polymers easier than using crazable polymers. Generally speaking, when a broad range of thermoplastic matrix

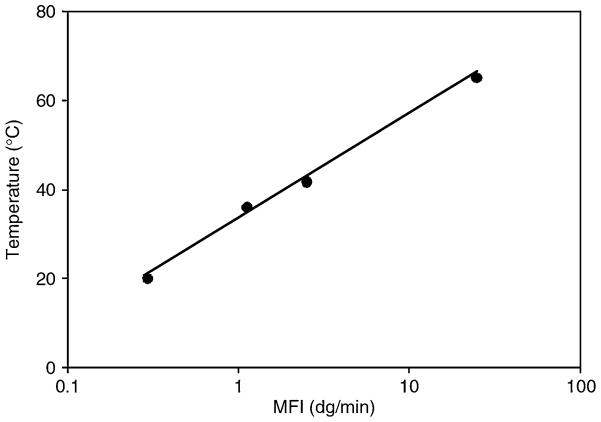

Fig. 11.24 Brittle-to-ductile transition temperature as a function of matrix molecular weight, 30 wt.% PP-$CaCO_3$ composites (From Zuiderduin et al. (2003); reproduced with permission of Elsevier)

polymers are examined, the observation is that the toughest rubber-modified materials will be those which possess the toughest matrices (Bucknall 1977).

Besides the stiffness of the chain and entanglement density, the molecular weight appears also an important factor (Kausch 1991) as it influences the properties of the molecular network, important for an initiation and development of both crazing and shear yielding. Moreover, polymers of high molecular weight demonstrate usually an increased fracture stress relative to the yield stress and the brittle-to-ductile transition shifted to a lower temperature. This relationship can be illustrated by an example of semicrystalline polypropylene (here modified with rigid particles) shown in Fig. 11.24. It can be observed there that an increasing molecular weight, depicted by decreasing melt flow index (MFI), results in the shift of the brittle–ductile transition towards lower temperature (Zuiderduin et al. 2003). Similar dependence of T_{BD} on molecular weight was observed also in various blends with elastomers (Dijkstra and Gaymans 1994b; Oshinski et al. 1996a, b, d; van Der Wal et al. 1998).

The chemical structure of the polymer, including the structure of the repeat unit, chain architecture, and molecular weight determine also the ability of the polymer to crystallization. The presence of crystalline phase influences deeply the toughness of the polymer as well as deformation mechanisms governing it, as the polymer crystals are allowed to absorb energy upon their deformation according to typical mechanisms of crystal plasticity. Moreover, they can facilitate additional relaxation modes of the amorphous phase which can simplify shear yielding of the amorphous component. The crystalline regions in semicrystalline polymers constitute the physical cross-links that stabilize and hold material together, particularly above its glass transition temperature. Above T_g, the modulus and the yield strength increase with increasing crystallinity of the matrix (Ward 1983). Below T_g, the effect of crystallinity on the modulus and yield strength is much smaller as the number of crystalline cross-links is small compared to the number of frozen (immobilized) entanglements, which act now similarly to permanent cross-links. Increasing crystallinity has a strong negative effect on the brittle-to-ductile transition, causing an increase of T_{BD} (van Der Wal et al. 1998).

The yield stress in a semicrystalline polymer increases with increasing crystallinity as well as with increasing lamellar thickness, which, in turn, is controlled by the temperature at which crystallization had occurred (Kazmierczak et al. 2005; Sirotkin and Brooks 2001; Ward 1983). Moreover, crystallization leads frequently to an increase of the entanglement density in the amorphous phase, as most of the entanglements were not resolved by crystallization but merely swept into amorphous interlamellar regions (Strobl 1997), especially when the molecular weight of polymer is high. For obtaining high toughness, the crystallinity level must be carefully balanced, since too high crystallinity can constrain excessively deformation of the amorphous component, which would manifest in an increase of T_{BD} and eventually lead to material embrittlement. On the other hand, the balance of all properties is of practical interest. Usually, it is demanded to have high ductility combined with a possibly high modulus and high yield strength. A highly crystalline polymer, demonstrating relative high modulus but being more brittle than its low crystallinity counterpart, can be successfully modified to obtain material that exhibits low temperature ductility by adding more rubber. In practice, the best balance of properties is obtained just with highly crystalline grades. As blending with a second polymer can in some cases modify significantly crystallization kinetic of the matrix as well as the resultant lamellar thickness and degree of crystallinity (Bartczak et al. 1995), this factor must be also taken into account when selecting the type and grade of the rubber to be used for toughening of a particular polymer. Also the processing conditions, especially the cooling rate, must be controlled to prevent an excessively high crystallinity. However, these effects are minor as compared to others, as, e.g., those related to the rubber content or its average particle size.

11.5.6.2 Dispersed-Phase Parameters

The Type of Elastomers

The function of the dispersed-phase material that in most instances is an elastomer is to induce an adequate toughening mechanism in order to shift the T_{BD} temperature down and increase notably the toughness of the material above T_{BD}. Therefore, it is expected that the choice of the elastomer type is important. It appears that the type of rubber may have a little influence on the notched Izod impact strength in the tough region, but give a strong effect on the temperature of brittle-to-ductile transition, T_{BD}, as it was observed by Borggreve et al. (1989b) in PA6 blended with various elastomers (Fig. 11.25).

A good correlation between T_{BD} and the modulus of an elastomer was found by Gaymans et al. (1990) in PA6 modified with olefinic rubbers: T_{BD} decreases steadily with rubber modulus (all at constant rubber concentration and average particle size). The volume strain experiments (Borggreve et al. 1989a; Bucknall et al. 1989) demonstrated that the blends with the highest impact resistance cavitated most easily. The correlation of T_{BD} and modulus is possibly due to both the cavitational stress and the tensile modulus being related to the cohesive energy density of the elastomer.

The type and grade of elastomer, through its chemical composition, molecular weight, and viscosity, determine miscibility with the matrix, the state of dispersion,

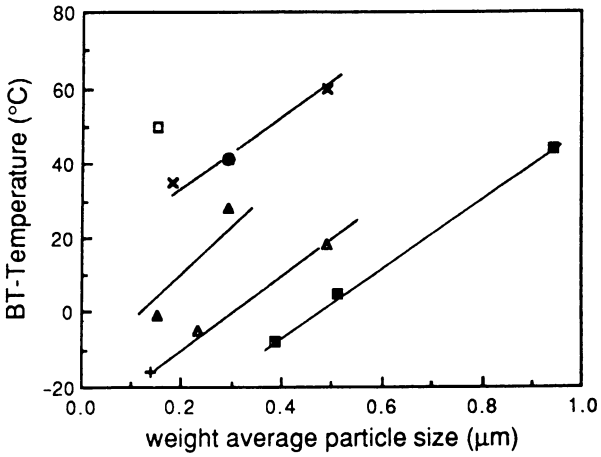

Fig. 11.25 Temperature of brittle–tough transition as a function of the weight-average particle size for blends of PA6 and 10 wt.% rubber, with different types of rubbers: ■, EPDM; +, EPR; ×, LDPE; ▲, Keltaflex®; ●, polyester TPE (From Borggreve et al. (1989b); reproduced with permission of Elsevier)

and the interfacial strength between rubber particles and the matrix, which in turn influence profoundly the impact behavior of the blend. The toughening effect is additionally dependent on the glass transition temperature of the rubber, as below T_g the cavitation stress increases drastically, so that rubber particles do not cavitate and consequently are not able to activate any toughening mechanism.

There are a great variety of elastomers applied to improve toughness of engineering polymers, including polyisoprene, butadiene elastomers (e.g., polybutadiene, styrene–butadiene, or butadiene–acrylonitrile copolymers), olefinic elastomers (e.g., ethylene–propylene, ethylene–octene-1 copolymers), styrene-butadiene-styrene (SBS), or styrene–ethylene–butene-1–styrene (SEBS) block copolymers, ionomers, polyurethanes, and many others, also functionalized with various groups, like maleic anhydride (MA) or glycidyl methacrylate (GMA), used for reactive extrusion. Elastomers used as toughness modifiers for various engineering polymers were reviewed, e.g., by Kesskula and Paul (1994). As an example, in Table 11.2 a survey of elastomers and compatibilization techniques tested for polyamides is presented (Akkapeddi 2001). Due to the polar nature of polyamides and apolar nature of elastomers, obtaining a very small rubber particles (0.2–0.4 μm in diameter) and their good dispersion, necessary for toughening of polyamides, is not easy and usually requires an adequate compatibilization, mainly through a reactive blending process, in order to produce blends containing appropriate small rubber particles.

Rubber Modulus

Because of very low stiffness, the rubber dispersed in the rigid matrix causes a decrease of the modulus and the yield strength of the blend. An extent of reduction depends, however, on the concentration of the rubber, rather than on its type or elastic properties (provided rubber is not highly cross-linked), since modulus of practically all elastomers above their glass transition is very much lower than modulus of the rigid matrix.

Table 11.2 Some common reactive rubbers and tougheners for polyamides (From Akkapeddi 2001)

Reactive rubber/toughener	Functionality	Reactivity	Other features
Maleic anhydride grafted ("maleated"), ethylene-propylene rubber (m-EPR)	Anhydride 0.3–0.9 % MA	High reactivity with the amine (NH_2) end group of PA	Amorphous rubber, low T_g leads to high-impact toughness down to –40 °C
Maleated, styrene–ethylene/butylene–styrene block copolymer rubber (m-SEBS)	Anhydride 0.5–2 % MA	High reactivity with the amine (NH_2) end group of PA	Amorphous rubber, low T_g leads to high-impact toughness down to –40 °C
Ethylene–ethyl acrylate–maleic anhydride (E-EA-MA) terpolymer	Anhydride 0.3–3 % MA	High reactivity with the amine (NH_2) end group of PA	Moderate T_g limits low-temperature toughness
Zinc neutralized, ethylene–methacrylic acid copolymer ionomer (E-MAA, Zn)	Zinc carboxylate, carboxylic acid	Low reactivity with amine but good polar interaction of Zn with amide and amine groups (interfacial complexation)	T_g and hardness limit low-temperature toughness; good solvent resistance
Zinc neutralized, ethylene–butyl acrylate–methacrylic acid terpolymer ionomer (E-BA-MAA, Zn)	Zinc carboxylate, carboxylic acid	Same as above	Low T_g and high-impact modification efficiency
Ethylene–glycidyl methacrylate copolymer (E-GMA)	Epoxide 3–8 % GMA	Moderate high reactivity with carboxyl group of PA	T_g and hardness limit achievable toughness; cross-linking tendency
Ethylene–ethyl acrylate–glycidyl methacrylate terpolymer (E-EA-GMA)	Epoxide 1–8 % GMA	Moderate high reactivity with carboxyl group of PA	Lower T_g, better impact; high viscosity
Acrylate core–shell rubber, functionalized	Carboxyl	Low reactivity with amine	Small rubber particle (<0.5 μm) aggregation
Ethylene–acrylic acid copolymers (E-AA)	Carboxyl	Low reactivity with amine	Not rubbery enough; modest impacts
Ethylene–ethyl acrylate or butyl acrylate copolymers (E-EA or E-BA)	Ester	No reactivity with amine	No impact improvement. Used only as codiluent

The stiffness of the rubber relative to the matrix determines the intensity of stress concentrations around rubber particles upon sample loading prior to their cavitation, as discussed in Sect. 11.4.3.1. The stress concentrations at the particle surface reach values very close to 2 already when G_R/G_M goes below 0.1 and are only slightly higher when G_R/G_M decreases below 0.01. That ratio of the moduli $G_R/G_M < 0.1$ facilitating high level of stress concentrations is easily reached for most of the rubber–matrix pairs at temperatures above T_g of the rubber. The situation changes when temperature decreases below T_g: the stress concentrations

diminish and additionally the stress required to induce cavitation in a glassy now particles increases dramatically, which practically inhibits any internal cavitation of particles and leads to the termination of the rubber toughening effect. Under impact loading conditions, the modulus is increased additionally due to high deformation rate and, therefore, the ductile-to-brittle transition is shifted to the "impact brittle point," which is about 10°C above T_g (Bergen 1968). The impact strength can decrease then even below the level of unmodified material (see Sect. 11.4.3.1).

The modulus of the rubber can be increased notably also by cross-linking, either intentional or induced by material aging. It has long been known that some cross-linking is necessary to preserve the structure of the particles and avoid their coalescence at further stages of material processing (compression molding, injection molding, etc.). Bucknall (1977) reasoned that light cross-linking of the rubber, which does not increase significantly its modulus, is desirable also for other reasons: as during impact loading the rubber cavitates and then undergoes high strains, the light cross-linking would allow the rubber to reach high strains by fibrillation rather than of expansion of the shell around a single void in the center of the particle, and the fibrils would then participate more effectively in stabilization of the matrix deformation by strain hardening and help to avoid a premature fracture. On the other hand, excessive cross-linking impairs fracture resistance, notably by reducing notched impact strength. High levels of cross-linking shift T_g of the rubber highly upwards. Moreover, it results in a dense molecular network leading to a significant increase of the cavitation stress and serious reduction of the ultimate stretch. Therefore, a decrease of toughness of the blend with increasing cross-link density of the rubber can be expected: a heavy cross-linking should suppress substantially cavitation of rubber particles, and as a consequence, the impact strength would decrease either. Experimental results for PA6/SBS blends with different degree of rubber cross-linking, obtained by Suo et al. (1993), supported this view. The same, sometimes even dramatic, decrease of the impact strength can be a result of an excessive cross-linking which has occurred unwanted on improper processing or when material was exposed to prolonged sunshine during its outdoor use. It is known that HIPS and ABS can embrittle seriously if they have been processed too long or at too high temperatures, which leads to excessive thermal cross-linking of the rubbery phase. Embrittlement was also observed if the rubbery phase in the particles were intentionally cross-linked, either chemically or by radiation (Steenbrink et al. 1998; Suo et al. 1993). Similarly, these and other rubber-modified materials are known to turn brittle after long exposure to UV light or sunshine.

Structure of the Rubber Particles

Internal structure of the rubber particles is very important from the point of view of both initiation and stabilization of the matrix deformation. Generally, three types of rubber particles are used for toughening. In HIPS and solution ABS, salami particles obtained during polymerization process are preferred. These particles contain much occluded matrix so that the particles are sufficiently large for initiating crazing, while the rubber content is relatively low, which limits the

decrease of Young's modulus. The crazes are initiated near the equatorial region of the rubber particles, perpendicular to the tensile stress direction, as shown in Fig. 11.8. In this region, the normal stress component of the stress tensor is the highest.

Core–shell particles are used frequently with transparent polymer matrices. In this type of particle, the core is very often formed from a material similar or identical to the matrix and is covered with a relatively thin rubbery shell, which is grafted with an outer second shell of the polymer identical to the matrix. If the thickness of the rubber shell is small compared to the wavelength of light, then light scattering is reduced, and the final blend maintains some transparency (Heckmann et al. 2005). Due to the rigid core and relative low amount of the rubber, such multilayer particles with rigid core facilitate also a fairly good balance between toughness and stiffness of the toughened material. Core–shell particles are obtained by emulsion polymerization and their size as well as size distribution can be controlled precisely in a certain range, so that particles of the optimum size can be prepared for a particular blend. The only problem, rather minor, during compounding of such particles with the matrix polymer is in obtaining a good dispersion and avoiding agglomerates in the final blend. The other very important benefit of core–shell particles is that the cavitation of such particles proceeds usually via nucleation of many small nanovoids in the rubber intermediate shell (Michler and Bucknall 2001). With subsequent expansion of these voids, a fibrillar morphology develops easily within the rubber shell with many elongated fibrils very well bonded to a rigid core and the outer shell (cf. Fig. 11.12). Stress and strain are distributed uniformly in these fibrils, which prevents their premature fracture, stabilizes cavities, and allows for effective stress transfer across the rubber shell and eventually leads to a significant contribution of particles in strain hardening and stabilization of material extensive deformation. Consequently, a high impact strength can be reached (see Sect. 11.4.4).

The last group of rubber particles constitutes particles obtained by dispersion of an elastomer in the matrix by blending of molten polymers in the extruder. The size of particles and the state of dispersion depend on rheological properties of both constituents of the blend as well as parameters of the mixing process. Frequently, to obtain a blend with rubber particles of desired size and satisfactory dispersion, reactive rubbers or other components (e.g., compatibilizers) must be added to the blend. If the elastomer used was thermoplastic, then the small crystallites formed inside particles on cooling constitute heterogeneities that can act as nucleation sites for multiple nanovoids within particles. Such a multiple cavitation is followed by formation of fibrils rather than a single rubber shell, which fibrils then can participate effectively in strain hardening and stabilization of the deformation process. Rubber fibrillization on cavitation usually fosters enhanced impact strength. The same effect of fibrillization can be obtained also by using block copolymers in which small sub-inclusions can be formed inside the particles. Grafting particles to the matrix by using functionalized rubbers in the reactive extrusion process or using adequate compatibilizers can control the size and interfacial strength of the rubber particles.

Interfacial Effects

A low interfacial energy between components of the blend is essential for obtaining a fine elastomer particle dispersion, which in turn is necessary for effective toughening. This condition is relevant not only for dispersing of bulk rubber by melt blending but also for dispersing aggregated core–shell particles or rigid particles during compounding. A low interfacial tension can be obtained either by careful selection of a rubber suitable for modification of a given rigid polymer or through a grafting reaction at the interface or by adding selected third polymeric component as compatibilizer. Grafting at the interface or using compatibilizers reduces interfacial tension while increases the adhesion (interfacial strength) between elastomer particles and the matrix.

Wu (1985) studied the PA-EPR rubber blends with different levels of adhesion between components, prepared by reactive melt extrusion. He found that the minimum interfacial strength needed for toughening was around 10^3 J/m^2, which is about the tearing stress of a rubber. This level of an interfacial strength can be obtained already by van der Waals bonding (Gaymans 2000). When interfacial strength becomes higher, due to, e.g., compatibilization or grafting at interface, the rubber particles in the blend tend to fail by internal cavitation. Lower interfacial strength (weaker bonding) is usually not desirable since particle debonding at interfaces rather than internal cavitation can take place. Debonding is less favorable than cavitation since there is no stress transfer from the matrix to the debonded particles so that these particles practically do not deform and hence do not participate in the strain hardening as the deformation of the matrix in the plastic zone advances. Voids created by debonding, not stabilized by stretching rubber, may become quickly crack initiators that would lead to premature fracture resulting in relative low impact strength.

Borggreve and Gaymans (1989) studied the PA-EPR blends, in which the amount of maleic anhydride grafted on the rubber, used to bond rubber and the matrix, varied in the range of 0.1–0.7 wt.%. These blends had different particle size for a given PA/rubber composition but exhibited identical relationship between T_{BD} and average particle size. Thus, the interfacial strength, seriously modified by chemical bonding of the rubber and PA chains through MA groups, appeared to control the dispersion process and the final size of the rubber particles, but did not influence the impact behavior at the constant particle size, because in all blends studied, toughening was related to the same mechanism of particle cavitation initiating extensive shear deformation of the matrix. These results demonstrate the actual role of grafting and use of compatibilizers – their primary function is to reduce the average particle size to the desired level effective for toughening, and not to increase interfacial adhesion between particles and the matrix. The process of reactive compounding, during which rubber particles are formed by shear forces and grafted to the matrix, appears relatively simple and effective method of preparation of tough blends with controlled particle sizes.

The modification of the interfacial tension influences the particle size obtained in the blend, but does not influence yield stress and modulus, which both depend on rubber concentration rather than on particle size (Borggreve et al. 1987).

Rubber Concentration

Rubber concentration in the blend is a very important factor in deformation and fracture of all rubber-toughened polymer blends. The impact strength of ductile polymers was found to increase as a function of rubber content (Gaymans 1994; Harrats and Groeninckx 2005). The brittle–ductile transition, which is a crucial parameter in toughened polymers, shifts towards lower temperature as the rubber content is increased (Argon et al. 2000; Bucknall 1977; Michler and Balta-Calleja 2012). Unfortunately, this comes at a price of an inevitable reduction of the material stiffness (lowered modulus) and the yield strength. When the material is loaded, the particles of soft compliant rubber transfer the load to the stiffer matrix, thence set up stress concentrations and reduce in this way the modulus and the yield stress, as already discussed in Sect. 11.4.3.1. The reduction of the modulus or yield strength can be described with the simple theoretical "effective area" model of Ishai and Cohen (Ishai and Cohen 1968) (cf. Eq. 11.11) or with the empirical dependence found by Gloagen et al. (1993) for rubber-toughened PMMA:

$$\sigma_y(\phi) = (1 - 1.375\phi)\,\sigma_y(0) \tag{11.27}$$

Both relationships show a dependence of the yield strength solely on the rubber volume concentration. The same holds for the modulus. It can be concluded then that in order to get an acceptable balance between toughness and stiffness of the modified material, the rubber content cannot be too high. The other reason for reducing the rubber content in the blend is related to the problems which may arise with appropriate rubber dispersion and particle size. When a bulk elastomer is dispersed in the matrix by high shear forces upon the melt compounding, a low rubber concentration is advantageous from the point of view of particle size and size distribution. Concentrations higher than 25–30 vol.% usually result in coalescence of inclusions already formed and consequently in an increase of the final average particle size and broad distribution of particle size, which in most cases appears negative for toughening. Similarly, when the ready particles of the core–shell type are used, their high concentration can bring on serious problems related to their dispersion, and particle agglomerates can survive the compounding process, which is also detrimental for toughening. Therefore, in most of the commercial formulations, the rubber concentration is kept usually rather low, in the range from 5 % to 20 % of the elastomer phase. Working within this concentration range usually allows to obtain a blend with sufficiently small rubber particles that are dispersed well enough in the matrix, which results in a tough material, while the unavoidable deterioration of its stiffness and yield strength is still at an acceptable level.

Particle Size and Interparticle Distance

It has been already well established that the impact resistance of rubber- toughened blends depends strongly not only on a concentration but also on size and size distribution of the rubber particles (Bucknall 1977). Generally, small particles (average diameter in the range 0.2–0.4 μm) are the most efficient in toughening

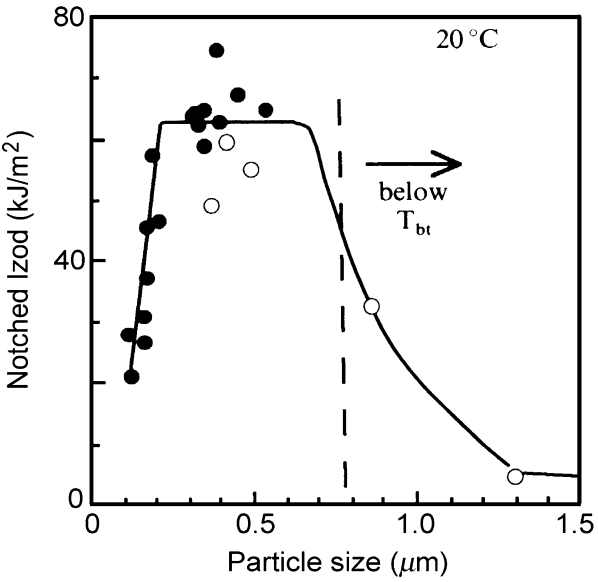

Fig. 11.26 Impact strength of PA-6/EPR blends as a function of particle size (26 vol.% of EPR rubber; notched Izod impact test at 20 °C): the different symbols refer to different manufacturing methods (From Gaymans (1994); reproduced with permission of Springer)

of these polymers for which shear yielding is the dominating mechanism of deformation and energy absorption. Significantly larger particles (D = 2–3 μm) appear, in turn, more effective when multiple crazing is the main mechanism of deformation.

It is now commonly recognized that the rubber particles play two major roles in the toughening of polymers: they generate a local stress concentrations (Bucknall 1977, 2000; Kausch 1983; Kausch 1987, 1990; Kinloch and Young 1983), and secondly, they modify the yield conditions for the matrix by altering significantly the stress state around cavitated particles and by increasing sensitivity of the yield to the mean stress, through transformation of the once continuous solid material into the porous (cellular) due to either particle cavitation or debonding (Bucknall and Paul 2009, 2013). The particles themselves should not initiate any fracture process; therefore, they should be sufficiently small to avoid excessive growth of voids up to the size of the critical flaw that can already cause crack initiation. On the other hand, in order to promote a necessary cavitation, they cannot be too small either (Bucknall 2000, 2007b; Bucknall and Paul 2009; Dompas and Groeninckx 1994; Lazzeri and Bucknall 1993). Numerous studies confirmed that for a given blend composition, optimum (high) toughness can be obtained only in certain, limited range of particle size. This size window was frequently found to be quite narrow. This feature can be illustrated by the results obtained for PA6/EPR blends of the constant overall compositions (26 vol.% of the rubber), in which the average particle size of the rubber was adjusted by variation in processing method or conditions, reported by Gaymans, Borggreve, and coworkers (Borggreve and Gaymans 1989; Borggreve et al. 1987, 1988, 1989a, b; Gaymans 2000; Gaymans et al. 1990) and presented in Fig. 11.26. They included in their study the blends with

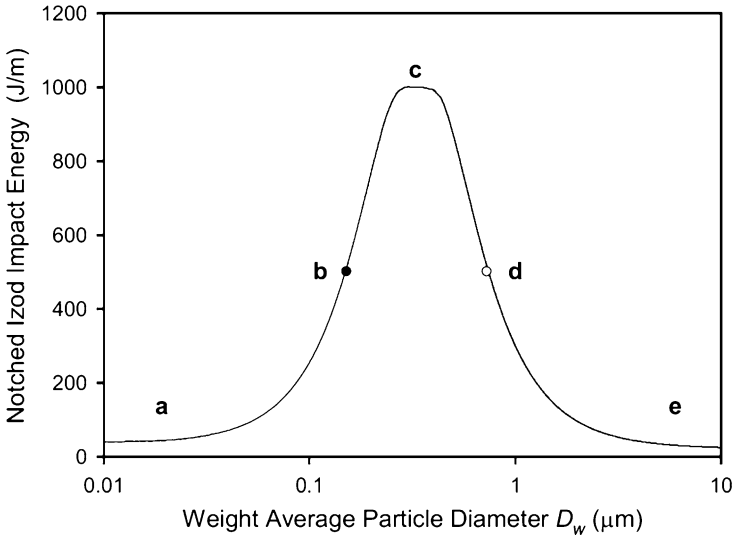

Fig. 11.27 Relationship between particle size and impact behavior for a typical "super-tough" thermoplastic blend. Points *b* and *d* mark *lower* (●) and *upper* (o) ductile–brittle transitions. Schematic representation based broadly on data of Huang et al. (2006a) for a series of 80/20 rubber-toughened PA6 blends (From Bucknall and Paul (2009); reproduced with permission of Elsevier)

large, medium, but also very small particles and performed impact tests at various temperatures. The obtained results demonstrated that these PA6/EPR blends exhibited both a lower and an upper ductile–brittle (DB) transition with respect to the particle size and that the upper critical particle size appeared temperature dependent, varying continuously from 0.5 μm at $T = -10^{\circ}C$ to 1.5 μm at $T = 50^{\circ}C$ as found in blends containing 20 wt.% (26 vol.%) of grafted EPDM rubber. Further extensive work has confirmed the existence of a minimum particle size for effective toughening in other semicrystalline as well as amorphous blends containing a variety of different elastomers (Dompas and Groenickx 1994; Dompas et al. 1994a, b; Huang et al. 2006a, b; Majumdar et al. 1994d; Okada et al. 2000; Oshinski et al. 1996c). There is now a substantial collection of papers which evidenced the effects of particle size on impact behavior in a wide range of polyamide (Borggreve and Gaymans 1989; Borggreve et al. 1987, 1989a, b; Gaymans 1994, 2000; Gaymans et al. 1990; Hobbs et al. 1983; Majumdar et al. 1994a, b, c, d, e; Oshinski et al. 1992a, b, 1996c; Takeda and Paul 1992; Wu 1983, 1985), polyesters (Gaymans 2000; Hage et al. 1997, 1999a, b, c, d, e), and polypropylene blends (Jang et al. 1984, 1985; Jiang et al. 2000, 2004a, b; Liang and Li 2000).

On the basis of numerous experimental data, Bucknall and Paul (2009) have proposed a model general curve illustrating the dependence of impact strength on average particle size. That curve, shown in Fig. 11.27, was drawn to follow the

results obtained for a representative "super-tough" rubber-toughened PA6 blend (Huang et al. 2006a). Similar curves can be obtained with appropriate scaling for other rubber-toughened blends as well. As illustrated in Fig. 11.27, moving beyond the preferred size range (around the optimum marked by **c**) in either direction results in a ductile–brittle transition, where **b** and **d**, respectively, mark the lower and upper transitions. These points define lower and upper critical particle sizes.

In his pioneering work, Wu (1985) studied PA6,6 blends with10–25 % of grafted polyolefin rubber and average particle sizes varying from 0.3 to 3.0 μm. He observed in these blends a ductile-to-brittle transition similar to that shown in section **c**–**e** of Fig. 11.27, as expected. He also found the critical average particle size D_{crit} increasing systematically with rubber content (see Fig. 11.28a), which seems against the prediction of the model curve in Fig. 11.27, which shows also a lower critical particle size while does not predict any dependence on the rubber concentration. This behavior is probably because only blends with particles larger than 0.3 μm were studied, i.e., still above the expected lower DB transition. The intriguing observation was, however, that when plotting impact strength against the calculated average interparticle distance ID, a single critical value, ID_{crit} was found. This critical interparticle distance was independent on rubber concentration and appeared to control exclusively the upper ductile–brittle transition, cf. Fig. 11.28b. On this basis, Wu concluded that the average particle size is not the primary parameter controlling the impact resistance. He proposed then to use the interparticle distance ID instead, which, in his opinion, is the principal parameter. The interparticle distance ID, which was defined as the distance between surfaces of two adjacent rubber particles, referred later to as the matrix ligament thickness is, according to Wu, the crucial morphological parameter which governs the toughening efficiency in rubber-modified blends.

Making two simplifying assumptions that all particles have the same diameter D and are packed in a regular array, Wu derived the following expression for ID (Wu 1992):

$$\mathrm{ID} = \mathrm{D}\left[k\left(\frac{\pi}{6\phi}\right)^{\frac{1}{3}} - 1\right] \tag{11.28}$$

where D is the particle diameter and k is a parameter dependent on lattice packing arrangement, with $k = 1$ for simple cubic lattice and $k = 1.12$ for face-centered cubic (fcc) or hexagonal closed packing (hcp). Margolina and Wu have introduced the term "matrix ligament thickness" to describe ID, in order to shift the focus from the rubber particles to the matrix material (Margolina and Wu 1988). To explain the dependence of BD transition on ligament thickness, they use the percolation concept (Margolina and Wu 1988; Wu 1992). If the particles cavitating internally are close enough, then the zones of yielded matrix around both particles come into contact, so that the thin matrix ligaments between particles become fully yielded across. For small ID, these ligaments become interconnected, and the yielding process percolates across the specimen, stimulating its ductile

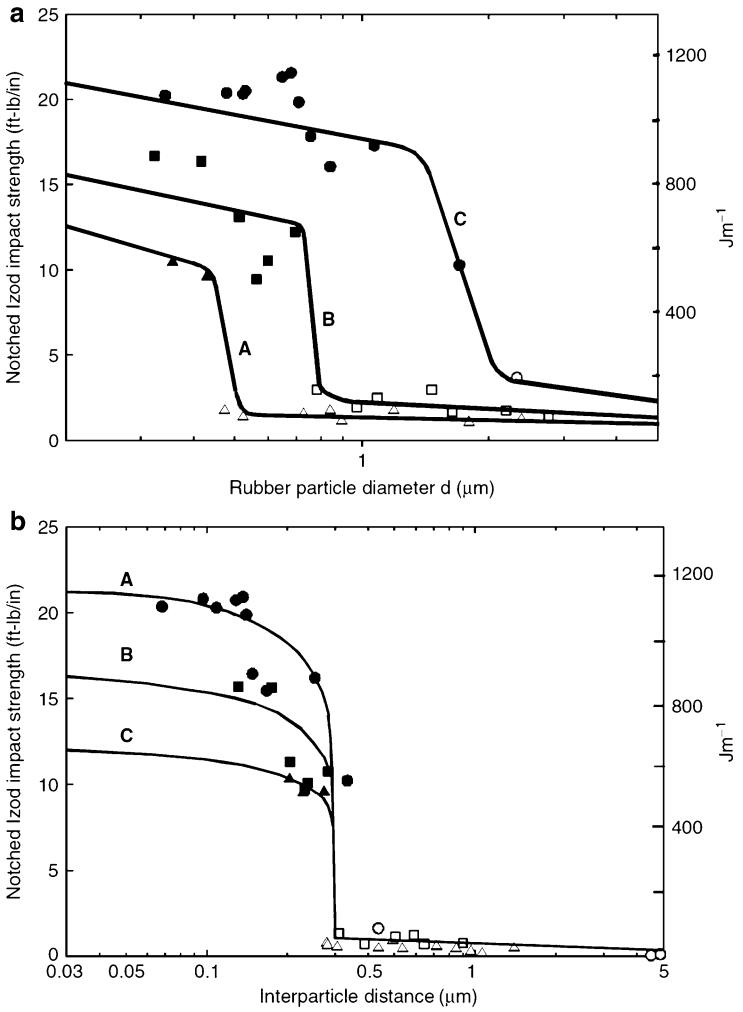

Fig. 11.28 (**a**) Notched Izod impact strength versus rubber particle diameter in PA 6,6/reactive rubber blends (curve A, 10 wt.% rubber; curve B, 15 wt.%; curve C, 20 wt.% rubber). (**b**) The same Izod impact strength data plotted versus interparticle distance (From Wu (1985); reproduced with permission of Elsevier)

deformation behavior. This occurs when the thickness of the matrix ligaments falls below the critical thickness. Such a state can be achieved for a given rubber volume fraction by decreasing the particle size and enhancing their dispersion. These ideas have been elaborated over the years by other researchers (Jiang et al. 2000, 2004a, 2008; Liu et al. 1998a, b, 1999; Sjoerdsma 1989).

To explain the observed effect of the interparticle distance, Wu proposed first that a strong overlap of the stress fields around particles induces shear yielding in PA6,6 matrix, turning the blend ductile. Later, however, Wu recognized

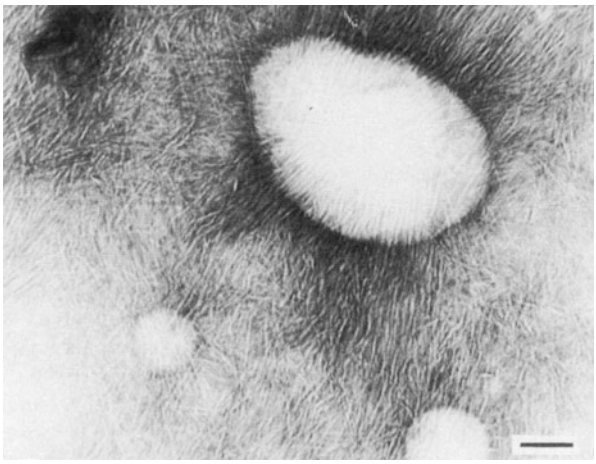

Fig. 11.29 TEM micrograph of PA6 modified with EPDM-g-MA. The sample was negatively stained with phosphotungstic acid. The *dark lines* are the amorphous regions and the *white lines* are the lamellae. The rubber particles are not stained and appear white. The scale bars represents 100 nm (From Muratoglu et al. (1995d); reproduced with permission of Elsevier)

deficiencies of this model, since the local stress level depends on the ratio of the center-to-center distance (L = D + ID) to the diameter of the particle, L/D (Wu 1988). This ratio scales to volume fraction of particles and remains constant at a given volume fraction regardless of particle size, so that according to the stress field overlap model, toughening should be unaffected by the presence of large particles at any given L/D ratio. This, however, does not agree with the experimental results which demonstrate that small particles are certainly more effective in toughening than large ones (Borggreve et al. 1987; Bucknall and Paul 2009). A second proposed model was based on the transformation of the matrix material from a state of plane-strain to plane-stress when the volume fraction of cavitating rubber particles increases and the interparticle distance reduces below the critical size. This approach also fails because it attributes the embrittlement directly to the presence of high triaxial stresses. Those triaxial stresses in interparticle ligaments can be affected only by changing the geometrical ratios, but these ratios actually remain constant for a given volume fraction of the particles irrespective of their size.

To explain the sense of the ligament thickness parameter in semicrystalline polymers, Muratoglu et al. (1995d) proposed a model based on an specifically oriented crystalline layer of limited thickness (~0.15 μm for PA6,6 matrix) which forms upon matrix crystallization and extends radially from the surface of each rubber particle (Muratoglu et al. 1995a, b, c, d). This approach considered that in a tough blend where the rubber particles are closer than double the thickness of the oriented layer (~0.3 μm for PA6,6), the crystalline structure within the entire cross section of the interparticle ligament is well and specifically oriented. Crystalline lamellae oriented perpendicularly to the rubber–matrix interface were evidenced by TEM. Such a morphology surely induces a real anisotropy within the interparticle ligament zones, cf. Fig. 11.29. In these anisotropic zones, a considerable fraction of crystals is oriented with hydrogen-bonded (001) plane that appears as the plane of the easiest crystallographic slip, parallel to the rubber–matrix interface in the

interparticle ligament. As a result, the plastic shear resistance of ligaments is significantly reduced as compared to the isotropic matrix. Due to percolation effect, the entire deformation zone can deform extensively at the reduced stress, which eventually results in a super-tough material response. This approach was supported by microscopic observations of morphological features in the stress-whitened plastic process zones of tensile and Izod impact specimens, confirming the important role of the local orientation within ligaments. Similar local orientation behavior, leading to much enhanced impact strength, was postulated also for blends of polyethylene with various rubbers as well as those with stiff particles of $CaCO_3$ mineral filler (Bartczak et al. 1999a, b, c). In the latter case, debonding of stiff particles played the same role as rubber cavitation for yield initiation. Bucknall and Paul (2009) remarked critically that "the hypothesis of Muratoglu is not consistent with the strong relationship observed by Gaymans and co-workers (Borggreve and Gaymans 1989; Borggreve et al. 1988, 1989a, b; Gaymans 2000) between critical particle size and temperature, nor with recent work by Huang et al. which shows that the impact behavior of 80/20 rubber-toughened blends based on the amorphous polyamide Zytel 330 is very similar to that of 80/20 blends based on PA-6" (Huang et al. 2006a, b; Huang and Paul 2006).

Corte and Leibler (Corte et al. 2005; Corte and Leibler 2007) compared the characteristic lengths and deformation processes involved in toughening. On this basis they tried to explain a critical ligament thickness governing toughening of semicrystalline polymers by the existence of a characteristic confinement length that is governing the fracture behavior. They envisaged fracture of a semicrystalline polymer as a process in which a great number of very small nano- or submicron-sized cracks open in poorly cohesive amorphous layers and accumulate in the semicrystalline material long before its final rupture. A brittle fracture eventually occurs when these submicron cracks coalesce to form a flaw bigger than critical which happens at certain critical concentration, ρ^*, estimated on the order of 10^{14}–10^{16} cm^{-3} for semicrystalline polymers. This critical concentration implies the existence of a critical distance between nano- and submicron cracks $\xi^* \propto \rho^{*-1/3}$, estimated on the order of 100 nm. Analyzing the stress and strain state across the interparticle matrix ligament between cavitated particles, Corte and Leibler predicted that a small zone near particle equator should begin to yield due to high stress concentrations. Such yielded zones around neighboring particles would confine the elastically strained central part of the ligament between these particles. Now, if the width of this central part of the ligament is larger than the critical distance between nano- and microcracks ξ^* characteristic for a given polymer, then the discussed confinement by yielded zones does not affect crack coalescence, and a brittle fracture can propagate as in unmodified polymer. However, if this distance is smaller than ξ^*, the confinement can appear strong enough to shield interactions between microcracks and inhibit their coalescence. As a consequence, a brittle fracture does not develop. Instead, a plastic deformation can be activated, resulting in enhanced toughness. According to this approach, material becomes tough when the initial ligament thickness ID is smaller than a critical confinement length ID_{crit}, given by the equation (Corte and Leibler 2007):

$$\mathrm{ID}_{\mathrm{crit}} = \xi^* + \mathrm{D}\left(\frac{C\sigma_B}{\sigma_y}\right)^2 \tag{11.29}$$

where ξ^* is the critical distance between microcracks; D is the particle diameter; σ_B and σ_y are fracture and shear yield stress, respectively; and C is a dimensionless parameter depending on the ability of particles to release the stress and on the criterion for brittle stress. This equation suggests that $\mathrm{ID}_{\mathrm{crit}}$ depends not only on the matrix characteristics given by the critical distance ξ^*, σ_B, and σ_y but also directly on the particle diameter D. This model was applied to an interpretation of experimental data of polyamide-based blends and to demonstrate how the critical confinement length depends on material properties, temperature, and processing history. The model revealed an initially unexpected particle size effect: the critical interparticle distance $\mathrm{ID}_{\mathrm{crit}}$ varied linearly with the particle diameter and inversely with the square of the shear yield stress (Eq. 11.29). These findings demonstrate according to Bucknall and Paul that there is practically no advantage in using ID instead of D as a basis for comparisons of toughness data, especially as D is easier to measure experimentally, and ID is usually estimated indirectly (Bucknall and Paul 2009).

Bucknall and Paul (2009, 2013) reviewed and commented on the deficiencies of the interparticle spacing concept. They finally concluded that "there are sound reasons for abandoning the concept of interparticle spacing altogether. The alternative is to base all discussions of impact behavior on the size and volume fraction of rubber particles, which are known to affect fracture resistance in all polymer blends. From this perspective, any correlations involving interparticle spacings should be regarded as purely fortuitous" (Bucknall and Paul 2009). Consequently, they proposed an alternative approach, based on a new model for deformation and fracture of blends under the constraints imposed on the notch tip in Izod or Charpy specimens. This model is based on three stress criteria, which define critical conditions for rubber particle cavitation, dilational shear yielding, and craze initiation, respectively, described already in Sects. 11.5.2, 11.5.3, 11.5.4, and 11.5.5. The three criteria were used together with stress field equations to determine limits within which each of these mechanism can be activated in the notched or sample, and find in this way the sequence in which the various criteria are satisfied in a developing plane-strain deformation zone. This allowed to identify the mechanisms that govern fracture toughness under specific loading conditions in notched impact tests and to predict the relationships between rubber particle diameter and the impact strength.

Void formation plays a key role in this description of rubber toughening. At initial deformation stage, prior to rubber particle cavitation, very high constraints are imposed on the shear yielding in the plane-strain region of the notched sample, and therefore the local stress in the yield zone can increase rapidly up to the point of initiation of brittle fracture from the notch tip, which happens before any significant plastic deformation and energy dissipation has taken place. In order to obtain higher toughness, the blend must be capable of activating a widespread cavitation at

stresses still below the level required to generate shear yielding in a fully constrained, void-free material, the level of which under plane-strain conditions ahead of notch tip appears very high. This is possible only if the blend contains particles of average size above the critical minimum size (which is about 0.03 μm in blends of polyamides with elastomers). On the other hand, large particles tend to induce crazing upon the early stages of the test which leads to premature failure of the plastic zone and much lower energy absorption. Therefore, large particles, especially above approximately 1 μm in diameter, are not desirable. It appears that for many high-performance blends, the optimum particle size is about 0.3 μm.

The basic relationships between deformation behavior and the particle size are presented in Fig. 11.30. These plots were prepared by Bucknall and Paul to summarize their model of particle size dependence (Bucknall and Paul 2009, 2013). They indicate the ranges of the particle size in which the phenomena of particle cavitation, matrix shear yielding, and crazing, in sequence, control the maximum stress which can be supported by the blend under the plane-strain conditions, as, e.g., in notched impact tests. The basis for comparison is the critical major principal stress, σ_{1c}, which is an important parameter, controlling both the radius of the plastic zone and its susceptibility to fracture. Using this parameter enables to compare the critical stresses for cavitation, shear yielding, and craze initiation directly by means of a simple two-dimensional plot of σ_{1c} against log(D), although, in fact, cavitation is governed by the mean stress (pressure), shear yielding by the pressure-modified effective shear stress, and craze initiation by the applied tensile stress. For purposes of illustration, the plots in Fig. 11.30 are based on calculations done for a virtual series of idealized blends of dry PA6 with 20 wt.% of an olefin rubber which can be regarded as a representative case. Very similar charts can be calculated for other materials and/or test conditions as well.

Figure 11.30a shows how competition between the various deformation mechanisms affects the yield stress. The solid line denotes σ_{1c}, the critical value of σ_1 at the onset of shear yield, whether before (the first straight section, calculated with Eq. 11.17) or after cavitation. The cavitation stress curve was calculated with Eq. 11.14 scaled accordingly to fit experimental data of the real PA6/rubber blend. Finally, the craze initiation stress curve, similar to those shown in Fig. 11.23, was calculated with Eq. 11.25.

Under plane-strain loading conditions, the stresses (σ_1, σ_2, σ_3) on the crack plane are equal to (σ,σ, $2\nu\sigma$). The highest calculated value of σ_{1c} is about 108 MPa, which corresponds to shear yielding of the void-free PA/rubber blend – cf. Fig. 11.21,which illustrates shear yielding of the non-cavitated blend under plane strain taking place when the mean stress $\sigma_m = 100$ MPa and the effective stress $\sigma_e = 21.5$ MPa, i.e., when stresses on the crack plane reach 108,108, 87 MPa. If the particles are very small, D $<$ 0.03 μm, the cavitation stresses are higher than this σ_{1y}, so that the rubber does not cavitate, and constraints on shear yielding remain very high in the plane-strain region ahead of the notch. Yielding in a confined region close to the notch tip could take place

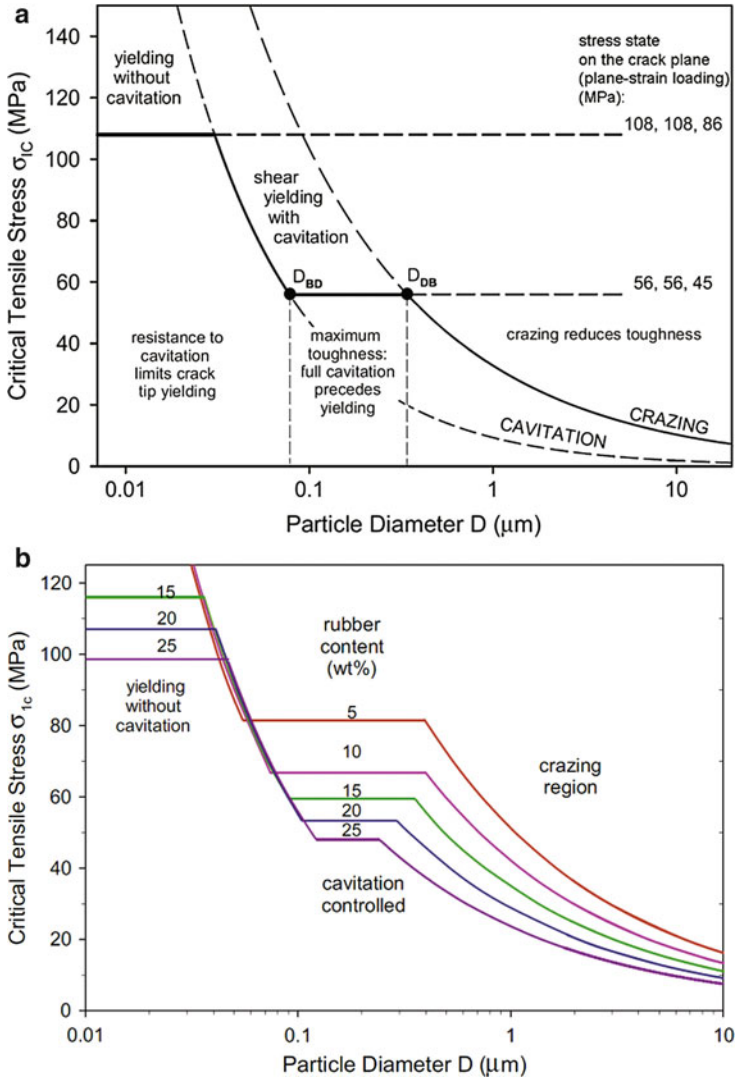

Fig. 11.30 (**a**) Critical stress map for PA6/rubber blends containing 20 % by weight (26.5 % by volume) of a lightly cross-linked olefin rubber, showing dependence of the critical major principal stress, on particle diameter. Craze line is calculated using Eq. 11.25 with E = 2.8 GPa and $G_{craze} = 0.2$ J/m^2. Shear yield stresses are calculated using Eq. 11.17, with pressure coefficient $\mu = 0.36$. *Solid line* defines critical stress for shear yielding, both with and without prior cavitation. Note that crazing and shear yielding can take place simultaneously in tough specimens containing relatively large particles (Adopted from Bucknall and Paul (2009); with permission of Elsevier). (**b**) Critical stress map for PA6/rubber blends containing various concentrations of rubber particles, showing the onset of rubber particle cavitation, shear yielding of cavitated blend, and crazing initiated by large particles (From Bucknall and Paul (2013); reproduced with permission of Elsevier)

without void formation, albeit at extremely high stresses (108,108, 87 MPa). Stresses of this magnitude do not develop in standard Izod or Charpy notched bars with rounded notch. Instead, local stresses increase quickly to the point of initiation of crack from the notch, leading to brittle fracture before reaching the high yield stress. By contrast, using the particle with size increasing above 0.03 μm enables the blend to cavitate before any fracture appears. Cavitation stress decreases with size, which causes a drop of the shear yield stress, down to $\sigma_{1c} = 56$ MPa (yield of the porous blend created by cavitation) at D ≈ 0.07 μm and to a significant increase of fracture toughness due to advancing plastic deformation. For even larger particles, the cavitation stress decreases below the shear yield stress of the fully cavitated blend; thus, the shear yield stress at plane strain is no longer a function of particle size. Consequently, an extensive dilatation shear yielding follows particle cavitation. This is the super-tough region, where K_I exceeds 3.5 $MPam^{0.5}$, and the radius of the plastic zone $r_p > 1$ mm. This dilatational shear yielding remains the dominating deformation mechanism until D ≈ 0.35 μm, the onset of the ductile–brittle transition, which occurs when the craze initiation curve crosses the line representing the shear yield. This crossing means that larger particles are likely to initiate crazes before the blend reaches its yield stress. Initiation and then propagation of crazes leads soon to failure of the plastic zone. As a result, impact strengths of the blend is reduced again. Summarizing, this chart explains the two brittle–ductile transitions, the lower brittle-to-ductile transition at $D_{BD} \approx 0.03$–0.08 μm, determined by the transition from brittle fracture in the absence of cavitation to dilatational shear yielding prompted by cavitation, and the upper ductile-to-brittle transition at $D_{DB} \approx 0.35$ μm, which is determined by the change from cavitation/yielding to crazing response. The optimum toughness is reached in the range of activity of cavitation and shear yielding, roughly at particle sizes between 0.1 and 0.3 μm.

Figure 11.30b is variant of Fig. 11.30a that illustrates the expected influence of the rubber concentration. It can be seen that critical stresses for yielding and for crazing tend to decrease with increasing concentration, but the same pattern of particle size dependence, discussed above, is valid for all composition. On the other hand, the range of particle size for which a super-tough behavior may be expected, limited by the upper ductile–brittle transition (transition from dilatational yield to crazing), drifts down with ϕ, which results in narrowing the size range optimum for toughening. What is more important, the yield stress goes down with increasing ϕ, which significantly reduces the probability of premature failure before the yield zone has fully developed. It must be noted, however, that once a high level of toughness has been achieved, any further increase of the rubber concentration becomes useless since the small expansion of the yield zone at the expense of a stronger reduction in the yield stress, so that total dissipated energy gradually decreases (Bucknall and Paul 2013).

The plots presented in Figs. 11.30a,b should be considered as diagrams which might appear useful in the interpretation of the notched impact toughness data, rather than a tool for predicting fracture resistance of any actual blend.

11.6 Concluding Remarks

Modification of polymers by blending with other polymers is known as an effective and economically justified method of enhancing their mechanical performance. Apart from modification of mechanical properties at low deformation rates, the most important target is the enhancement of toughness, especially at high deformation rates, including notched impact conditions.

Most of the amorphous glassy polymers tend to fracture in a brittle manner. Semicrystalline polymers, when unnotched, often fracture in a ductile manner, yet in the presence of a notch or other defects become brittle. Both amorphous and semicrystalline polymers can be made tougher by modification with particles of elastomers and in selected cases also with particles of other polymers or even stiff fillers. The change from brittle to ductile behavior is realized by promoting the deformation mechanism, either crazing or shear yielding, whichever is characteristic for a given polymer when in pristine form, in order to facilitate an extensive plastic deformation in possibly large volume of the sample that allows to dissipate large amounts of energy. The primary function of the particles is to cavitate (either internally or by debonding) and thereby produce changes in the local stress state in their adjacent vicinity that can facilitate the plastic response of the matrix. More importantly, cavitation transforms a continuous solid material into porous one, which demonstrates much higher sensitivity of the yield stress to the mean stress. This feature is crucial, especially in notched specimens, because it enables the blend to yield at moderate stresses still under plane-strain conditions found in front of the notch or crack tip. Recent studies indicate that the elimination of geometrical constraints and raising the state of plane-stress is not the primary role of cavitation, as some researchers have suggested in the past. Cavitation itself absorbs energy, but this is only a small fraction of the total fracture energy. The vast part of the impact energy is dissipated due to plastic deformation. Cavitation of the particles is, however, prerequisite for the enhanced ductile deformation.

The key to tough or super-tough impact behavior is the development of large and stable plastic zone, initially at the notch tip and then ahead of the propagating crack. One way of achieving this goal is to prepare the blend with high rubber contents ($>$25 % by volume), optimum particle sizes, and relatively low yield stresses. However, the high rubber content results also in a notably reduced material stiffness and therefore most frequently is not desirable. On the other hand, moderate yield stresses, obtained with the lower content of the rubber, and optimum particle sizes alone do not guarantee good toughening. Other material-related factors, including matrix chemistry and molecular weight, adhesion between particles and matrix, morphology of rubber particle shear modulus, and other properties of the rubber phase, are equally important in determining the total amount of energy absorbed and must be all taken into consideration when significant toughness improvement is demanded.

Average particle diameter of the rubber, D, and its volume fraction, ϕ, are among the most essential factors affecting the toughness of polymer blends. The concentration of the rubber must be well balanced in order to obtain material with

stiffness and strength, which are inevitably reduced, yet are still within acceptable limits. The optimum concentration of elastomer appears to be in the range from 5 to 20 wt.%. Regardless of the actual concentration, the average size of the rubber particles, together with its distribution, is the most important parameter. It is well known that there is an optimum range of particle sizes for which tough response in many systems may be expected, which is roughly from 0.1 to 0.5 μm for the majority of the blends, in which the shear yielding is the principal energy-absorbing deformation mechanism. To obtain tough materials on the basis of crazable polymers, larger particles, usually 2–3 μm in diameter, are necessary.

Acknowledgments The project was financed in part from funds of the National Science Centre of Poland on the basis of the decision number 2012/04/A/ST5/00606. Statutory fund of the Centre of Molecular and Macromolecular Studies, Polish Academy of Sciences is also acknowledged.

11.7 Cross-References

▶ Miscible Polymer Blends
▶ Morphology of Polymer Blends
▶ Polyethylenes and Their Blends
▶ Polymer Blends: Introduction
▶ Properties and Performance of Polymer Blends
▶ Reactive Compatibilization

Notations and Abbreviations

Symbols

C_∞ Chain stiffness parameter
D Particle diameter
$\mathbf{D_{BD}}$, $\mathbf{D_{DB}}$ Diameter of particle for brittle–ductile and ductile–brittle transition
d_e Entanglement mesh size
DB Ductile–brittle transition
E, $\mathbf{E_M}$ Young's modulus, modulus of the matrix
$\mathbf{E_R}$ Young's modulus of the rubber particle
f_z Function of the free volume accounting for the effect of the physical aging on crazing stress
f_y Function of the free volume accounting for the effect of the physical aging on yieldstress
G_{craze} Energy absorbed in formation of unit area of a craze
$\mathbf{G_{IC}}$ Fracture surface energy
$\mathbf{G_M}$ Shear modulus of the matrix
$\mathbf{G_R}$ Shear modulus of the rubber particle

ID Interparticle distance (matrix ligament thickness)
$\mathbf{ID_{crit}}$ Critical interparticle distance
K Bulk modulus
$\mathbf{K_I}$ Stress intensity factor
l^2 Mean-square length of a statistical unit of the chain
$\mathbf{M_v}$ Molecular mass of a statistical skeletal unit
m_p Plastic constraint factor
n_v Number of statistical skeletal units in the chain
P Pressure
R_o^2 Mean-square end-to-end distance of an unperturbed chain
R Radius of the particle
r_p Radius of the plastic zone
r_{vd} Radius of the void
$\mathbf{T_{BD}}$ Temperature of brittle–ductile transition
$\mathbf{T_g}$ Temperature of glass transition
U_{ch} Bond energy of polymer chain
U_p Potential energy of the rubber particle
α Coefficient of thermal expansion
δ Cohesive energy density
ε_v Volume strain
ϕ Volume concentration of the rubber in the blend
$\mathbf{\Phi_p}$ Volume fraction of particles
$\mathbf{\Phi_{vd}}$ Volume fraction of voids
Ψ Inclination angle of the dilatation band
Γ Surface energy of the craze
$\mathbf{\Gamma_r}$ Surface energy of rubber particle
γ Van der Waals surface energy
λ_f Extension ratio of the rubber at fracture
ν_e Entanglement density
ν Poisson's ratio
μ Pressure sensitivity coefficient
ρ_a Density of amorphous polymer
ρ^* Critical concentration of submicron-sized cracks
ξ^* Critical distance between submicron cracks
σ_1 Applied tensile stress
σ_{1c} Critical major tensile stress
σ_{craze} Craze initiation stress
σ_{1craze} Critical tensile stress for craze initiation
σ_B Fracture strength
σ_e Effective (deviatoric) yield stress
σ_m Mean stress
σ_y Yield stress
σ_{y0} Yield stress in pure shear
σ_{yt} Yield stress in tension

Abbreviations

ABS Acrylonitrile–butadiene–styrene copolymer
EPDM Ethylene–propylene–diene terpolymer
EPR Ethylene–propylene copolymer
GMA Glycidyl methacrylate
HDPE High-density polyethylene
HIPS High-impact polystyrene
MA Maleic anhydride
PA Polyamide
PBA Poly(butyl acrylate)
PBT Poly(butylene terephthalate)
PC Polycarbonate
PE Polyethylene
PET Poly(ethylene terephthalate)
PMMA Poly(methyl methacrylate)
POM Polyoxymethylene
PP Polypropylene
PPO Poly(phenylene oxide)
PS Polystyrene
PVDF Polyvinylidene fluoride
PVC Poly(vinyl chloride)
SAN Styrene–acrylonitrile copolymer
SBS Styrene-butadiene-styrene block copolymer
SEBS Styrene–ethylene–butene-1–styrene block copolymer

References

M. Abate, V. Di Liello, E. Martuscelli, P. Musto, G. Ragosta, G. Scarinzi, Polymer **33**, 2940–2948 (1992)
I.A. Abu-Isa, C.B. Jaynes, J.F. O'Gara, J. Appl. Polym. Sci. **59**, 1957–1971 (1996)
A.M. Aerdts, G. Groenickx, H.F. Zirkzee, H.A.M. van Aert, J.M. Geurts, Polymer **38**, 4247–4252 (1997)
K. Akkapeddi, Rubber toughening of polyamides by reactive blending, in *Reactive Polymer Blending*, ed. by W. Baker, C. Scott, G.-H. Hu (Hanser Publishers, Munich, 2001), pp. 207–253
A.S. Argon, Polymer **52**, 2319–2327 (2011)
A.S. Argon, *The Physics of Deformation and Fracture of Polymers* (Cambridge University Press, Cambridge, 2013)
A.S. Argon, R.E. Cohen, Polymer **44**, 6013–6032 (2003)
A.S. Argon, J.G. Hannoosh, Philos. Mag. **36**, 1195–1216 (1977)
A.S. Argon, M.M. Salama, Philos. Mag. **36**, 1217–1234 (1977)
A.S. Argon, R.E. Cohen, A.C. Patel, Polymer **40**, 6991–7012 (1999)
A.S. Argon, Z. Bartczak, R.E. Cohen, O.K. Muratoglu, Novel mechanism of toughening semi -crystalline polymers, in *Toughening of Plastics: Advances in Modelling and Experiments*, ed. by R.A. Pearson, H.-J. Sue, A.F. Yee. ACS Symposium Series, vol. 759 (Oxford University Press, London, 2000), pp. 98–124

A.S. Argon, A. Galeski, T. Kazmierczak, Polymer **46**, 11798–11805 (2005)
A. Arostegui, J. Nazabal, Polymer **44**, 5227–5237 (2003)
B.M. Badran, A. Galeski, M. Kryszewski, J. Appl. Polym. Sci. **27**, 3669–3681 (1982)
F.J. Balta-Calleja, G.H. Michler (eds.), *Mechanical Properties of Polymers Based on Nano-Structure and Morphology* (Taylor and Francis, Boca Raton, 2005)
L.L. Ban, M.J. Doyle, M.M. Disko, G.R. Smith, Polym. Commun. **29**, 163–165 (1988)
Z. Bartczak, J. Macromol. Sci. Phys. **B41**, 1205–1229 (2002)
Z. Bartczak, A. Galeski, Macromol. Symp. **294**, 67–90 (2010)
Z. Bartczak, E. Martuscelli, A. Galeski, Primary spherulite nucleation in polypropylene-based blends, in *Polypropylene. Structure, Blends and Composites*, ed. by J. Karger-Kocsis. Copolymers and Blends, vol. 2 (Chapman and Hall, London, 1995), pp. 25–49
Z. Bartczak, A.S. Argon, R.E. Cohen, T. Kowalewski, Polymer **40**, 2367–2380 (1999a)
Z. Bartczak, A.S. Argon, R.E. Cohen, M. Weinberg, Polymer **40**, 2331–2346 (1999b)
Z. Bartczak, A.S. Argon, R.E. Cohen, M. Weinberg, Polymer **40**, 2347–2365 (1999c)
F.S. Bates, R.E. Cohen, A.S. Argon, Macromolecules **16**, 1108–1114 (1983)
J.-C. Bauwens, J. Polym. Sci **A2 5**, 1145–1156 (1967)
R.S. Beck, S. Gratch, S. Newman, K.C. Rusch, J. Polym. Sci. Part B Polym. Lett. **6**, 707–709 (1968)
R.L. Bergen, Appl. Polym. Symp. **7**, 41–51 (1968)
L.L. Berger, Macromolecules **23**, 2926–2934 (1990)
N. Billon, J.M. Haudin, Polym. Eng. Sci. **37**, 1761–1769 (1997)
R.J.M. Borggreve, R.J. Gaymans, Polymer **29**, 1441–1446 (1988)
R.J.M. Borggreve, R.J. Gaymans, Polymer **30**, 63–70 (1989)
R.J.M. Borggreve, R.J. Gaymans, J. Schuijer, J.F. Ingen-Housz, Polymer **28**, 1489–1496 (1987)
R.J.M. Borggreve, R.J. Gaymans, A.R. Luttmer, Macrolol. Symp. **16**, 195–207 (1988)
R.J.M. Borggreve, R.J. Gaymans, H.M. Eichenwald, Polymer **30**, 78–83 (1989a)
R.J.M. Borggreve, R.J. Gaymans, J. Schuijer, Polymer **30**, 71–77 (1989b)
P.B. Bowden, R.J. Young, Nature **229**, 23–25 (1971)
P.B. Bowden, R.J. Young, J. Mater. Sci. **9**, 2034–2051 (1974)
A.J. Brady, H. Kesskula, D.R. Paul, Polymer **35**, 3665–3672 (1994)
N.W.J. Brooks, M. Mukhtar, Polymer **41**, 1475–1480 (2000)
N. Brown, I.M. Ward, J. Mater. Sci. **18**, 1405–1420 (1983)
H.R. Brown, A.S. Argon, R.E. Cohen, O.S. Gebizlioglu, E.J. Kramer, Macromolecules **22**, 1002–1004 (1989)
R.A. Bubeck, D.J. Buckley, E.J. Kramer, H. Brown, J. Mater. Sci. **26**, 6249–6259 (1991)
R. Buchdahl, E. Nielsen, J. Appl. Phys. **21**, 482–487 (1950)
C.B. Bucknall, *Toughened Plastics* (Applied Science Publishers, London, 1977)
C.B. Bucknall, Adv. Polym. Sci. **27**, 121–148 (1978)
C.B. Bucknall, Rubber toughening, in *The Physics of Glassy Polymers*, ed. by R.N. Haward, R.J. Young, 2nd edn. (Chapman and Hall, London, 1997), pp. 363–412
C.B. Bucknall, Deformation mechanisms in rubber-toughened polymers, in *Polymer Blends, Vol. 2: Performance*, ed. by D.R. Paul, C.B. Bucknall (Wiley-Interscience, New York, 2000), pp. 83–117
C.B. Bucknall, Polymer **48**, 1030–1041 (2007a)
C.B. Bucknall, J. Polym. Sci. Part B Polym. Phys. **45**, 1399–1409 (2007b)
C.B. Bucknall, D.R. Paul, Polymer **50**, 5539–5548 (2009)
C.B. Bucknall, D.R. Paul, Polymer **54**, 320–329 (2013)
C.B. Bucknall, R.R. Smith, Polymer **6**, 437–446 (1965)
C.B. Bucknall, P. Davies, I.K. Partridge, J. Mater. Sci. **21**, 307–313 (1986)
C.B. Bucknall, P.S. Heather, A. Lazzeri, J. Mater. Sci. **24**, 2255–2261 (1989)
C.B. Bucknall, A. Karpodinis, X.C. Zhang, J. Mater. Sci. **29**, 3377–3383 (1994)
M.F. Butler, A.M. Donald, A.J. Ryan, Polymer **39**, 39–52 (1998)
A. Cecere, R. Greco, G. Ragosta, G. Scarinzi, Polymer **31**, 1239–1244 (1990)

V.P. Chacko, K.E. Karasz, R.J. Ferris, E.L. Thomas, J. Polym. Sci. B **20**, 2177 (1982)
C.M. Chan, J. Wu, J.X. Li, Y.K. Cheung, Polymer **43**, 2981–2992 (2002)
S. Cimmino, F. Coppola, L. D'Orazio, R. Greco, G. Maglio, M. Malinconico, C. Mancarella, E. Martuscelli, Polymer **27**, 1874–1884 (1986)
B. Cioni, A. Lazzeri, Compos. Interfac. **17**, 533–549 (2010)
A.A. Collyer (ed.), *Rubber Toughened Engineering Plastics* (Chapmann and Hall, London, 1994)
L. Corte, L. Leibler, Macromolecules **40**, 5606–5611 (2007)
L. Corte, B. Beaumeb, L. Leiblerer, Polymer **46**, 2748–2757 (2005)
B. Crist, C.J. Fisher, P.R. Howard, Macromolecules **22**, 1709–1718 (1989)
C.A. Cruz-Ramos, Core-shell impact modifiers, in *Polymer Blends, Vol. 2: Performance*, ed. by D.R. Paul, C.B. Bucknall (Wiley-Interscience, New York, 2000), pp. 137–176
O. Darras, R. Seguela, J. Polym. Sci. B **31**, 759–766 (1993)
A. Dasari, Q.-X. Zhang, Z.-Z. Yu, Y.-W. Mai, Macromolecules **43**, 5734–5739 (2010)
C. Deshmane, Q. Yuan, R.D.K. Misra, Mater. Sci. Eng. A **452–453**, 592–601 (2007)
K. Dijkstra, R.J. Gaymans, J. Mater. Sci. **29**, 3231–3238 (1994a)
K. Dijkstra, R.J. Gaymans, Polymer **35**, 332–335 (1994b)
K. Dijkstra, J. ter Laak, R.J. Gaymans, Polymer **35**, 315–322 (1994a)
K. Dijkstra, H. Wevers, R.J. Gaymans, Polymer **35**, 323–331 (1994b)
D. Dompas, G. Groeninckx, Polymer **35**, 4743–4749 (1994)
D. Dompas, G. Groeninckx, M. Isogawa, T. Hasegawa, M. Kadokura, Polymer **35**, 4750–4759 (1994a)
D. Dompas, G. Groeninckx, M. Isogawa, T. Hasegawa, M. Kadokura, Polymer **35**, 4760–4765 (1994b)
A.M. Donald, Failure mechanisms in polymeric materials, in *Rubber Toughened Engineering Plastics*, ed. by A.A. Collyer (Chapmann and Hall, London, 1994), pp. 1–28
A.M. Donald, Crazing, in *The Physics of Glassy Polymers*, ed. by R.N. Haward, R.J. Young, 2nd edn. (Chapman and Hall, London, 1997), pp. 295–341
A.M. Donald, E.J. Kramer, J. Mater. Sci. **17**, 1765 (1982)
I.L. Dubnikova, S.M. Berezina, A.V. Antonov, J. Appl. Polym. Sci. **94**, 1917–1926 (2004)
B. N. Epstein, U.S. Patent 4,174,358, 1979 (to du Pont)
A.G. Evans, Philos. Mag. **26**, 1327–1344 (1972)
J.D. Ferry, *Viscoelastic Properties of Polymers*, 2nd edn. (Wiley, New York, 1970)
E.A. Flexman, Polym. Eng. Sci. **19**, 564–571 (1979)
E.A. Flexman, ACS Polym. Prep. **29**, 189–190 (1988)
M.E. Fowler, J.W. Barlow, D.R. Paul, Polymer **28**, 1177–1184 (1987)
Q. Fu, G. Wang, J. Shen, J. Appl. Potym. Sci. **49**, 673–677 (1993)
A. Galeski, e-Polymers art. no. 026, 1–28 (2002)
R.J. Gaymans, Toughened polyamides, in *Rubber Toughened Engineering Plastics*, ed. by A.A. Collyer (Chapmann and Hall, London, 1994), pp. 210–242
R.J. Gaymans, Toughening of semicrystalline thermoplastics, in *Polymer Blends, Vol. 2: Performance*, ed. by D.R. Paul, C.B. Bucknall (Wiley-Interscience, New York, 2000), pp. 177–224
R.J. Gaymans, K. Dijkstra, Polymer **31**, 971–971 (1990)
R.J. Gaymans, J.W. van der Werff, Polymer **35**, 3658–3664 (1994)
R.J. Gaymans, R.J.M. Borggreve, A.J. Oostenbrink, Makromol. Chem. Macromol. Symp. **38**, 125–136 (1990)
O.S. Gebizlioglu, H.W. Beckham, A.S. Argon, R.E. Cohen, H.R. Brown, Macromolecules **23**, 3968–3974 (1990)
R. Gensler, C.J.G. Plummer, C. Grein, H.-H. Kausch, Polymer **41**, 3809–3819 (2000)
A.N. Gent, Rubber Chem. Techn. **63**, 49–53 (1990)
J.M. Gloagen, P. Steer, P. Gallliard, C. Wrotecki, J.M. Lefebvre, Polym. Eng. Sci. **33**, 748–753 (1993)
G. Gong, B.H. Xie, W. Yang, Z.M. Li, S.M. Lai, M.B. Yang, Polym. Test. **25**, 98–106 (2006)

A. Gonzales-Montiel, H. Kesskula, D.R. Paul, Polymer **36**, 4587–4603 (1995a)
A. Gonzales-Montiel, H. Kesskula, D.R. Paul, Polymer **36**, 4605–4620 (1995b)
A. Gonzales-Montiel, H. Kesskula, D.R. Paul, Polymer **36**, 4621–4637 (1995c)
M. Gordon, J.S. Taylor, J. Appl. Chem. **2**, 493–500 (1952)
D.J. Green, P.S. Nicholson, J.D. Emberg, J. Mater. Sci. **14**, 1657–1661 (1979)
A.L. Gurson, J. Eng. Mater. Technol. Trans. ASME **99**, 2–15 (1977a)
A.L. Gurson, in *CF 4 Fracture 1977, Waterloo, Canada, Vol. 2A*, ed. by D.M.R. Taplin (Pergamon Press, Oxford, 1977b), p. 357
E. Hage, H. Kesskula, D.R. Paul, Polymer **38**, 3237–3250 (1997)
W.R. Hale, H. Keskkula, D.R. Paul, Polymer **40**, 365–377 (1999a)
W.R. Hale, H. Keskkula, D.R. Paul, Polymer **40**, 3665–3676 (1999b)
W.R. Hale, H. Keskkula, D.R. Paul, Polymer **40**, 3353–3365 (1999c)
W.R. Hale, J.H. Lee, H. Keskkula, D.R. Paul, Polymer **40**, 3621–3629 (1999d)
W.R. Hale, L.A. Pessan, H. Keskkula, D.R. Paul, Polymer **40**, 4237–4250 (1999e)
C. Harrats, G. Groeninckx, Deformation mechanisms and toughness of rubber and rigid filler modified semicrystalline polymers, in *Mechanical Properties of Polymers based on Nano-Structure and Morphology*, ed. by F.J. Balta Calleja, G.H. Michler (Taylor and Francis, London, 2005), pp. 481–546
J.M. Haudin, Plastic deformation of semicrystalline polymers, in *Plastic Deformation of Amorphous and Semi-crystalline Materials*, ed. by B. Escaig, C. G'Sell (Les Editions de Physique, Paris, 1982), p. 291
R.N. Haward, R.J. Young (eds.), *The Physics of Glassy Polymers*, 2nd edn. (Chapman and Hall, London, 1997)
C. He, A.M. Donald, M.F. Butler, Macromolecules **31**, 158–164 (1998)
W. Heckmann, G.E. McKee, F. Ramsteiner, Structure-property relationship in rubber modified amorphous thermoplastic polymers, in *Mechanical Properties of Polymers Based on Nano-Structure and Morphology*, ed. by F.J. Balta-Calleja, G.H. Michler (Taylor and Francis, London, 2005), pp. 429–479
C.S. Henkee, E.J. Kramer, J. Polym. Sci. B **22**, 721–737 (1984)
M. Hert, Angew. Makromol. Chem. **196**, 89–99 (1992)
S.Y. Hobbs, R.C. Bopp, V.H. Watkins, Polym. Eng. Sci. **23**, 380–389 (1983)
J.J. Horst, J.L. Spoormaker, Polym. Eng. Sci. **36**, 2718–2726 (1996)
R.M. Hosti-Miettinen, M.T. Heino, J.V. Sappala, J. Appl. Polym. Sci. **57**, 573–586 (1995)
D.J. Hourston, S. Lane, Toughened polyesters and polycarbonates, in *Rubber Toughened Engineering Plastics*, ed. by A.A. Collyer (Chapmann and Hall, London, 1994), pp. 243–265
D.J. Hourston, S. Lane, H.X. Zhang, Polymer **32**, 2215–2220 (1991)
D.J. Hourston, S. Lane, H.X. Zhang, Polymer **36**, 3051–3054 (1995)
J.J. Huang, D.R. Paul, Polymer **47**, 3505–3519 (2006)
J.J. Huang, H. Keskkula, D.R. Paul, Polymer **47**, 639–651 (2006a)
J.J. Huang, H. Keskkula, D.R. Paul, Polymer **47**, 624–638 (2006b)
W.R. Hwang, G.W.M. Peters, M.A. Hulsen, H.E.H. Meijer, Macromolecules **39**, 8389–8398 (2006)
G.R. Irwin, Appl. Mater. Res.. **3**, 65–71 (1964)
G.R. Irwin, P.C. Paris, in *Fracture, an Advanced Treatise*, ed. by H. Liebowitz, vol. 3 (Academic, New York, 1971), p. 13
O. Ishai, L.J. Cohen, J. Compos. Mater. **2**, 302–315 (1968)
B.Z. Jang, D.R. Uhlmann, J.B. Vander Sande, J. Appl. Polym. Sci. **29**, 3409–3420 (1984)
B.Z. Jang, D.R. Uhlmann, J.B. Vander Sande, Polym. Eng. Sci. **25**, 643–651 (1985)
H. Janik, R.J. Gaymans, K. Dijkstra, Polymer **36**, 4203–4208 (1995)
W. Jiang, S.C. Tjong, R.K.Y. Li, Polymer **41**, 3479–3482 (2000)
W. Jiang, D. Yu, B. Jiang, Polymer **45**, 6427–6430 (2004a)
W. Jiang, D.H. Yu, L.J. An, B.Z. Jiang, J. Polym. Sci. B **42**, 1433–1440 (2004b)

W. Jiang, Y.X. Hu, J.H. Yin, J. Polym. Sci. B **46**, 766–769 (2008)
M. Kamal, C.S. Sharma, P. Upadhyaya, V. Verma, K.N. Pandey, V. Kumar, D.D. Agrawal, J. Appl. Polym. Sci. **124**, 2649–2656 (2012)
H. Kanai, A. Auerbach, A. Sullivan, J. Appl. Polym. Sci. **53**, 527–541 (1994)
T.-K. Kang, Y. kim, G. kim, W.-J. Chp, C.-S. Ha, Polym. Eng. Sci. **37**, 603–614 (1997)
H.H. Kausch (ed.), *Crazing in Polymers*. Advances in Polymer Science, vol. 52/53 (Springer, Berlin, 1983)
H.H. Kausch, *Polymer Fracture* (Springer, Berlin, 1987)
H.H. Kausch (ed.), *Crazing in Polymers, Vol. II*. Advances in Polymer Science, vol. 91/92 (Springer, Berlin, 1990)
H.H. Kausch, Macromol. Chem. Macromol. Symp. **41**, 1–8 (1991)
Y. Kayano, H. Kesskula, D.R. Paul, Polymer **37**, 4505–4518 (1996)
Y. Kayano, H. Kesskula, D.R. Paul, Polymer **38**, 1885–1902 (1997)
T. Kazmierczak, A. Galeski, A.S. Argon, Polymer **46**, 8926–8936 (2005)
A. Kelly, W.R. Tyson, A.H. Cottrell, Philos. Mag. **15**, 567–586 (1967)
M.A. Kennedy, A.J. Peacock, L. Mandelkern, Macromolecules **27**, 5297–5310 (1994)
H. Kesskula, Appl. Polym. Symp. **15**, 51–78 (1970)
H. Kesskula, D.R. Paul, Toughening agents for engineering polymers, in *Rubber Toughened Engineering Plastics*, ed. by A.A. Collyer (Chapmann and Hall, London, 1994), pp. 136–164
G.-M. Kim, G.H. Michler, Polymer **39**, 5689–5697 (1998a)
G.-M. Kim, G.H. Michler, Polymer **39**, 5699–5703 (1998b)
A.J. Kinloch, R.J. Young, *Fracture Behaviour of Polymers* (Applied Science Publishers, London, 1983)
F. Kloos, Angew. Makromol. Chem. **133**, 1–24 (1985)
M. Kowalczyk, E. Piorkowska, J. Appl. Polym. Sci. **124**, 4579–4589 (2012)
E.J. Kramer, Microscopic and molecular fundamentals of crazing, in *Crazing in Polymers*, ed. by H.H. Kausch. Advances in Polymer Science, vol. 52/53 (Springer, Berlin, 1983), pp. 1–56
E.J. Kramer, L.L. Berger, Fundamental processes of craze growth and fracture, in *Crazing in Polymers, Vol. II*, ed. by H.H. Kausch. Advances in Polymer Science, vol. 91/92 (Springer, Berlin, 1990), pp. 1–68
T. Kyu, J.M. Saldanka, M.J. Kiesel, Toughness enhancement in polycarbonate/polymethylmethacrylate blend via phase separation, in *Two-Phase Polymer Systems*, ed. by L.A. Utracki (Hanser Publishers, Munich, 1991), pp. 259–275
J. Laatsch, G.-M. Kim, G.H. Michler, T. Arndt, T. Sufke, Polym. Adv. Technol. **9**, 716–720 (1998)
F.F. Lange, Philos. Mag. **22**, 983–992 (1970)
P. Laurienzo, M. Malinconico, E. Martuscelli, G. Volpe, Polymer **30**, 835–841 (1989)
R.E. Lavengood, L. Nicolais, M. Narkis, J. Appl. Polym. Sci. **17**, 1173–1185 (1973)
A. Lazzeri, C.B. Bucknall, J. Mater. Sci. **28**, 6799–6808 (1993)
A. Lazzeri, C.B. Bucknall, Polymer **36**, 2895–2902 (1995)
A. Lazzeri, C.B. Bucknall, Recent development in the modelling of dilatational yielding, in *Toughening Plastics, Advances in Modeling and Experiments*, ed. by R.A. Pearson, H.J. Sue, A.F. Yee. ACS Symposium Series, vol. 759 (ACS, Washington, DC, 2000), p. 14
A. Lazzeri, Y.S. Thio, R.E. Cohen, J. Appl. Polym. Sci. **91**, 925–935 (2004)
A. Lazzeri, S.M. Zebarjad, M. Pracella, K. Cavalier, R. Rosa, Polymer **46**, 827–844 (2005)
J. Lei, R. Zhou, Polym. Eng. Sci. **40**, 1529 (2000)
J.Z. Liang, R.K.U. Li, J. Appl. Polym. Sci. **77**, 409–417 (2000)
L. Lin, A.S. Argon, Macromolecules **25**, 4011–4024 (1992)
L. Lin, A.S. Argon, J. Mater. Sci. **29**, 294–323 (1994)
Y. Lin, H. Chen, C.M. Chan, J. Wu, Macromolecules **41**, 9204–9213 (2008)
Y. Lin, H. Chen, C.-M. Chan, J. Wu, Polymer **51**, 3277–3284 (2010)
Y. Lin, H.B. Chen, C.M. Chan, J.S. Wu, J. Appl. Polym. Sci. **124**, 77–86 (2012)
Z.H. Liu, R.K.Y. Li, S.C. Tjong, Z.N. Qi, F.S. Wang, C.L. Choy, Polymer **39**, 4433–4436 (1998a)

Z.H. Liu, X.D. Zhang, X.G. Zhu, Z.N. Qi, F.S. Wang, R.K.Y. Li, C.L. Choy, Polymer **39**, 5047–5052 (1998b)
Z.H. Liu, R.K.Y. Li, S.C. Tjong, C.L. Choy, X.G. Zhu, Z.N. Qi, Polymer **40**, 2903–2915 (1999)
Z.H. Liu, K.W. Kwok, R.K.Y. Li, C.L. Choy, Polymer **43**, 2501–2506 (2002)
G. Liu, X. Zhang, Y. Liu, X. Li, H. Chen, K. Walton, G. Marchand, D. Wang, Polymer **54**, 1440–1447 (2013)
P.A. Lovell, M.S. El-Aaser (eds.), *Emulsion Polymerization and Emulsion Polymers* (Wiley, Chichester, 1997)
P.A. Lovell, J. McDonald, D.E.J. Saunders, R.J. Young, Polymer **34**, 61–69 (1993)
W. Loyens, G. Groeninckx, Polymer **43**, 5679–5691 (2002)
W. Loyens, G. Groeninckx, Polymer **44**, 4929–4941 (2003)
M. Lu, H. Kesskula, D.R. Paul, Polymer **34**, 1874–1885 (1993)
M. Lu, H. Kesskula, D.R. Paul, J. Appl. Polym. Sci. **58**, 1175–1188 (1995)
M. Lu, H. Kesskula, D.R. Paul, J. Appl. Polym. Sci. **59**, 1467–1477 (1996)
J.T. Lutz, D. Dunkelberger (eds.), *Impact Modifiers for PVC. The History and Practice* (Wiley, New York, 1992)
B. Majumdar, H. Kesskula, D.R. Paul, Polymer **35**, 4263–4279 (1994a)
B. Majumdar, H. Kesskula, D.R. Paul, J. Polym. Sci. B **32**, 2127–2133 (1994b)
B. Majumdar, H. Kesskula, D.R. Paul, Polymer **35**, 5468–5477 (1994c)
B. Majumdar, H. Kesskula, D.R. Paul, Polymer **35**, 1386–1398 (1994d)
B. Majumdar, H. Kesskula, D.R. Paul, Polymer **35**, 5453–5467 (1994e)
A. Margolina, S.H. Wu, Polymer **29**, 2170–2173 (1988)
J. Martinez-Salazar, J.C.C. Camara, F.J.B. Balta-Calleja, J. Mater. Sci. **26**, 2579–2582 (1991)
E. Martuscelli, P. Musto, G. Ragosta (eds.), *Advanced Routes for Polymer Toughening* (Elsevier, Amsterdam, 1996)
Y. Men, J. Riegel, G. Strobl, Phys. Rev. Lett. **91**, 95502-95501–95502-95504 (2003)
E.H. Merz, G.C. Claver, M. Baer, J. Polym. Sci. **22**, 325–341 (1956)
G.H. Michler, Micromechanical mechanisms of toughness enhancement in nanostructured amorphous and semicrystalline polymers, in *Mechanical Properties of Polymers Based on Nano-Structure and Morphology*, ed. by F.J. Balta Calleja, G.H. Michler (Taylor and Francis, London, 2005), pp. 375–428
G.H. Michler, F.J. Balta-Calleja, *Nano- and Micromechanics of Polymers* (Carl Hanser, Munich, 2012)
G.H. Michler, C.B. Bucknall, Plastics Rubber Compos. **30**, 110–115 (2001)
G.H. Michler, J.U. Starke, Investigation of micromechanical and failure mechanisms of toughened thermoplastics using electron microscopy, in *Toughened Plastics II: Novel Approaches in Science and Engineering*, ed. by C.K. Riew, A.J. Kinloch (American Chemical Society, Washington, DC, 1996), pp. 251–277
D.E. Mouzakis, N. Papke, J.S. Wu, J. Kerger-Korcsis, J. Appl. Polym. Sci. **79**, 842–852 (2001)
O.K. Muratoglu, A.S. Argon, R.E. Cohen, Polymer **36**, 2143–2152 (1995a)
O. K. Muratoglu, A. S. Argon, R. E. Cohen, M. Weinberg, Polymer **36**, 4787–4795 (1995b)
O.K. Muratoglu, A.S. Argon, R.E. Cohen, M. Weinberg, Polymer **36**, 4771–4786 (1995c)
O.K. Muratoglu, A.S. Argon, R.E. Cohen, M. Weinberg, Polymer **36**, 921–930 (1995d)
M.M. Nasef, H. Saidi, Mater. Chem. Phys. **99**, 361–369 (2006)
R. Neuber, H.A. Schneider, Polymer **42**, 8085–8091 (2001)
D. Neuray, K.-H. Ott, Angew. Makromol. Chem. **98**, 213–224 (1981)
S. Newman, in *Polymer Blends*, ed. by D.R. Paul, S. Newman, vol. 2 (Academic, New York, 1978), pp. 63–89
K.H. Nitta, K. Okamoto, M. Yamaguchi, Polymer **39**, 53–58 (1998)
K.H. Nitta, Y.-W. Shin, H. Hashiguchi, S. Tanimoto, M. Terano, Polymer **46**, 965–975 (2005)
W.J. O'Kane, R.J. Young, A.J. Ryan, J. Macromol. Sci. Phys. B **34**, 427–458 (1995)
O. Okada, H. Keskkula, D.R. Paul, Polymer **41**, 8061–8074 (2000)

K. Okamoto, K. Shiomi, T. Inoue, Polymer **35**, 4618–4622 (1994)
E.F. Oleinik, Polym. Sci. C **45**, 17–117 (2003)
E. Orowan, Rep. Prog. Phys. **12**, 185–232 (1949)
A.J. Oshinski, H. Kesskula, D.R. Paul, Polymer **33**, 268–283 (1992a)
A.J. Oshinski, H. Kesskula, D.R. Paul, Polymer **33**, 284–293 (1992b)
A.J. Oshinski, H. Keskkula, D.R. Paul, Polymer **37**, 4891–4907 (1996a)
A.J. Oshinski, H. Keskkula, D.R. Paul, Polymer **37**, 4919–4928 (1996b)
A.J. Oshinski, H. Keskkula, D.R. Paul, J. Appl. Polym. Sci. **61**, 623–640 (1996c)
A.J. Oshinski, H. Kesskula, D.R. Paul, Polymer **37**, 4909–4918 (1996d)
Y.C. Ou, F. Yang, Z.-Z. Yu, J. Polym. Sci. B **36**, 789–795 (1998)
R.J. Oxborough, P.B. Bowden, Philos. Mag. **28**, 547–559 (1973)
R.J. Oxborough, P.B. Bowden, Philos. Mag. **30**, 171–184 (1974)
J.-G. Park, D.-H. Kim, K.-D. Suh, J. Appl. Polym. Sci. **78**, 2227–2233 (2000)
D.S. Parker, H.J. Sue, J. Huang, A.F. Yee, Polymer **31**, 2267–2277 (1990)
M. Penco, M.A. Pastorino, E. Ochiello, F. Garbassi, R. Braglia, G. Gianotta, J. Appl. Polym. Sci. **57**, 329–334 (1995)
J.M. Peterson, J. Appl. Phys. **37**, 4047–4050 (1966)
J.M. Peterson, J. Appl. Phys. **39**, 4920–4928 (1968)
E. Piorkowska, A.S. Argon, R.E. Cohen, Polymer **34**, 4435–4444 (1993)
F. Polato, J. Mater. Sci. **20**, 1455–1465 (1985)
J. Qin, A.S. Argon, R.E. Cohen, J. Appl. Polym. Sci. **71**, 2319–2328 (1999)
F. Ramsteiner, W. Heckmann, Polym. Commun. **26**, 199–200 (1985)
T. Ricco, M. Rink, S. Caporusso, A. Pavan, An analysis of fracture initiation and crack growth in ABS resins, in *Toughening of Plastics II*, ed. by C.B. Bucknall (Plastics & Rubber Institute, London, 1985), pp. 27/21–27/29
J.A. Roetling, Polymer **6**, 311–317 (1965)
J.H. Rose, J.R. Smith, J. Ferrante, Phys. Rev. **28**, 1835–1845 (1983)
A. Rozanski, A. Galeski, Int. J. Plast. **41**, 14–19 (2013)
A. Sanchez-Solis, M.R. Estrada, J. Cruz, O. Manero, Polym. Eng. Sci. **40**, 1216–1225 (2000)
J.A. Schmitt, J. Appl. Polym. Sci. **12**, 533–546 (1968)
C.E. Schwier, A.S. Argon, R.E. Cohen, Philos. Mag. A **52**, 581–603 (1985)
C.E. Scott, C.W. Macosko, Int. Polym. Process. **10**, 36–45 (1995)
R. Seguela, J. Polym. Sci. B **40**, 593–601 (2002)
R. Seguela, O. Darras, J. Mater. Sci. **29**, 5342–5352 (1994)
R. Seguela, e-Polymers art. no. 032 (2007)
L.G. Shadrake, F. Guiu, Philos. Mag. **34**, 565–581 (1976)
N. Shah, J. Mater. Sci. **23**, 3623–3629 (1988)
S.J. Shaw, Rubber modified epoxy resins, in *Rubber Toughened Engineering Plastics*, ed. by A.A. Collyer (Chapmann and Hall, London, 1994), pp. 165–209
R.O. Sirotkin, N.W. Brooks, Polymer **42**, 3791–3797 (2001)
S.D. Sjoerdsma, Polymer **30**, 106–108 (1989)
J.U. Starke, R. Godehardt, G.H. Michler, C.B. Bucknall, J. Mater. Sci. **32**, 1855–1860 (1997)
A.C. Steenbrink, V.M. Litvinov, R.J. Gaymans, Polymer **39**, 4817–4825 (1998)
S.S. Sternstein, L. Ongchin, Polym. Preprint. Am. Chem. Soc. Div. Polym. Chem. **10**, 1117 (1969)
G. Strobl, *The Physics of Polymers. Concepts for Understanding Their Structures and Behavior* (Springer, New York, 1997)
H.-J. Sue, J. Mater. Sci. **27**, 3098–3107 (1992)
H.-J. Sue, A.F. Yee, Polym. Eng. Sci. **36**, 2320–2326 (1996)
M. Suess, J. Kressler, H.W. Kammer, Polymer **28**, 957–960 (1987)
J.N. Sultan, F.J. McGarry, Polym. Eng. Sci. **13**, 29–34 (1973)
Y. Suo, S.S. Hwang, K.U. Kim, J. Lee, S.I. Hong, Polymer **34**, 1667–1676 (1993)
Y. Takeda, D.R. Paul, J. Polym. Sci. B **30**, 1273–1284 (1992)
Y. Takeda, H. Kesskula, D.R. Paul, Polymer **33**, 3394–3407 (1992)

V. Tanrattanakul, A. Hiltner, E. Baer, W.G. Perkins, F.L. Massey, A. Moet, Polymer **38**, 2191–2200 (1997)
Y.S. Thio, A.S. Argon, R.E. Cohen, M. Weinberg, Polymer **43**, 3661–3674 (2002)
R.R. Tiwari, D.R. Paul, Polymer **52**, 5595–5605 (2011)
P.A. Tzika, M.C. Boyce, D.M. Parks, J. Mech. Phys. Solids **48**, 1893–1929 (2000)
L.A. Utracki, M.M. Dumoulin, Polypropylene alloys and blends with thermoplastics, in *Polypropylene: Structure, Blends and Composites*, ed. by J. Karger-Kocsis, vol. 2 (Chapman & Hall, London, 1995)
A. van Der Wal, J.J. Mulder, J. Oderkerk, R.J. Gaymans, Polymer **39**, 6781–6787 (1998)
F. Vazquez, M. Schneider, T. Pith, M. Lambla, Polym. Int. **41**, 1–12 (1996)
P. Vincent (ed.), *Mechanical Properties of Polymers* (Wiley Interscience, New York, 1971)
Y. Wang, J. Lu, G.J. Wang, J. Appl. Polym. Sci. **64**, 1275–1281 (1997)
I.M. Ward, *Mechanical Properties of Solid Polymers* (Wiley, New York, 1983)
S.T. Wellinghoff, E. Beaer, J. Appl. Polym. Sci. **22**, 2025–2045 (1978)
J.-I. Weon, K.-T. Gam, W.-J. Boo, H.-J. Sue, C.-M. Chan, J. Appl. Polym. Sci. **99**, 3070–3076 (2006)
M.W.L. Wilbrink, A.S. Argon, R.E. Cohen, M. Weinberg, Polymer **42**, 10155–10180 (2001)
H. Wilhelm, A. Paris, E. Schafler, S. Bernstorff, J. Bonarski, T. Ungar, J. Mater. Sci. Eng. A **387–389**, 1018–1022 (2004)
S. Wu, J. Polym. Sci. B **21**, 699–716 (1983)
S. Wu, Polymer **26**, 1855–1863 (1985)
S. Wu, Polym. Eng. Sci. **27**, 335–343 (1987)
S. Wu, J. Appl. Polym. Sci. **35**, 549–561 (1988)
S. Wu, J. Polym. Sci. B Polym. Phys. Ed. **27**, 723–741 (1989)
S. Wu, Polym. Eng. Sci. **30**, 753–761 (1990)
S. Wu, Polym. Int. **29**, 229–247 (1992)
H.Q. Xie, D.S. Feng, J.S. Guo, J. Appl. Polym. Sci. **64**, 329–335 (1997)
K. Yang, Q. Yang, G.X. Li, Y.J. Sun, D.C. Feng, Polym. Compos. **27**, 443–450 (2006)
K. Yang et al., Polym. Eng. Sci. **47**, 95–102 (2007)
A.F. Yee, J. Mater. Sci. **12**, 757–765 (1977)
A. F. Yee, Polymer Prepr. **17** (1976)
A.F. Yee, J. Du, M.D. Thouless, Toughening of epoxies, in *Polymer Blends, Vol. 2: Performance*, ed. by D.R. Paul, C.B. Bucknall (Wiley-Interscience, New York, 2000), pp. 225–268
R.J. Young, Philos. Mag. **30**, 85–94 (1974)
R.J. Young, Mater. Forum. **11**, 210–216 (1988)
Q. Yuan, J.S. Shah, K.J. Bertrand, R.D.K. Misra, Macromol. Mater. Eng. **294**, 141 (2009)
W.C.J. Zuiderduin, C. Westzaan, J. Huetink, R.J. Gaymans, Polymer **44**, 261–275 (2003)
W.C.J. Zuiderduin, J. Huetink, R.J. Gaymans, Polymer **47**, 5880–5887 (2006)